1-1-2016

The Roles Of Human Cytomegalovirus Tegument Proteins Pul48 And Pul103 During Lytic Infection

Daniel Angel Ortiz
Wayne State University,

THE ROLES OF HUMAN CYTOMEGALOVIRUS TEGUMENT PROTEINS pUL48 AND pUL103 DURING LYTIC INFECTION

by

DANIEL ANGEL ORTIZ

DISSERTATION

Submitted to the Graduate School

of Wayne State University,

Detroit, Michigan

in partial fulfillment of the requirements

for the degree of

DOCTOR OF PHILOSOPHY

2015

MAJOR: IMMUNOLOGY & MICROBIOLOGY

Approved by:

_____

Advisor Date

_____

_____

_____

DEDICATION

This work is dedicated to my family and friends that have supported me throughout my journey as a graduate student. Moving to a Michigan was an adventure all in itself, as I have never lived outside of Illinois. Having my uncle Tony and aunt Bobbie close by made the transition much easier. I always knew I had a place to eat, relax, and vent. Their generosity and hospitality have redefined my definition of “family” which will always resonate with me.

I also want to thank my parents, Javier and Esperanza Ortiz, who have been there for me throughout this whole process. They have encouraged me since I was young to pursue my dreams, from which, has led me pursue my interest in microbiology. Their love and support has not only made me the person I am today, but has also guided me to a better future. I could not be more thankful for their instrumental role in my life.

Finally, I would like to acknowledge my friends, old and new. Without their help I would not have been able to mentally escape from the life of a graduate student. Although laboratory experiment consumed my life, being able to “check out” was both necessary and sufficient to completing my PhD.

ACKNOWLEDGEMENTS

We gratefully acknowledge Wade Gibson (Johns Hopkins University) for antibodies against UL48, Dong Yu (Washington University) for the HCMV (AD169) BAC, the Wandless lab for sharing the BioID construct, Bonita Biegalke (Ohio University) for anti-pUL34, and the Donald Court (National Cancer Institute) for bacterial strains used for generation of BAC mutants. We thank Mary Olive, Carmel Harkins, and the staff of the Wayne State University Microscopy and Imaging Resources Laboratory for their assistance; Hong Yi of the Robert P. Apkarian Integrated Microscopy Core of Emory University for electron microscopy; Paul Stemmer and Namhee Shin of the Karmanos Cancer Center Proteomics Core for mass spectrometry analysis.

This work was supported by Wayne State University, NIH NIGMS R25GM058905-13, and NIAID (1 R21 AI076591-01 and 1 R56 AI099390-01). The Wayne State University Microscopy and Imaging Resources Laboratory are supported in part by NIH grants and by NIH Center grant P30CA22453 to the Karmanos Cancer Institute, Wayne State University, and the Perinatology Research Branch of the National Institutes of Child Health and Development, Wayne State University. The Robert P. Apkarian Integrated Microscopy Core of Emory University is supported by NIH (1 S10 RR025679 01). The Wayne State University and Karmanos Cancer Center Proteomics Core is supported by NIH Grants P30 ES020957, P30 CA022453 and S10 OD010700.

TABLE OF CONTENTS

LIST OF TABLES

LIST OF FIGURES

CHAPTER ONE

GENERAL INTRODUCTION

Human herpesviruses. Indication of herpesviruses causing human disease dates back to the early days of medicine when Hippocrates used the Greek word “herpes” to describe lesions that appeared to creep across the skin. The term herpes, however, was used ubiquitously to define several skin conditions. It was Vidal that proved a herpesvirus, herpes simplex virus (HSV), is the infectious agent responsible by conducting human-to-human transmission studies (1). Future experiments by Andrews and Carmichael showed that HSV could cause recurrent infections in adults with neutralizing antibodies, but it was Burnet and Williams that recognized HSV can establish a lifelong latent infection that can still cause herpetic lesions in the presence of external stimuli (2).

All viruses classified under the *Herpesviridae* family have similar virion structures. Each virion is composed of a double stranded DNA genome packaged inside an icosahedral capsid. Surrounding the capsid is an amorphous proteinacious coat labeled the tegument layer that forms a scaffold between the capsid and the outer lipid envelope (Fig. 1). There are over 200 viruses that belong to the *Herpesviridae* family with only 8 known to primarily infect humans (3). The human herpesviruses belong to three different subfamilies (*Alphaherpesvirinae, Betaherpesvirinae,* and *Gammaherpesvirina)* based on biological properties. The *Alphaherpesvirinae* consist of HSV 1 and 2, and varicella-zoster virus (VZV), with a broad host range and short replication cycle. The *Betaherpesvirinae* include human cytomegalovirus (HCMV), human herpesvirus 6 (type A and B), and human herpesvirus 7, which have a narrow

host range and a long replication cycle. The last subfamily *Gammaherpesvirinae,* are composed of Epstein-Barr virus and Kaposi's sarcoma virus that have the most restricted host range.

Although the rate of the replication varies between the subfamilies, they share a common life cycle. Infection is initiated upon attachment of viral glycoproteins to species specific cellular receptors. Fusion of the viral envelope with the host membrane at the plasma membrane or inside endocytic vesicles mediates entry of the capsid and the release of tegument proteins into the cytoplasm (4, 5). The tegument proteins modulate host cell immune responses, regulate host cell protein synthesis, and facilitate the transport of the nucleocapsid to the nucleus. Docking of the nucleocapsid to the nuclear pore releases viral DNA into the nucleus where tegument proteins trans-activate viral gene expression. This initiates the lytic gene cascade consisting of three major kinetic classes (immediate early, early, and late) which lead to the production of viral particles. Released infectious viral progeny are capable of establishing a life-long latent infection, which can be reactivated in response to various stimuli.

HCMV clinical relevance. HCMV is an opportunistic pathogen that has spread worldwide. Primary infections occur through contact with infected blood and urine, or mucosal secretions. The seroprevalence rate in the United States hovers around 50%, but rates are significantly higher in under developed countries (6, 7). Infection of healthy individuals is usually mild and self-limiting, yet results in a life-long latent infection with periodic episodes of reactivation.

Primary infection or reactivation of HCMV presents a concern to the immunocompromised, such as AIDS patients and transplant recipients. The assault on CD4 lymphocytes by HIV leaves the immune system depleted and allows HCMV proliferation and dissemination, leading to retinitis, gastrointestinal disease, and pneumonitis (8). HCMV retinitis once accounted for 90% of AIDS related vision loss until the development of highly effective antiretroviral and anti-CMV therapies (9, 10). Unfortunately, low income countries have limited access to these drugs which leaves AIDS patients at risk for acquiring HCMV retinitis (11). Also at risk of HCMV disease are solid organ and hematopoietic stem cell transplant patients as a result of life-long immunosuppressive drug regimens. Infection and invasion of HCMV into tissues can cause pneumonia, hepatitis, encephalitis, and even death. Fortunately, ganciclovir, high-dose acyclovir, and valacyclovir treatment have been shown to prevent early onset HCMV disease in hematopoietic stem cell transplants (12-15). Delayed onset HCMV disease still presents a major problem for clinicians who have turned to monitoring patients long term through pp65 antigenemia and PCR testing (12, 16).

HCMV infection is also a concern for pregnant mothers who can vertically transmit the virus to their child during pregnancy or childbirth. In developed countries, HCMV is the most common viral congenital infection with 0.2% to 2.5% of newborns being affected (17). Infected children can be symptomatic or asymptomatic at birth, but all are at risk of developing severe neurological abnormalities that cause mental retardation, microcephaly, seizures, and hearing loss. In fact, HCMV is the leading cause of non-genetic sensorineural hearing loss among infants (7, 18). Anti-viral

treatment is recommended and effective in symptomatic congenital HCMV cases, but an HCMV vaccine would address asymptomatic and in utero infections (19).

HCMV virion structure and genome. HCMV is the largest known human herpesvirus. The diameter of a single virion ranges from 150- 200 nm, which houses a linear double stranded DNA (230 kbp). The genome contains a unique long (UL) and a unique short region (US), flanked by sets of internal repeats (TRL/IRL and IRS/TRS respectively). Inversion of the UL and US regions allows up to four different isoforms of the HCMV genome. The coding capacity of the laboratory strain AD169 genome is around 190 translated open reading frames (ORFs) which all show high similarity to clinical isolates (20, 21). However, the total number of translated ORFs can be as high as 750 when including small codons (<80) and alternative transcript start, stop and splice sites, thus demonstrating the complexity of HCMV infection (22).

HCMV attachment and entry. The broad cell tropism of HCMV is an essential component to multi-organ spread and disease. Clinical strains of HCMV have the ability to infect epithelial cells, endothelial cells, fibroblasts, smooth muscle cells, monocytes, and macrophages. The proteoglycan heparin sulfate is found on the all of these cells and is the primary site of attachment for HCMV glycoproteins gB and gM/gN (23). Other cell surface receptors have been proposed (i.e. EGFR and PDGFR), however, neutralizing antibody against these ligands proved unsuccessful at preventing entry, alluding to the possibility of alternative entry pathways (24, 25). Integrins, specifically α2β1, α6β1, and αvβ3, have also been considered attachment sites. Studies using anti-integrin antibodies inhibited entry, yet binding still occurred, suggesting integrins are involved in virus-cell membrane fusion (26). The location of the fusion step differs

depending on cell type. In fibroblasts, fusion takes place at the outer cell membrane, which involves the viral glycoproteins gH and gL (5, 27), but in epithelial and endothelial cells, gH/gL forms a complex with proteins pUL128, pUL130 and pUL131 to initiate a pH dependent fusion that occurs after endocytosis of the virus particle (4).

Following fusion, viral tegument proteins are released into the cytoplasm of the cell to facilitate a productive infection. Some include viral proteins that can counteract the host antiviral response. TRS1 and IRS1 prevent the phosphorylation of eukaryotic translation initiation factor eIF-2alpha and the activation of RNase L, which blocks cellular protein synthesis (28). Another viral mechanism of immune evasion is inhibiting antigen presentation. One of the most abundant tegument proteins, pp65, blocks the antigen processing of IE2 to avoid cytotoxic killing by $CD8^+$ T cells (29), and degrade HLA class II molecules to prevent recognition by $CD4^+$ T cells (30). Other capsid associated tegument proteins are responsible for mediating the transport of the nucleocapsid to the nuclear pore via microtubules. Docking of the capsid initiates release of the viral genome into the host cell nucleus.

HCMV gene expression and replication. Once the HCMV genome enters the nucleus, it circularizes and localizes to nuclear domain 10 sites, where tegument proteins initiate the lytic gene cascade. Although transfection of viral DNA alone results in productive infection, infectivity substantially increases in the presence of viral transactivators, such as pp71 and pUL35 (31). The association between pp71 and pUL35 act cooperatively to stimulate the major immediate early promoter and begin lytic gene expression (32). The primary products of the major immediate early promoter are immediate early genes IE1-p72 and IE2-p86. These proteins are involved in a variety of

functions, including evasion of host innate immunity, regulation of the cell cycle, and transactivation of viral and host genes (33-35). Although only IE2 is essential for replication (36), both IE1 and IE2 work synergistically with other viral and cellular components to drive early gene expression (37, 38).

Early genes are the second kinetic class of genes expressed during a lytic infection and are required for viral DNA replication. HCMV DNA synthesis follows the assembly of viral and cellular proteins at the origin of lytic replication, termed *ori*Lyt. To date, 11 viral genes are associated with *ori*Lyt replication: UL44 (DNA processivity factor), UL54 (DNA polymerase), UL57 (single stranded-DNA-binding protein), UL70 (primase), UL84 (replication initiator protein), UL102 (primase-associated factor), UL105 (helicase), IRS1/TRS1, and UL36–38, UL112/113, and IE2 (39-41). Localization of UL84 and IE2 to replication centers initiates *ori*Lyt-dependent replication in fibroblasts (41). Viral DNA is replicated via a rolling circle mechanism that generates concatemeric HCMV genomes. Concurrent with viral DNA replication is the expression of late genes.

HCMV assembly and egress. The production of late proteins leads to procapsid assembly. These preformed capsids recognize and target the concatemeric viral DNA for encapsidation. Cleavage of the concatemer packages a single HCMV genome per capsid. The formation of the nucleocapsid is followed by an envelopment and de-envelopment process to exit the nucleus (42). At the inner nuclear membrane, primary envelopment is triggered by the pUL97 mediated phosphorylation of the nuclear egress complex, subunits pUL50 and pUL53 (43). Subsequent de-envelopment occurs at the outer nuclear membrane and releases the nucleocapsid into the cytoplasm.

While some tegument proteins are added to the nucleocapsid during nuclear egress, most are acquired in transit towards sites of secondary envelopment. Envelopment occurs at specialized, HCMV induced, cytoplasmic vesicles that contain markers for trans-Golgi, multi vesicular bodies, and endosomes (44-46). Budding of particles into these vesicles is followed by exocytosis, in which the mature virion is released from the cell. The cytoplasmic process of assembly, envelopment, and egress all occur inside the HCMV induced cytoplasmic virion assembly complex (cVAC).

Cytoplasmic virion assembly complex. A hallmark of HCMV infection is nuclear and cytoplasmic enlargement or cytomegaly. Following 3 to 4 days post infection, the host cell nucleus takes on a kidney bean-like shape that partially wraps around a perinuclear structure termed the cVAC. This structure is the final site of virion maturation and necessary for efficient virion production. The formation of the cVAC involves the structural rearrangement of multiple cellular organelles. The interior compartment consists of a microtubule organizing center (MTOC) and EEA1 positive endosomes that are encircled by a ring of intertwined Golgi and trans-Golgi components (47). Microtubules emanating from the MTOC are thought to be responsible for the trafficking of virions through the cVAC (Fig. 2). Also, Rab GTPases and endosomal sorting complex required for transport (ESCRT) gather at the cVAC and are implicated in virion maturation; perturbing components of either pathway results in decreased viral titers (48-50). Rab proteins are master regulators that control the flow of membrane traffic and target viral proteins to their appropriate destination. ESCRT machinery perform membrane bending and scissioning events that may contribute to the budding

of nucleocapsids into endocytic vesicles (The role of ESCRT proteins is described further in the following section).

In addition to cellular proteins, many viral tegument proteins and glycoproteins heavily localize to the cVAC for virion production (51, 52). A mature HCMV virion is composed of 70 different viral proteins with at least 32 being tegument proteins (53, 54). The process of virion assembly is incompletely understood, but requires, in part, tegument proteins pUL32 (pp150), pUL99 (pp28), pUL94, pUL71 and pUL103 (55-58).

The second most abundant tegument protein, pUL32, serves a multifunctional role during infection. At early times, pUL32 localizes to the nucleus and is tightly bound to capsids (59-61). Initial studies with pUL32 antisense mRNA appeared to block the translocation of nucleocapsids to the cytoplasm, indicating a role in nuclear egress (62). In support of these knockdown studies, a UL32 deletion virus grown on complementing cells showed an accumulation of viral DNA in the cytoplasm, but few discernable nucleocapsids (63). In addition, mutagenizing pUL32 conserved region 1 (CR1) or CR2 perturbed cVAC organization and virion maturation (63). This data indicates a dual role of pUL32 in stabilizing nucleocapsids and virion assembly.

The UL99 protein is a highly conserved myristoylated and phosphorylated protein (64). The deletion or mislocalization of HCMV pUL99 (pp28) causes a defect in viral replication and irregular Golgi structures (56, 64, 65). Interesting, only the N-terminal 50 amino acids that carry the multimerization, myristoylation, and pUL94 binding domain are necessary for virion production (64, 66). Disruption of a single cysteine residue at position 250 of pUL94, or the deletion of pUL99 residues 37-39 disrupts the pUL94-

pUL99 interaction, which causes the dispersal of both proteins from the cVAC (55, 67). The proper localization of pUL94 and pUL99 is essential for virus production.

Equally as important in the process of envelopment is pUL71. In the absence of pUL71, the cVAC contains abnormally large cytoplasmic inclusions labeled with LAMP1 and CD63, markers for late endosomes and multivesicular bodies (68, 69). Virus particles located at these enlarged vesicles have delayed envelopment and thus impaired release. In transfection experiments, pUL71 binds to pUL103 with localization of pUL103 dependent on the pUL71interaction (70). Interestingly, a pUL103 deletion mutant also shows nucleocapsids suspended in the process of secondary envelopment and lower viral titers (58). These results suggest that pUL71 and pUL103 form a protein complex that functions during the final stages of virion maturation.

The process of HCMV assembly and egress in the cVAC is highly complex and requires the concerted effort of viral and cellular proteins. A recent study shows viral proteins are able to subvert the antiviral function of interferon-induced transmembrane proteins (IFITMs) for cVAC formation and efficient virus production (71). Also, host proteins contribute to the proper localization of viral proteins, as in how Rab6 interacts with and traffics pUL32 to the cVAC during infection (50). The functions of these viral and cellular interactions are only beginning to be uncovered. Understanding the interplay between viral and cellular proteins in the cVAC will provide further insight to late stages of HCMV infection, as well as basic cell biology.

ESCRT machinery. The process of subverting host cell machinery for virion production is a common theme among multiple viruses. Although not much is known about HCMV secondary envelopment, there is evidence that HCMV obtains its

envelope in endocytic compartments. (i) In HCMV infected cells incubated with horseradish peroxidase (HRP), virions and HRP were present in the same compartment (44). (ii) Purified infectious HCMV virions contain CD63, a multivesicular body marker (45). (iii) Dominant negative ESCRT components, CHMP1A and VPS4A reduce infectious yield (48).

The formation of these endocytic vesicles is mediated by ESCRT machinery (Fig. 3). The ESCRT pathway is initiated by ESCRT-0 subunits binding phosphatidylinositol 3-phosphate, ubiquitinated proteins, and TSG101 of ESCRT-I. Sequential recruitment of ESCRT-I and ESCRT-II subunits concentrates ubiquitinated cargo to begin the membrane invagination process. Activation of the ESCRT-III complex completes the membrane scissioning and releases the newly formed vesicle. HCMV may use all or a combination of these players during secondary envelopment.

In retroviruses, ESCRT machinery is recruited to sites of envelopment by signal motifs found on viral proteins. These signals are often the same or similar to those present on host cell proteins, and are termed “late” or “L” domains: P(T/S)AP, PPXY, and YPX_nL. The P(T/S)AP late domain is used to recruit TSG101, and thus ESCRT-I, to sites of virion envelopment (72, 73). The PPXY motif binds WW domains of NEDD4 family members that target specific proteins for ubiquitination (74). YPX_nL late domains in retroviruses bind the V domain of ALG-2 interacting protein X (ALIX) to facilitate viral budding at the cell membrane (75-77).

Although ESCRT machinery is critical for retrovirus budding, evidence of ESCRT involvement during HCMV envelopment is conflicting. siRNA knockdown of TSG101, ALIX, Vps4A and Vps4B in retinal pigment epithelial cells had either no effect or a slight

increase in HCMV virion production (78). However, dominant negative versions of CHMP1A and VPS4A in human fibroblasts reduced infectious yields by 100-fold at 6 dpi indicating the necessity of ESCRT-III in virion production (48). In the same study, CHMP1A and Vps4A localized in or around the cVAC, but how these ESCRT-III components are recruited to sites of HCMV envelopment remains a mystery. Sequence analysis of HCMV tegument and glycoproteins revealed numerous late domains. One P(T/S)AP motif in pUL32, two PPXY motifs in gB and pUL48, and 7 HCMV proteins (including pUL103) with ALIX binding domains YPX_nL. With this redundancy and multiple pathways leading to ESCRT-III recruitment (ESCRT-II, NEDD4, ALIX, or an unidentified viral protein), identification of functional late domains in HCMV may provide insight to the process of secondary envelopment.

UL103. The HCMV UL103 gene encodes a tegument protein that is conserved among all human herpesviruses. Early work on the alphaherpesvirus homolog UL7 has shed light on the process of UL103 gene transcription. The UL7 gene is located on the unique long region of the genome and overlaps the upstream UL6 gene (homolog of HCMV UL104) at its 5' end. Analysis of the UL7 and UL6 transcript reveals a shared poly A tail with both genes being transcribed simultaneously in herpes simplex virus 1 (HSV-1) and psuedorabies virus 1 (PrV-1) (79, 80). The UL6 gene product is essential in forming the entry portal for packaging viral DNA in preformed capsids (81), while the UL7 gene is a nonessential structural protein with late transcription kinetics (79, 80, 82).

The HCMV UL103 gene is similar to its alphaherpesvirus counterpart (UL7) in a variety of ways. (i) The UL103 gene shares 53 base pairs with the neighboring UL104 gene, indicating cotranscription. (ii) Expression of UL103 is regulated as a late gene

with the protein incorporated into virions ((54, 83)). (iii) Disruption or deletion of the UL103 ORF causes smaller plaque size, decreased viral titers, and defects in virion release (58, 82, 84-87). (iv) pUL103 and the HSV-1 homolog accumulate in the cytoplasm at late times post infection and colocalize with cytoplasmic membranes (58, 88). (v) The localization of pUL103 is dependent on its interaction with pUL71, which is also evident in the HSV-1 homologs pUL7 and pUL51 (70, 88). However, some properties of pUL103 are HCMV specific. For instance, HCMV produces sacs of enveloped tegument proteins called dense bodies during infection. The formation of dense bodies is independent of virion assembly, but the release of both particles is controlled by pUL103 (58). The properties of the highly conserved HCMV pUL103 have been explored extensively, yet the function of pUL103 during infection has yet to be elucidated.

Insight to the possible functions of pUL103 can be gathered from previous studies on pUL7. For instance, the UL7 protein of HSV-2 appears in the nucleus and is weakly associated with A, B, and C capsids (89). Although HCMV pUL103 has not been identified as nuclear, it does contain a conserved G-F-x(8)-E-D-x-V-x(12)-R domain with similarity to DNA topoisomerase III of fission yeast, hinting to a possible role in packaging or DNA transcription. Also, co-immunoprecipitation of HSV-1 pUL7 pulled down cellular mitochondrial proteins ANT2 and ANT4 (82). The biological significance of these interactions was not pursued, but could be involved in regulating mitochondrial function to facilitate a productive infection.

This work. Currently, there are only four drugs approved for HCMV treatment, but all target steps of DNA replication. Because of this, resistance to these types of

drugs is increasing. An alternative approach is to prevent cVAC assembly, and thus inhibit viral production. However, the viral proteins involved in cVAC formation have yet to be characterized.

The focus of this work was to identify individual viral proteins that control cVAC biogenesis. The formation of the cVAC follows viral DNA synthesis, which implies a connection to late genes. Although this does not exclude immediate early and early gene involvement, it provides an initial starting point for viral genes to pursue. Also, a fully formed cVAC is critical for efficient virus production, so we chose to focus on late genes that display a growth defect when the ORF is disrupted. This led to the screening of 26 genes, from which three viral proteins (pUL48, pUL94, and pUL103) were identified as important for cVAC biogenesis. These three viral proteins as well as their interacting partners, whether they are viral or cellular proteins, can provide potential targets for developing anti-viral drugs.

To further understand the functions of pUL103, we conducted a dual method approach of affinity purification followed by mass spectrometry to elucidate pUL103 binding partners. By using two different methods and enriching for interactions identified by both, we were able to reduce the amount of false positives while also improving the likelihood of a true interaction. We identified and verified pUL103 interactions with multiple nuclear viral proteins (IE2, pUL34, and pUL44), an antiviral (IFI16) and ESCRT associated protein (ALIX). These interaction partners revealed a nuclear association of pUL103, as well as possible functions in the antiviral response and ESCRT machinery recruitment, suggesting a multifaceted role of pUL103 during HCMV infection.

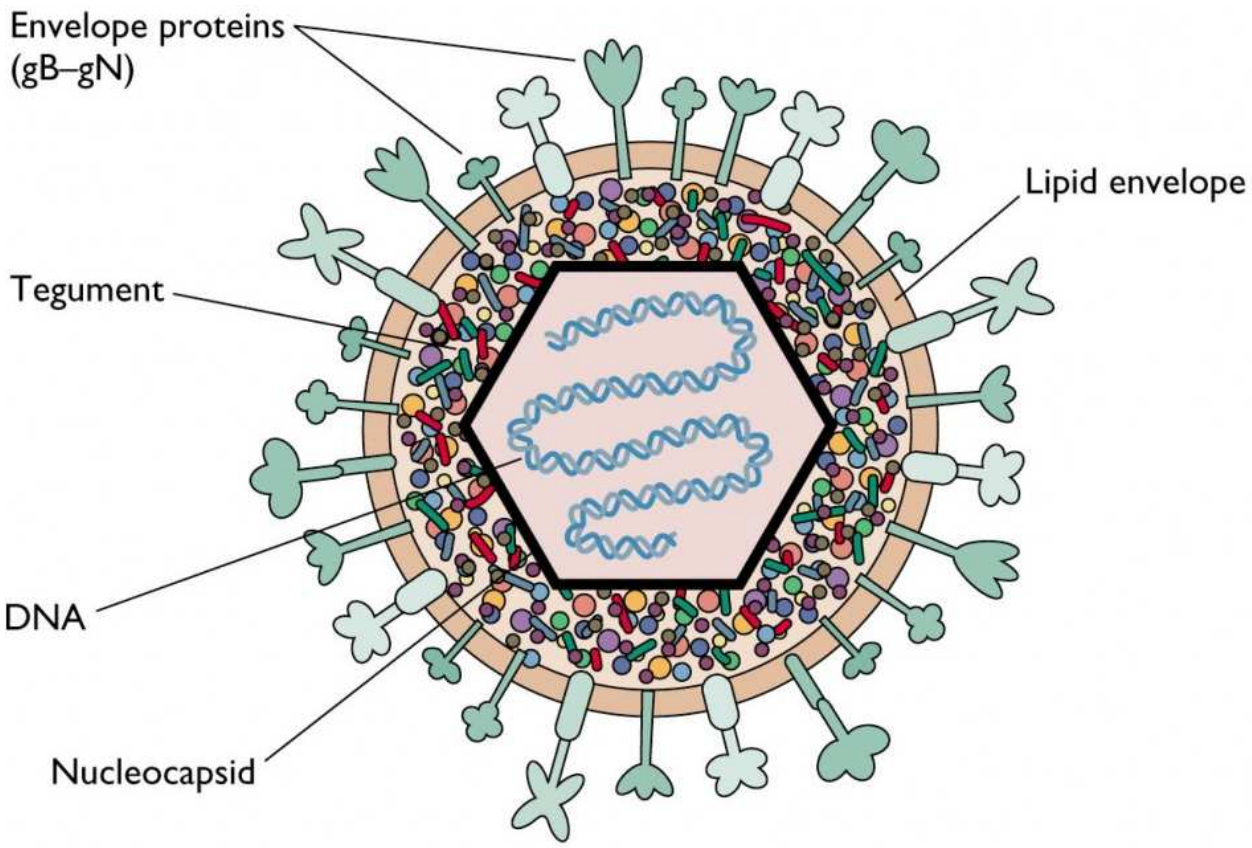

Figure 1. Herpesvirus virion structure

Used with permission from http://www.twiv.tv/virus-structure/

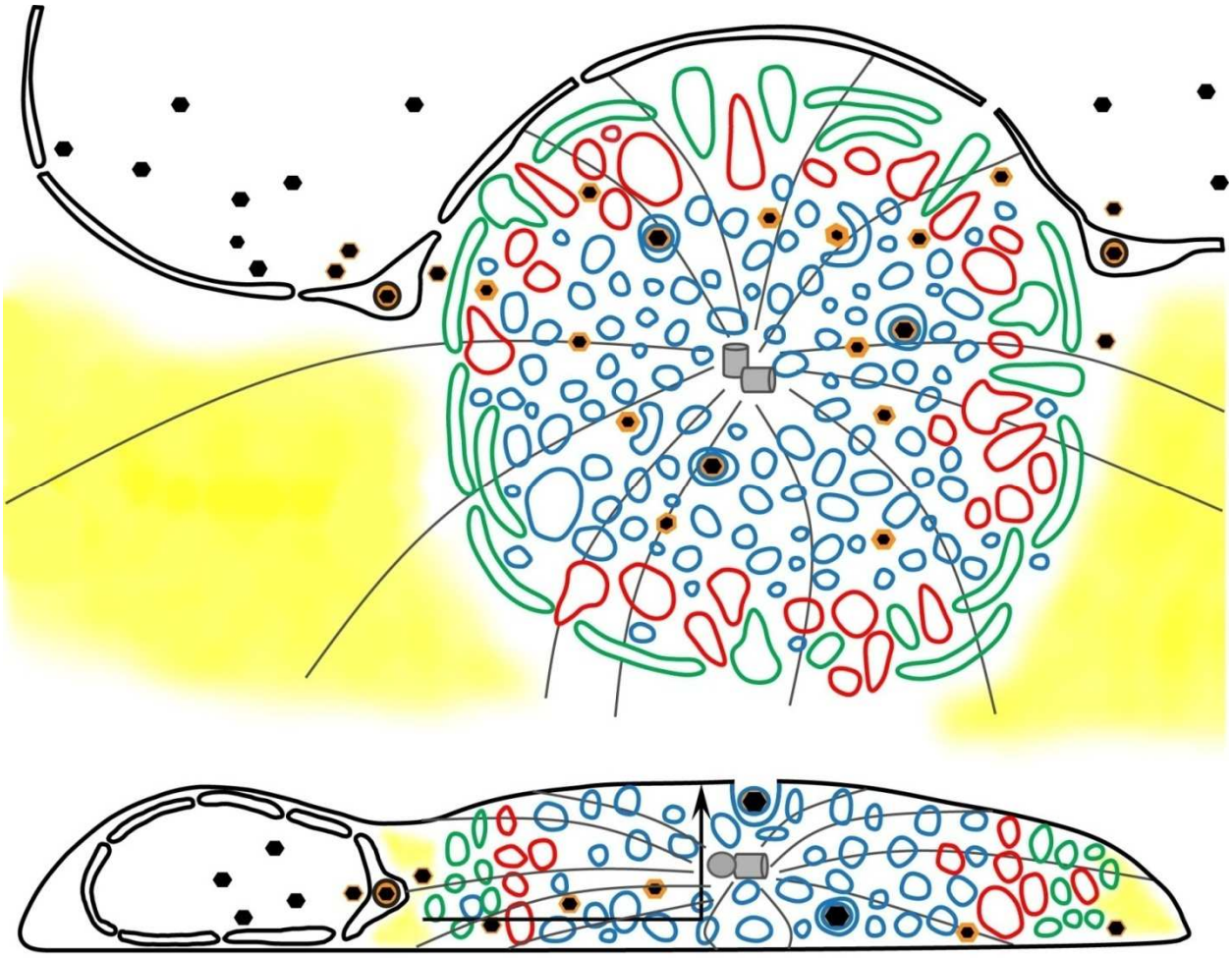

Figure 2. Schematic representation of the cVAC and proposed path of virion egress

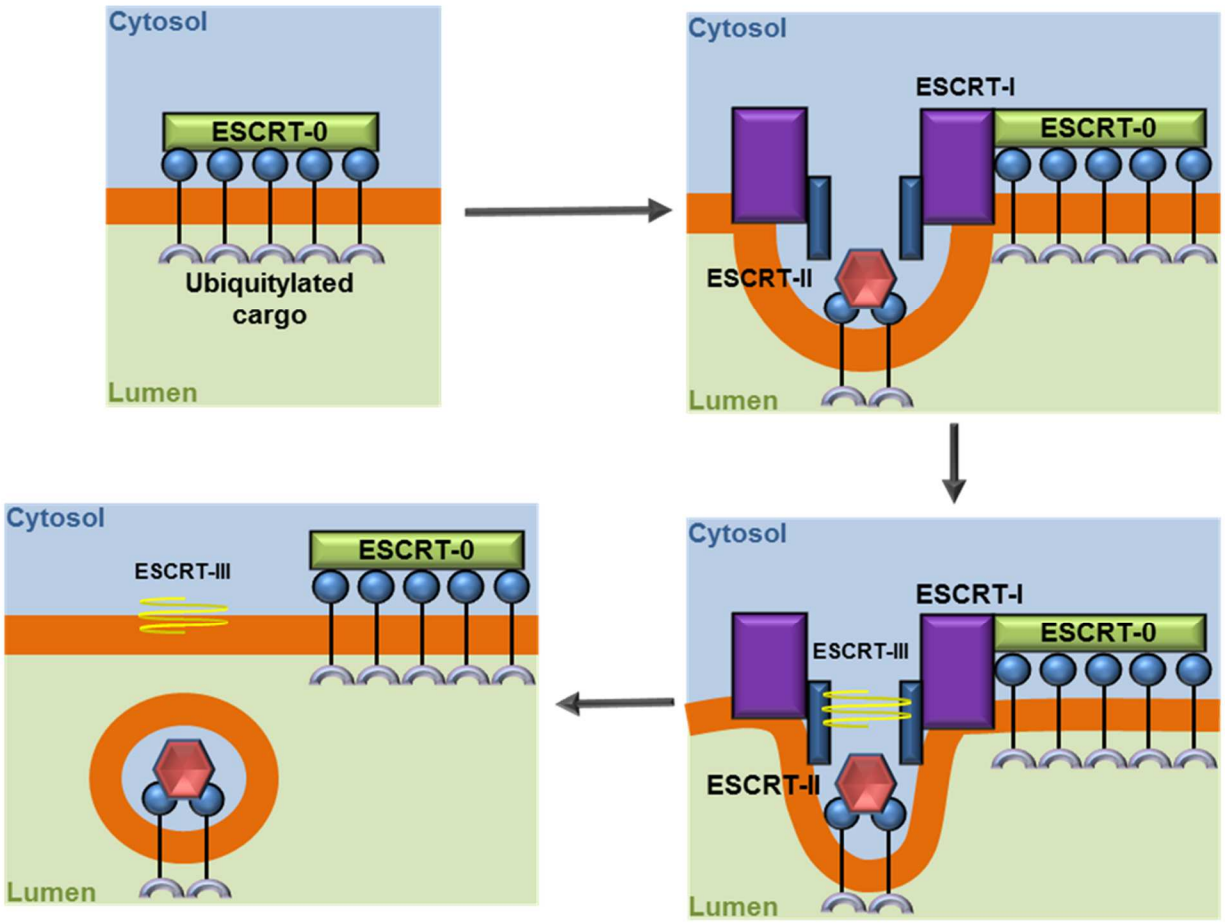

Figure 3. Formation of intraluminal vesicles by ESCRT machinery; the proposed pathway for HCMV virion envelopment

CHAPTER TWO

VERIFYING THE ROLES OF pUL48 AND pUL103 IN CVAV BIOGENESIS

This chapter is written as published in the Journal of Virology, August 2014. Subhendu Das PhD conducted the siRNA screen to identify viral candidates involved in assembly complex biogenesis (figures 3-5). I constructed and characterized two recombinant viruses to verify the siRNA screen results (figures 6-13).

Introduction

Herpesvirus virion assembly is a complex process (reviewed in (90, 91)). A portion takes place in the nucleus, which is the site of viral DNA replication, formation of and filling the nucleocapsid with viral DNA, and acquisition of the initial tegument layer. The major pathway of virion maturation involves the nascent capsid budding through the inner nuclear membrane into the lumen of the nuclear membrane, thus acquiring the primary envelope. Subsequently, the virion "infects" the cytoplasm through the outer nuclear membrane, leading to loss of the primary envelope. Tegument components are added during movement through the cytoplasm to a vesicle into which the particle buds, acquiring its mature envelope. The vesicle housing the virion is transported to the cell surface where the virion is released in an exocytic process.

Human cytomegalovirus (HCMV) induces cytopathic effects that include cytoplasmic and nuclear enlargement, and development of characteristic cytomegalic nuclear and cytoplasmic inclusions (reviewed in (92)). The large cytoplasmic inclusion corresponds to the cytoplasmic virion assembly complex (cVAC) (51). cVAC are large cylindrical structures that are present one per infected cell, even in multinucleate

syncytia. Nuclei take on a kidney-like (reniform) shape as they bend partially around the cVAC (93). Electron microscopic evidence indicates that the cVAC is the site of final tegumentation and envelope acquisition (44, 94, 95). Viral tegument proteins, envelope proteins, and some non-structural proteins localize to the cVAC, and cytoskeletal filaments appear to radiate from a microtubule organizing center in the cVAC (46, 51, 96, 97). The cVAC is relatively devoid of endoplasmic reticulum (ER) markers. The ER-to-Golgi intermediate compartment (ERGIC), Golgi apparatus, and *trans*-Golgi network (TGN) form a cylindrical ring that outlines the cVAC (47, 51, 96).

Tooze et al. (44) treated cells with soluble horseradish peroxidase, which is taken up by recycling endosomes, and found its reaction product of oxidized diaminobenzidine in cytoplasmic vesicles that contained what appeared to be tegumented and enveloped HCMV virions, providing direct evidence that the virion exit vesicle is related to recycling endosomes. Consistent with this, we and others found that molecular markers of recycling endosomes (early endosome antigen 1 (EEA1) and Rab11) stain vesicles that cluster at the center of the cVAC (45, 47, 58, 96, 98). Exactly how virions mature in the cVAC remains a mystery, and it has not been demonstrated whether a fully formed cVAC is necessary for efficient virion production. Although structures morphologically similar to the HCMV cVAC have not been described for other herpesviruses, a recent study found that herpes simplex virus 1 virions acquire their envelope at tubular structures that share many properties with recycling endosomes (99).

Although the full set of viral regulators of cVAC biogenesis has not been identified, some things are known: (i) cVAC do not form in the absence of viral DNA synthesis ((97) and our unpublished observations), indicating that its formation is

dependent on expression of one or more viral late genes; gene(s) from an earlier kinetic class may also be involved. (ii) Treatment of cells with nocodazole, which depolymerizes microtubules, leads to rapidly reversible cVAC disruption (100). While microtubules are important (even essential) components of the cVAC, they are not likely to be regulators of cVAC biogenesis. (iii) The kinase activity of pUL97 is required for formation of perinuclear complexes that correspond to cVAC and for efficient production of infectious virions, but UL97 activity alone is insufficient for cVAC development (97, 101, 102). (iv) Although not examined in detail, images in papers describing some HCMV mutants that have defects at late stages of virion assembly are consistent with at least some features of cVAC-like structures forming in the absence of UL32, UL91, UL96, UL99 (56, 57, 69, 103). (v) In contrast, insertion of a stop codon into the UL103 open reading frame resulted in the absence of well-formed Golgi rings, but the recycling endosomal compartment was not studied (58). In addition, in cells infected with a pUL71-deficient virus, viral proteins that normally associate with the cVAC are mislocalized (69). (vi) cVAC form in cells infected with highly passaged laboratory strains of HCMV that lack some genes present in wild type viruses (preceding references), as well as after infection with a low passage virus that encodes a nearly complete complement of HCMV genes (104). Interestingly, an HCMV locus spanning UL133 to UL138 is required for cVAC development in human microvascular endothelial cells, but not in embryonic lung fibroblasts (104), indicating that cell-specific viral factors can be involved. (vii) In addition to protein regulators of cVAC biogenesis, HCMV microRNAs miR UL112-1, US5-1, and US5-2 target mRNAs of several host proteins involved in regulation of the cellular secretory apparatus (105). A recombinant virus that

does not express these miRNAs did not induce formation of cVAC and produced significantly fewer infectious virions. Ectopic expression of these microRNAs had some effects on Golgi structures, but full cVAC did not form.

In prior studies we described the three dimensional structure of the cVAC, and the extensive remodeling of the cytoplasm and shifts in organelle identity that occur during cVAC development (98). The objective of this work was to identify HCMV protein-coding genes that regulate cVAC biogenesis. Using siRNAs that target a set of 26 candidates, we identified three HCMV genes (UL48, UL94, and UL103) whose absence results in abrogation of cVAC development, without affecting expression of other viral genes. Our results expand the set of functions assigned to HCMV genes, and will enable identification of the network of interactions between HCMV and the host cell secretory apparatus, provide new information about the process of virion assembly, and define new targets for development of novel antivirals.

Materials and Methods

Cells and virus. HCMV (AD169) (American Type Culture Collection, Manassas, VA) was grown in low passage human foreskin fibroblasts (HFF) in complete Dulbecco's modified Eagle (DMEM) medium plus sodium pyruvate and MEM nonessential amino acids (Invitrogen, Carlsbad, CA), GlutaMAX (Invitrogen), and 5% FBS (HyClone, Logan, UT). Virus was titrated by plaque assay on low passage diploid human foreskin fibroblasts. For growth curves, supernatant virus was collected, purified, and stored at -80°C. The siRNA experiments reported here were performed in low-passage human lung fibroblasts (HLF) (a gift from John Stewart, Centers for Disease Control and Prevention, Atlanta, GA) that were propagated in the medium described above but with 10% FBS and penicillin and streptomycin. Antibiotics were omitted during experiments.

siRNA screening and immunofluorescence assay. Cocktails of four siRNAs that specifically target each candidate HCMV regulator of cVAC biogenesis were designed and synthesized by Dharmacon Inc. (Lafayette, CO). For the transfection experiments, 2 x 10^4 HLF cells per well were seeded onto 0.2% gelatin coated 8-well glass chamber slides (LabTek, Nunc, Rochester, NY; catalog number 177402) for 1 h at 37°C. The following day, cells were transfected with 50 pmol SMARTPOOL siRNA using Lipofectamine 2000; 6 h after transfection, cells were infected at a multiplicity of infection (MOI) of 0.2 in DMEM containing 5% fetal bovine serum. As previously described (16), after 120 h, cells were washed with PBS, fixed with 4% paraformaldehyde in PBS (lacking Ca^{2+} and Mg^{2+}) at pH 7.4, and then autofluorescence was quenched by incubation for 15 min in 50 mM ammonium chloride. Cells were subsequently permeabilized and then successively incubated with the primary

antibodies (described in Table 1) and fluorescent tagged secondary antibodies (Alexa Fluor 488- conjugated goat anti-mouse IgG and Alexa Fluor 568-conjugated goat anti-rabbit IgG both from Molecular Probes, Carlsbad, CA). Mounting was done with Vectashield containing DAPI (4', 6-diamidino-2-phenylindole) (Vector Laboratories Inc., CA). Imaging was done on a Leica TCS SP5 laser scanning confocal microscope.

Construction of recombinant viruses. Recombinant HCMV viruses were generated by recombineering using the AD169 bacterial artificial chromosome, pAD/Cre in SW105 (gift from Donald L. Court, National Cancer Institute), an *E. coli* strain which contain a temperature sensitive recombinase gene and an arabinose inducible Flp gene (106, 107). pAD/Cre contains the AD169 genome flanked by loxP sites that excise the bacterial component of the BAC upon transfection into mammalian cells. Due to overlapping adjacent coding regions at the 5' end of the UL48 and UL103 genes, the FKBP segment (108), was inserted at the 3' end of the target genes. Selective markers (galK and kanamycin) flanked by FKBP and FRT sequences were PCR amplified from pYD-C630 (provided by Dong Yu, Washington University) (109). Primers for recombineering are listed in Table 2. Positive selection of the FKBP GalK/kanamycin cassette was carried out on kanamycin Luria broth agar plates. Selection markers were removed by inducing the SW105 Flp recombinase, leaving UL48-FKBP or UL103-FKBP with an FRT site in frame at the C-terminus. Removal of the GalK selection marker was verified by selection on galactose indicator plates. Galactose negative colonies were picked, and verified by restriction enzyme analysis, PCR, and DNA sequencing. To create UL103-FKBP-V5, the GalK/kanamycin cassette was replaced by amplifying and recombining the V5 tag. Negative selection of the GalK was performed on M63 minimal

media plates supplemented with glycerol, D-biotin, L-leucine, 2-deoxygalactose, and chloramphenicol. Loss of the GalK was verified as described above. All viruses were reconstituted by using Lipofectamine 2000 to transfect HFFs with 8-10 µg of BAC DNA, followed by propagation in the presence of 1 µM Shield-1 (Cat no. CIP-AS1, Cheminpharma, Farmington, CT), which was replaced every 48 hours to maintain its activity. Virus was collected when the monolayer showed >80% cytopathic effect. Virus stocks were grown by infecting HFFs at a multiplicity of infection of 0.01 in the presence of 2 µM Shield-1; extracellular virions were partially purified by centrifugation through a 20% sucrose cushion.

Immunoblots. HFFs were grown to confluence in T25 flasks and mock infected or infected at an MOI of 0.1. At 5 dpi, cells were washed with PBS and then lysed with RIPA buffer (0.1 M Hepes pH 7.4, 0.1% sodium deoxycholate, 150 mM NaCl, 1% NP-40, 0.1% SDS, and Roche protease inhibitor). Protein concentrations were determined by BCA assay (Pierce, Rockford, IL). Equal amounts of protein solubilized in 2X SDS Laemmli buffer with 2-mercaptoethanol were separated in 10% SDS polyacrylamide gels, transferred to nitrocellulose membranes (Whatman, Florham Park, NJ), probed with primary antibodies, and then reacted with HRP-conjugated goat anti-rabbit/mouse IgG secondary antibodies (Thermo Scientific, Rockford, IL). Reactions were detected with the Supersignal West Pico Chemiluminescent substrate (Thermo Scientific, Rockford, IL) on autoradiography film (GE Healthcare, Pittsburgh, PA). Antibodies are listed in Table 1.

Electron microscopy. Transmission electron microscopy was done by Dr. Hong Yi at the Robert P. Apkarian Integrated Electron Microscopy Core Facility of

Emory University, Atlanta, GA, using methods developed Dr. Yi in collaboration with Ahlqvist, Tandon, and Mocarski (58, 103). Briefly, HFF were infected in the presence and absence of Shield-1 with the parental (pAD/Cre) or the UL103-FKBP virus at MOI = 0.3. At 120 hpi cells were washed with fixative (2.5% glutaraldehyde in 0.1 M sodium phosphate buffer (pH 7.4)), and then incubated in fixative for 20 min at room temperature. After overnight storage in fixative at 4°C, cells were shipped submerged in the fixative. Cells were postfixed in the same buffer with 1% osmium tetroxide, dehydrated through a graded series of ethanol, and then embedded in an epoxy resin. Cell culture dishes were broken, and ultrathin sections were then cut and counterstained with uranyl acetate and lead citrate. The Hitachi H-7500 was operated at 75 kV, and images were captured using a Gatan BioScan (Pleasanton, CA) charge-coupled device camera.

Results

Screening strategy to identify viral genes required for cVAC development. Based on the requirement for viral DNA synthesis for cVAC biogenesis, and the hypothesized importance of the cVAC in virion maturation, we identified 26 HCMV genes as possible regulators of cVAC biogenesis (Table 3) and used siRNAs to individually silence them during infection. Effects on cVAC development were visualized by confocal microscopic analysis of markers that are collectively diagnostic for cVAC structure.

The synthetic siRNAs used were mixtures of 4 siRNA duplexes, each of which independently targets the transcript of interest (Dharmacon SMARTpools). Use of such pools instead of single siRNAs increases specificity by reducing the input concentration of individual siRNAs, thereby reducing off target effects. Pools also increase the likelihood of successful silencing because four regions of the target gene are targeted at once. Although antibodies are not available against most of the proteins whose expression we targeted, similarly designed siRNA pools that target HCMV proteins for which we have antibodies (IE2, MDBP, UL99, US17, and US18) delivered satisfactory results for every target tested ((110) and data not shown). Nonetheless, negative effects of individual siRNA pools should not be taken as proof that the targeted gene has no effect on cVAC biogenesis.

Screening experiments were done in 8-well glass chamber slides. Human lung fibroblast (HLF) cells were transfected with the siRNAs 6 to 8 hr prior to infection with fully infectious HCMV (AD169). As a reminder, siRNAs do not affect input protein

levels, but reduce levels of proteins expressed from genes transcribed during infection. At 120 hpi, cells were fixed and stained with the indicated antibodies.

The antibodies used in our antibody cocktails give reliable and distinct staining patterns that are collectively diagnostic for cells being infected, expression of viral late genes, and formation of the cVAC (Fig. 4A; Table 4). To validate the screening strategy, we used 100 μg/ml phosphonoacetic acid (PAA)-treated, HCMV-infected cells as a prototype of a gene silencing experiment. PAA inhibits viral DNA synthesis, consequently inhibiting cVAC biogenesis in HCMV infected cells. As shown in Fig. 4B, in the presence of PAA, markers of the secretory apparatus in infected cells resembles those in uninfected cells.

HCMV genes involved in cVAC biogenesis identified through the use of siRNAs. Over 400 confocal images were analyzed as part of the screening process. Phenotypes observed after siRNA treatment included: no effect, toxic effects, absence of HCMV late gene expression, and inhibition of cVAC formation in cells where HCMV late genes are expressed. Candidate regulators of cVAC biogenesis were defined as genes whose silencing did not affect HCMV gene expression but prevented formation of perinuclear Golgi rings surrounding concentrations of EEA1 staining, with emphasis on the EEA1 patterns.

The results from our siRNA screen of 26 HCMV genes are summarized in Table 5. Some siRNAs had no visible effects on infected cells, while others caused extensive cytopathic effects, including blobs of dead cells, small nuclei, and irregularly shaped nuclei. These diverse effects might be products of silencing viral genes that are

involved in regulating any of a variety of cellular processes, including protein secretory pathways, cellular metabolism, and anti-apoptotic activity.

The three genes whose siRNAs resulted in the most significant and specific effects on cVAC development were UL48, UL94, and UL103. In the presence of siRNAs against each of these genes, HCMV late genes were expressed, Golgi rings formed in few cells, and the early/recycling endosome machinery was dispersed, nearly absent, or otherwise disrupted (Fig. 5). An important pathognomonic change associated with HCMV infected cells is development of enlarged nuclei that take on a reniform (kidney bean) shape; these changes are important during cVAC biogenesis (93). Knockdown of all three of the candidate cVAC biogenesis regulators (UL48, UL94, and UL103) resulted in significantly lower ratios of reniform to oval nuclei compared to untreated cells and cells treated with siRNAs against several other genes targeted in our screening (Fig. 6). Some of the known properties of these candidate regulators are listed in Table 6.

Use of regulated protein destabilization to verify the siRNA screening results. To independently confirm the siRNA results, and to address specificity issues that might arise from overlapping transcripts previously described across UL48, UL94 and UL103, we employed regulated FKBP-mediated protein destabilization of the proteins of interest (Fig. 7; (108)). The FKBP moiety targets tagged proteins for rapid proteasomal degradation, and the stability of the proteins tagged with FKBP domains can be regulated by the concentration of Shield-1. Due to coding region overlaps between each of the genes of interest and their upstream neighbor, the FKBP domain was fused in place of the stop codon at the C-terminus of each protein. Recombinant

BACs were transfected into two cultures that were grown in the presence and absence of Shield-1. The UL48 recombinant (UL48-FKBP) produced many fewer and much smaller plaques in the absence of Shield-1 (data not shown), providing a preliminary indication that the FKBP domain was having the desired effect. As expected because UL103 deletion mutants are viable, the UL103 recombinants (UL103-FKBP and UL103-FKBP-V5) produced infectious virions under both conditions. We were not able to reconstitute a viable virus from a UL94-FKBP BAC.

We used immunofluorescence and immunoblots to verify our ability to regulate the stability of the proteins of interest. pUL48 was detected using an antibody against its N-terminus (kindly provided by Wade Gibson) (111). Because highly specific antibodies are not available for detection of pUL103, a 14 amino acid V5 epitope tag was added to the C-terminus of UL103-FKBP (UL103-FKBP-V5). For UL48-FKBP, addition of Shield-1 markedly increased the amount of pUL48 detected by immunofluorescence (Fig. 8A) (6.2-fold per cell based on 3D quantification of at least 8 cells for each condition). By densitometry, there was a 3.1-fold increase of pUL48 in the presence of Shield-1 (Fig. 8C). The amount of pUL48 expressed by the UL48-FKBP virus in the presence of Shield-1 is less than that produced by the parental virus. When UL103-FKBP-V5 is grown in the absence of Shield-1, the UL103-FKBP-V5 protein is very faint and dispersed when visualized by immunofluorescence, with marked increases when Shield-1 is present (3.1-fold by IFA and 4.2-fold in immunoblots) (Fig. 8B and 8D). Thus, addition of the FKBP destabilization domain to pUL48 and pUL103 enables regulation of their stability. Immunoblots showed little difference in expression of virus genes from all three lytic classes in the presence or absence of pUL48 or

pUL103 stabilization (Fig. 9), and only modest differences were seen in intracellular DNA levels by quantitative PCR (data not shown).

Having verified the intended effects of Shield-1 on viral proteins, the effect of regulated protein degradation on cVAC structure was analyzed by staining viral and cellular markers of the cVAC in the presence or absence of Shield-1 (Figs. 10 and 11). Shield-1 had no significant effect on cVAC development for the parental virus (Fig. 11). pUL48 destabilization in absence of Shield-1 led to dispersal of early/recycling endosomes, and absence of the characteristic Golgi ring, as was seen in the siRNA experiments. cVAC biogenesis appeared to be normal in most cells in which pUL48 was stabilized with Shield-1. Similar results were seen for UL103-FKBP. In an anaylsis of over 800 cells, cVAC disruption in the absence of Shield-1 was statistically significant ($p<0.0001$) (Fig. 11). Thus, in accordance with the siRNA screen, destabilization of pUL48 and pUL103 disrupted cVAC formation, verifying their importance in cVAC biogenesis.

Growth properties of recombinant viruses in the presence and absence of Shield-1. The siRNA and protein stability experiments described above were done at low multiplicity and employed cVAC morphology endpoints visible in infected cells at 4 or 5 dpi. To determine whether destabilization of pUL48 or pUL103 influences virus growth, we compared the growth of three recombinant viruses (UL48-FKBP, UL103-FKBP, and UL103-FKBP-V5) with their parent (pAD/Cre). Time courses of production of extracellular infectious virions were examined at low and high MOI (multi- and single-step growth curves, respectively). At low MOI, not all cells are infected at the time of inoculation. Thus, multiple rounds of replication can take place, enabling examination of

virus dissemination in terms of production of secondary plaques, features such as plaque size, and dependence on conditions created when cells are not exposed to large numbers of viral particles, many of which are not independently infectious (e.g., HCMV dense bodies and non-infectious enveloped particles). At high MOI, essentially every cell in the culture is infected simultaneously, and cells are also exposed to large numbers of bioactive non-infectious particles. Such synchronized infections provide information about how much infectious virus is produced during a single round of replication.

For UL48-FKBP, the single- and multi-step growth infections were done in the presence or absence of Shield-1 (Fig. 12A). Progeny extracellular virions were titered in triplicate in the presence of the drug. Somewhat unexpectedly, the single-step growth curves for UL48-FKBP showed one-log growth defects starting at 3 dpi, regardless of whether Shield-1 was present or absent; the defect persisted over the 6 day experiment. Likewise, in the multi-step analysis, UL48-FKBP growth was similar in the presence and absence of Shield-1; mutant infectious progeny were first detected at 6 dpi, and infectious yields lagged by ~3 logs until 15 dpi, when they were about 1 log lower than for the parental virus. Inefficient growth of the UL48-FKBP virus might be attributable in part to the lower overall level of pUL48 expressed in the presence or absence of Shield-1 (Fig. 8C).

The UL103-recombinant virus stocks were also grown with Shield-1. In single- and multi-step analyses, the presence of Shield-1 had little effect on the yield of extracellular infectious virus (Fig. 12B). Titers were similar when measured in the presence or absence of Shield-1 (data not shown), the only difference being plaque

sizes (see below). In the single-step experiment in the absence of Shield-1, the UL103-FKBP recombinant virus produced infectious extracellular virus at rates similar to its parent at most time points, with a <10- fold difference at 3 dpi. In contrast, Ahlqvist and Mocarski found up to a 50-fold decrease in extracellular infectious titer with a Towne-BAC mutant that does not express pUL103 (15). These results suggest that at high multiplicities of infection, there is some compensation for the absence of pUL103 by a complementary function likely provided by another viral protein. In multi-step experiments, the UL103-FKBP and UL103-FKBP-V5 viruses lagged in extracellular virus production by 2 to 3 logs at 3 and 6 dpi, ultimately reaching parental titers 9 to 15 dpi. In marked contrast, a pUL103-null virus produced ~3000-fold less extracellular infectious titer (15). This indicates that even small amounts of pUL103 expressed by the UL103-FKBP virus are sufficient to support near parental growth. The latter point is supported by our observations that (i) at low multiplicities, the small amount of pUL103 produced by our FKBP-tagged viruses is sufficient to rescue about two logs of the early (3 to 6 dpi) growth defect seen in the absence of pUL103, with the growth defect being overcome 9 to 15 dpi, and (ii) growth of these viruses at moi = 0.1 was similar to that in the single-step analysis (data not shown); the growth defect was only seen at low moi.

In other growth experiments with FKBP-tagged UL48 and UL103 viruses, we saw little effect of Shield-1 over concentrations ranging from 0 to 4 μM/ml (data not shown). These results suggest that although the FKBP domain enables regulated stability of pUL48 and pUL103, as well as regulation of their activity in cVAC biogenesis, for both proteins the FKBP tag inhibits some aspect of production or egress of infectious virions. As mentioned, for pUL103, this effect was largely overcome by 9 to 15 dpi.

Ahlqvist and Mocarski found that viruses deficient in expression of pUL103 produce significantly smaller plaques (58). Consistent with this, we found that Shield-1 could rescue the small plaque phenotype of the UL103-FKBP virus (Fig. 13). Thus, in addition to its roles in cVAC biogenesis and virion maturation or egress, pUL103 has a role in cell-to-cell spread of infection. In contrast, the UL48 recombinant virus produced small plaques in the presence and absence of Shield-1 (data not shown).

In ultrastructural analyses, in the absence of Shield-1, cytoplasmic UL103-FKBP virions were more likely to have aberrant appearances, including frequent appearance of virions that appeared to be arrested or greatly slowed down in the midst of acquiring their envelope (Fig. 14).

Discussion

Little is known of the effectors of HCMV cVAC biogenesis, a biological process that is distinct from cVAC operation. Structures architecturally similar to the cVAC (Golgi rings surrounding a cluster of early/recycling endosomes, and spatial segregation of the early/recycling and late endosomal systems) have been identified in uninfected cells (112-114). cVAC biogenesis may thus be a product of the virus activating, and possibly modifying, a previously programmed biological process. Like other biological pathways regulated by HCMV (e.g., immune responses, apoptosis, and the AKT/PI3K/mTOR pathway) (115, 116), we anticipate multiple points of control of the process by the virus, including the recently described role of HCMV microRNAs in cVAC biogenesis (105). In addition to the virologic lessons, elucidation of this pathway and its points of control will be informative with respect to important areas of cell biology.

Using siRNAs, we screened HCMV early/late and late genes known to be important for efficient lytic replication for their activity in cVAC biogenesis. Of the 26 genes tested, only inhibition of expression of UL48, UL94, and UL103 specifically prevented cVAC biogenesis: Golgi rings did not form and the early/recycling endosome complex was disrupted, in the context of infections that had proceeded to at least late gene expression.

The genes for all three candidate cVAC regulators have coding regions that overlap with coding regions of their neighboring genes, and polycistronic transcripts span each gene locus (Fig. 7). To address the possibility that the siRNA effects were due to silencing of overlapping transcripts, we tagged each candidate protein with a regulatable post-translational destabilization domain. Although we were not able to reconstitute a viable virus from a BAC containing a tagged version of UL94, viable

recombinants were reconstituted for UL48 and UL103, and we demonstrated regulated stability of the proteins of interest. HCMV IE, early, and late genes were expressed at near-parental levels regardless of pUL48 or pUL103 degradation. When pUL48 or pUL103 were destabilized, cVAC biogenesis was impaired, in a manner similar to what was seen following siRNA treatment, thus confirming the siRNA result and verifying its specificity for these genes.

Our siRNA results are consistent with prior reports that HCMV UL94 and UL103 are important for late stages of HCMV virion assembly and egress (55, 58). From the UL103-FKBP virus we learned that the pUL103 domain necessary for cVAC biogenesis is distinct from at least two other functional domains. Specifically, defects in plaque size (Fig. 13) and secondary envelopment (Fig. 14) were able to be rescued by Shield-1, and the C-terminal FKBP tag appears to alter production of extracellular infectious virus in a manner that is impervious to, and possibly worsened by stabilization of the tagged protein with Shield-1 (Fig. 12B). We also provide new evidence that HCMV pUL48 is important for production of infectious extracellular virus, perhaps analogous to the role of its herpes simplex virus 1 homolog in production of non-infectious light bodies (117). Similar to the behavior of the UL103-FKBP virus, this defect in the UL48-FKBP virus was not rescued by Shield-1, in contrast to the cVAC biogenesis activity. More detailed studies of the roles of these proteins in cVAC biogenesis will require generation of reagents that do not include tags that interfere with functions of the proteins of interest.

The three HCMV proteins whose silencing prevented cVAC formation are virion tegument proteins that are conserved across the *Herpesviridae* (Table 6). It has been suggested that HCMV UL103 and its orthologs in other herpesviruses play related roles

in the final stages of virion assembly (58). While structures analogous to the HCMV cVAC have not been identified for other herpesviruses, is possible that these conserved proteins are all involved in remodeling infected cells into virus production factories.

It is clear that multiple viral and cellular gene products play important roles in cVAC biogenesis. We hypothesize that collective interactions of these factors, with each other and with other viral and cellular proteins, establish an environment conducive to cVAC development. The viral proteins identified here as regulators of cVAC biogenesis will be useful probes for identifying and understanding the network of viral and cellular genes involved in cVAC biogenesis and virion maturation, a necessary prelude to developing novel antivirals that block the process.

TABLE 1. Antibodies used in IFA and immunoblot assays

Antibody target	Host/isotype, clone	Source, catalog no.
Epitope tag		
V5 (14 amino acids)	Mouse monoclonal/IgG2aκ	LifeTechnologies, R960-25
Cellular		
GAPDH (36 kDa)	Mouse monoclonal/IgG1, clone GA1R	ThermoScientific, MA5-15738
GM130 (130 kDa)	Mouse monoclonal/IgG1(κ),clone 35/GM130	BD Biosciences, 610822
EEA1 (180 kDa)	Rabbit polyclonal	Abcam, ab2900
HCMV		
IE1 and IE2 (IE1, 72kDa; IE2, 86kDa)	Mouse monoclonal/ IgG_1(k), clone CH160	Virusys, P1215
IE2 (86kDa)	Mouse monoclonal, clone 8B1.2	Chemicon (Millipore), MAB810
pUL44 (CMV ICP36), 46 kDa	Mouse monoclonal/ IgG1(k), clone 10D8	Virusys, CA006-100
UL48 (N-terminal region)	Rabbit polyclonal	Wade Gibson (Johns Hopkins University) (118)
pUL99 (pp28)	Mouse monoclonal/IgG2A(k), 5C3	Virusys, CA004-100
gB (55 kDa and 110 kDa)	Mouse monoclonal/ IgG1(k), clone 2F12	Virusys, CA005-100

TABLE 2. Primers used for generating recombinant viruses

Virus	Primer sequence*	Amplification target
UL48-FKBP	5'-CGCAATCCGTACAGGACACTATTCAACACATGCGGTTTCTCTATCTTTTGatgggagtgcaggtggaaaccatc-3'	FKBP-GalK/Kan tag
	5'-ACGATAAAAATCCTATTGTTTTTATTACCCGCTACTGTCAGTGTCGGTTAgctggagctccaccgcgggaagttc-3'	
UL103-FKBP	5'-GTTGCGTGTTTTTTTTTTTTCTATGATATGCGTGTCTAGTTCGCTTCTCAgctggagctccaccgcgggaagttc-3'	FKBP-GalK/Kan tag
	5'-TGCCCTCACCCCCCAAGCTGCCGCCGCGCTGGGAACGAGGAGAGGAAGAGatgggagtgcaggtggaaaccatc-3′	
UL103-FKBP-V5	5' -GTTGCGTGTTTTTTTTTTTTCTATGATATGCGTGTCTAGTTCGCTTCTCAcgtagaatcgagaccgagga- 3'	V5 tag
	5' -CACATGCCACTCTCGTCTTCGATGTGGAGCTTCTAAAACCGGAAGAATTCggtaagcctatccctaaccc- 3'	

*The uppercase sequences correspond to the 50-bp segments of viral DNA needed for recombination into the viral genome. The lowercase sequences are regions needed to enable amplification of exogenous sequences (e.g., the V5 epitope) intended to be inserted into the BAC

TABLE 3. Targets for siRNA screening: HCMV Early-Late and Late genes essential or important for viral growth

Function	Gene(s)
Tegument	R: UL97*
	E: UL32, UL48, UL82, UL94, UL99
Glycoproteins	E: UL55, UL73, UL75, UL100, UL115
Unknown	R: UL21, UL29, UL30, UL69, UL103, UL117
	E: UL34, UL49, UL71*, UL76*, UL91, UL92, UL93, UL95, UL96

R = reduced; viral growth reduced by at least 50-fold
E = essential; no viral replication its absence
Replication data are from (84) and (85), kinetic class assignments are from (83).
*Kinetic class not assigned in (83).

TABLE 4. Targets and purposes of antibody cocktails used in screening assays

	Antibodies[a]						
	Mouse Monoclonals				Rabbit Polyclonals		
Cocktail	IE2	pUL99	EEA1	GM130	MannII	US18	Purpose[b]
A	+				+		confirms infection and Golgi ring formation
B		+			+		confirms Golgi ring formation, and late gene expression and localization
C			+		+		confirms Golgi ring formation and EEA1 relocalization
D				+	+		confirms Golgi ring formation
E	+					+	confirms infection, and late gene expression and localization
F		+				+	confirms late gene expression
G			+			+	confirms EEA1 relocalization, and late gene expression and localization
H				+		+	confirms Golgi ring formation, and late gene expression and localization

[a]+, present in cocktail
[b]IE2, pUL99 and US18 detect different stages of infection, GM130 and Mann II stain Golgi rings, and EEA1 localizes at the center of cVAC.

TABLE 5. HCMV genes screened by siRNA: properties and silencing results

		siRNA results			
Gene	Gene properties[a]	Unusual cytopathic effects[b]	Late gene expression	Effect on Golgi and EEA1 markers	Candidate cVAC regulator[c]
UL21A	Enhances replication	Yes	No change in expression of pUS18/gB	Small effect on Golgi markers, but not on EEA1	
UL29	Unknown	Yes (Many nuclei are very small, blob of dead cells and empty patches)	No change in the expression of pUS18 and pUL99	None	
UL30	Unknown; alters PML morphology	Yes (Blob of dead cells and empty patches)	No change in expression of pUS18/gB	Small effect on Golgi markers, but not on EEA1	
UL32	Major tegument protein, binds to capsid	Yes (Blob of dead cells and altered nuclear form)	Reduced (Altered distribution of pUL99 [mainly cytoplasmic])	None	
UL34	Represses US3 transcription; shuttles between nucleus and cytoplasm	Yes	Altered distributions of pUL18 and pUL99	Golgi markers did not form good rings, but EEA1 was still in tight perinuclear cluster.	
UL48	Large tegument protein; ubiquitin-specific protease (N-terminal region); involved in capsid transport	Yes	Higher proportion of pUS18 in non-cVAC cytoplasm; expression of pUL99 reduced	Fuzzy and diffuse EEA1; altered localization of Golgi markers, and absence of Golgi rings; few conventional cVACs	Yes
UL49	Unknown	Yes (Many small nuclei)	No change in expression of pUS18, but gB was more diffuse	Small effect on Golgi markers, but not on EEA1	
UL55 (gB)	Virion envelope glycoprotein, gB; involved in heparan sulfate mediated virion entry, and cell-to-cell spread	Yes	Altered distribution of pUS18, and reduced gB expression	Small effect on Golgi markers, but none on EEA1	
UL69	Tegument protein; multifunctional regulator; shuttles between nucleus and cytoplasm; inhibits pre-mRNA splicing; exports virus mRNA from nucleus	Yes (Empty patches, irregular forms of nucleus and sometimes stretched)	Higher expression of pUS18 in non-cVAC cytoplasm;altered expression pattern of pUL99	None	
UL71	Tegument protein; involved in virion morphogenesis	Yes (Blobs of dead cells)	Reduced; Altered distribution of pUL99	None	
UL73 (gN)	Virion envelope glycoprotein, gN, complexed with envelope gM; supports virion morphogenesis	Yes (Many small nuclei)	Expression of pUS18 reduced;altered distribution pattern of pUL99	None	
UL75 (gH)	Virion envelope protein, gH; complexed with envelope gL; involved in cell entry, and cell-to-cell spread	Yes (Many small nuclei)	Expression of pUS18 reduced;altered distribution pattern of pUL99, mostly cytoplasmic	Reduced expression of Golgi markers and EEA1 but no changes in their arrangement	
UL76	Virion protein; affects translation of UL77	Yes	Small altered expression of pUS18 and pUL99	Altered distribution of Golgi markers but not EEA1	
UL82	Tegument phosphoprotein pp71; upper matrix protein; involved in gene regulation	Yes (Many small nuclei)	No change in expression of US18, but reduced gB expression	Altered and reduced expression of Golgi markers, but not on EEA1	
UL91	Unknown	Yes (Many small nuclei)	No change in expression of pUS18 and pUL99	Altered distribution of Golgi markers but not EEA1	
UL92	Unknown; members of this family found in several herpesviruses, including EBV BDLF4, HCMV UL92, HHV8 ORF31 and HSV6 U63	Yes (Many nuclei are very small, blob of dead cells and empty patches)	Slightly altered expression of US18 and pUL99	None	

UL93	Capsid-associated; involved in DNA encapsidation and capsid transport	Yes (Blob of dead cells and empty patches)	Slight altered expression of pUS18, but not in pUL99	None	
UL94	Tegument protein; involved in virion secondary envelopment	Yes	No effect on pUL99 or pUS18 expression levels.	Greatly reduced EEA1 expression; partial effect on Golgi markers, forming small Golgi ring	Yes
UL95	Late gene activator; found in several herpesviruses, include EBV BGLF3 and other UL95 proteins (e.g., HCMV UL95, HSV-1 UL34, and HHV6 U67)	Yes (Blob of dead cells and empty patches)	Slightly altered expression of pUS18, but not pUL99	Altered distribution of Golgi markers but not EEA1	
UL96	Tegument protein; stabilization of nucleocapsids during nucleo-cytoplasmic translocation; possibly involved in virion morphogenesis	Yes (Many blob of dead cells)	Altered distribution; increased expression of pUL99	None	
UL97	Tegument protein; virion serine/threonine protein kinase	Yes	Reduced	None	
UL99	Myristylated tegument protein; involved in virion morphogenesis	Yes	Reduced	None	
UL100 (gM)	Virion envelope glycoprotein, gM; 8 transmembrane domains; complexed with envelope gN; involved in virion morphogenesis	Yes (Blob of dead cells withnuclear debris, patches of empty spaces and many small nuclei)	Slightly altered distribution of pUS18 and pUL99	Altered expression of Golgi markers, but not of EEA1	
UL103	Tegument protein; involved in virion and dense body egress; DNA encapsidation	Yes (Big empty patches)	US18 looks normal, but altered distribution of UL99	Golgi markers and EEA1 are greatly reduced; Altered distribution of Golgi markers	Yes
UL115	Virion glycoprotein gL; complexed with envelope gH; involved in cell entry andcell-to-cell spread	Yes (Blobs of dead cells)	Less abundant (late virion proteins/cVAC markers)	Reduced EEA1 expression; little effect on Golgi markers; Golgi rings with EEA1 center still present	
UL117	Enhances replication compartment formation; impairs cellular DNA synthesis	Yes (Many are very small and bright blue blobs [apoptotic debris?])	Expression of pUS18 altered fuzzier cVAC association; altered distribution pattern of pUL99 in some cell	Little effect on Golgi markers or EEA1	

[a] Gene function information is reviewed in (119).

[b] In most instances, unusual cytopathic effects consisted of numerous blobs of dead cells and altered nuclear forms (smaller, elongated, or irregular shapes).

[c] Candidate cVAC regulators are the genes we selected for further study; this does not preclude other genes being important in the process.

TABLE 6. Properties of candidate regulators of HCMV cVAC biogenesis[a]

HCMV gene	Homologs			Functions and properties of HCMV homolog	Interacting viral partners (HCMV only)
	HSV	γHV	HHV6		
UL48	UL36	ORF64	U31	Essential Largest tegument protein Has deubiquitinating enzyme activity Role in intracellular capsid transport	pUL45, pUL47, pUL50, pUL69, pUL88, pUL103, and pUL132
UL94	UL16	ORF33	U65	Essential Tegument protein Binds single-stranded DNA Cytoplasmic egress	pUS22, pUL72, pUL82, and pUL99
UL103	UL7	ORF42	U75	Elimination of pUL103 expression reduces virus replication by 10^2 to $>10^4$-fold, and results in reduced plaque size. May have a role in viral replication Tegument protein Associated with the cVAC Virus particle and dense body egress	pUL22A, pUL48N, and pUL103

[a]Information in this table is from the following references: (55, 58, 67, 84, 85, 120-123)

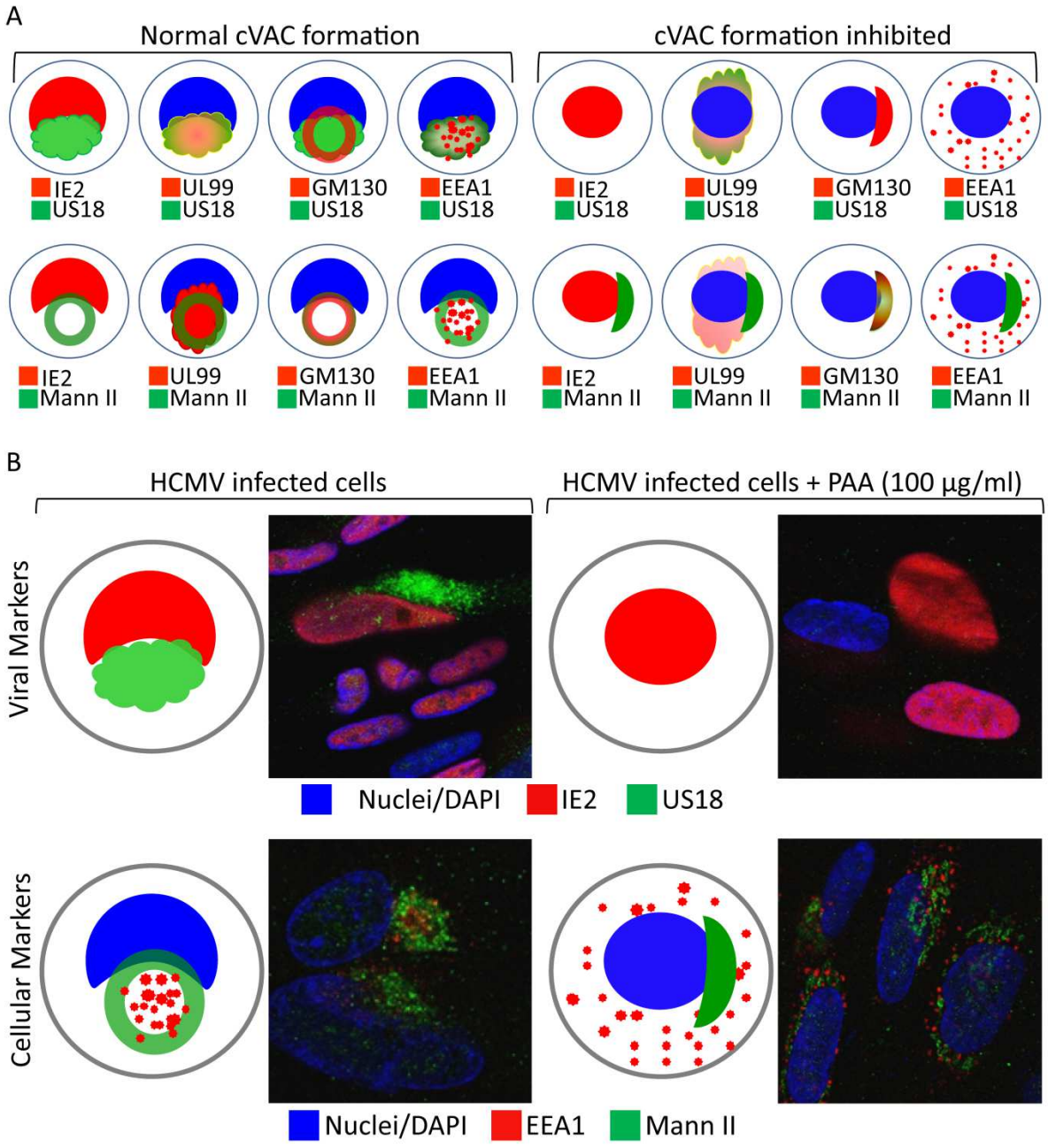

Figure 4. **Validation of siRNA screening system.** (A) Diagrammatic representation of cVAC staining pattern in the HCMV infected human lung fibroblasts, and the predicted outcomes following silencing of cVAC biogenesis regulators**.** The illustrated patterns are representations of previously published data (47, 96, 98). (B) Inhibition of cVAC biogenesis by PAA (Cat. no. P6909, Sigma-Aldrich, St. Louis, MO) treatment in HCMV infected fibroblasts; confocal images are shown alongside the predicted patterns.

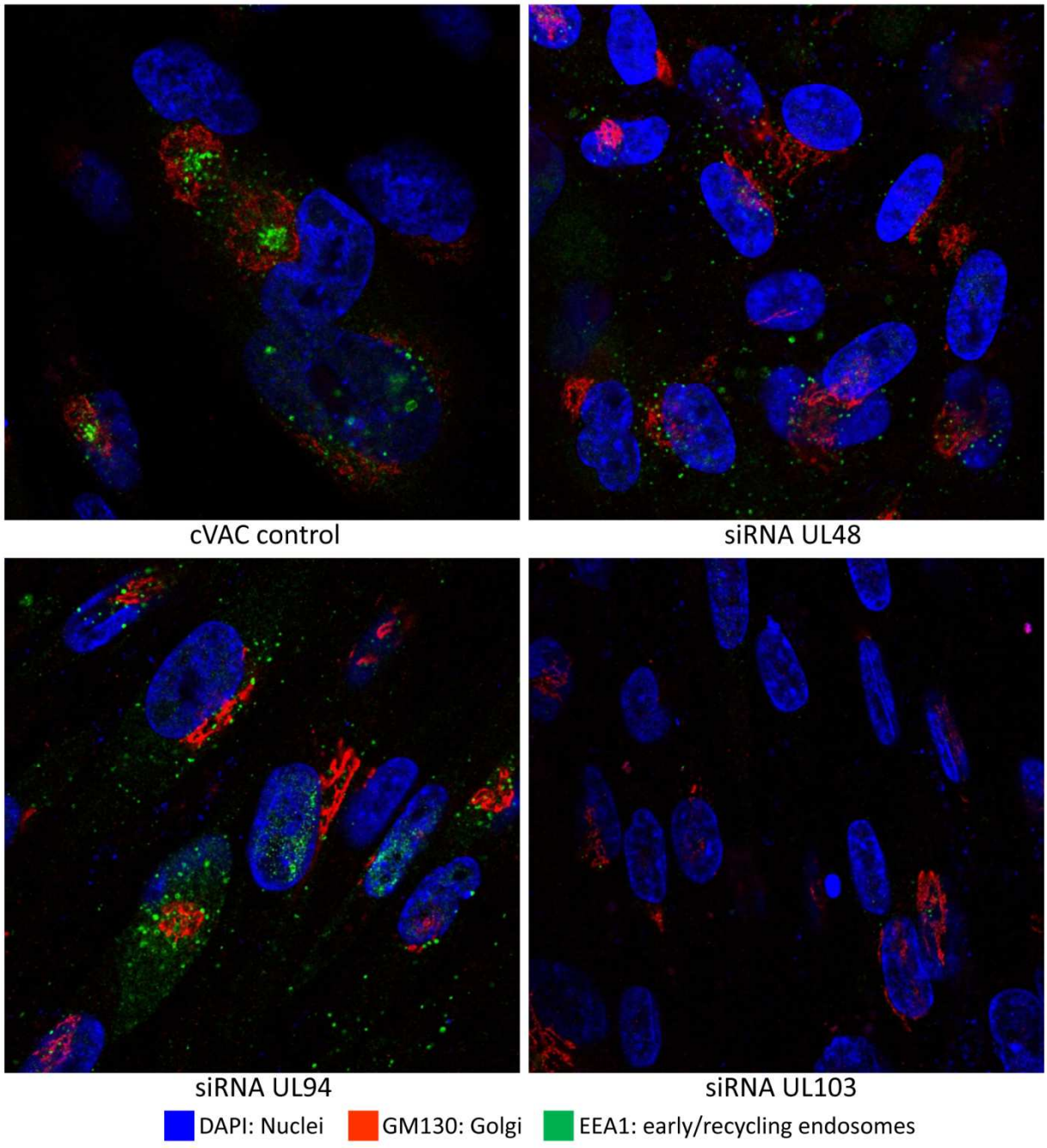

Figure 5. **siRNA-based identification of UL48, UL94, and UL103 as candidate regulators of cVAC biogenesis.** Cells were treated with siRNA pools designed to target the indicated HCMV genes, stained with antibodies against the indicated cellular markers and then examined by confocal microscopy. A subset of the results obtained using the full panel of markers illustrated in FIG. 3 is shown here. The staining patterns for the full set of markers were consistent with UL48, UL94, and UL103 playing important roles in cVAC biogenesis.

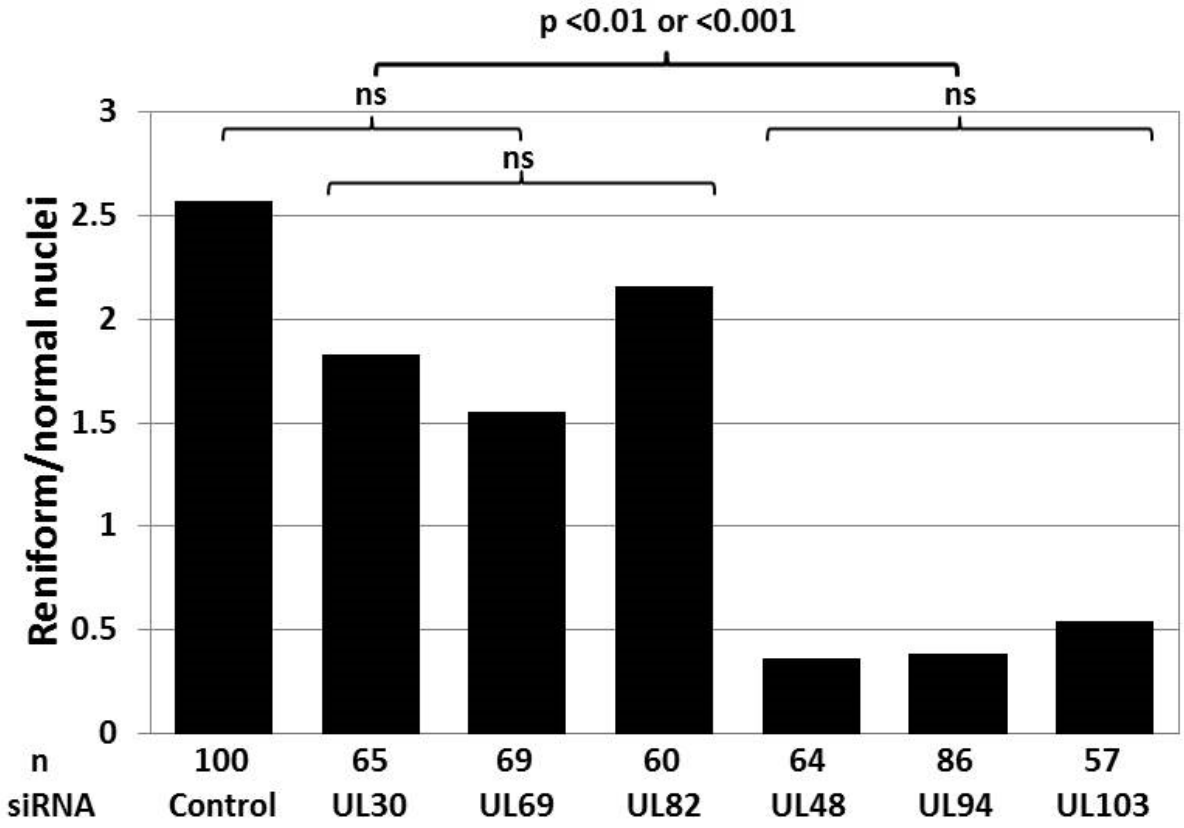

Figure 6. **Ratios of reniform and oval nuclei in HCMV infected cells after gene silencing.** HCMV infected cells with reniform or oval shaped nuclei were counted in cells with or without silencing of the indicated genes. The significance of the differences were evaluated using the Chi Square test. n, number of cells examined for each condition; p, level of significance.

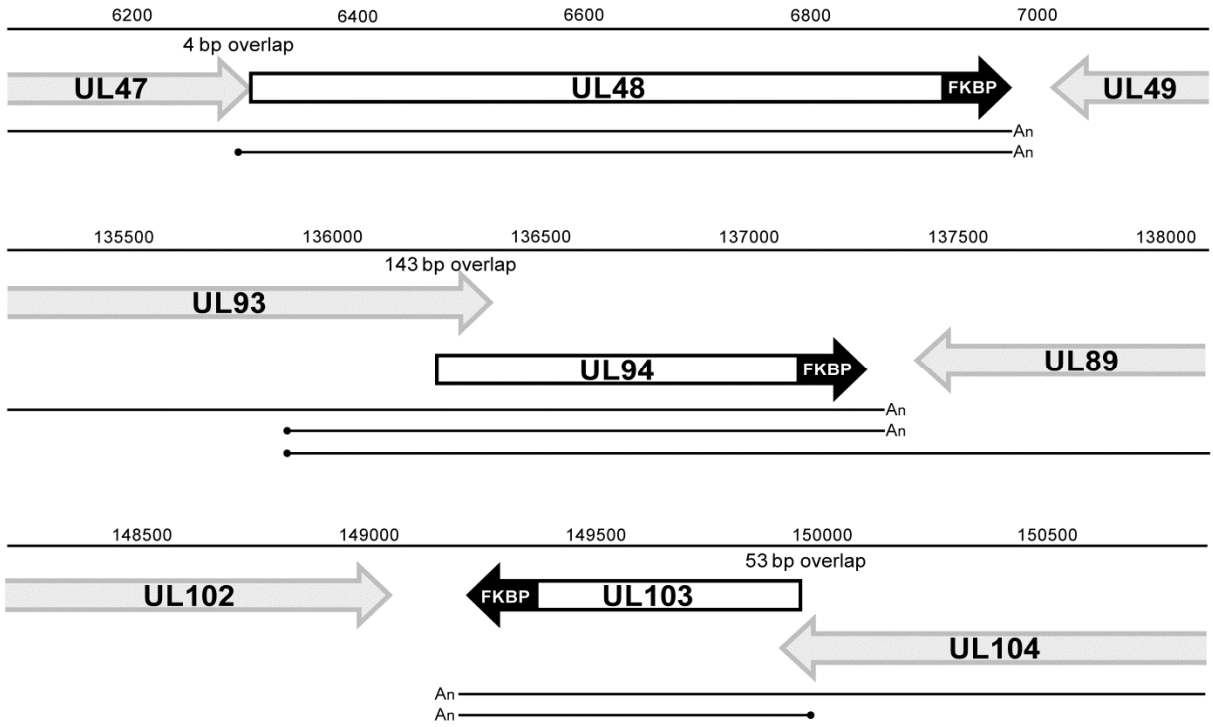

Figure 7. **Gene arrangements and transcripts in the vicinity of the candidate regulators of cVAC biogenesis.** 5' ends of mRNAs are indicated with balls, and 3' polyadenylated regions with "An". Genetic recombineering methods described in Materials and Methods were used to introduce the FKBP degradation domain into our genes of interest. All three genes overlap with neighboring genes at their 5' end. To avoid effects on overlapping coding regions at the N-termini of the three genes, the FKBP destabilization domain was added at the C-terminus of each gene. UL48 maps: (124); UL94 maps: (125-127); PRV UL7 (HCMV UL103 homolog) map: (124) and HCMV UL103 (22).

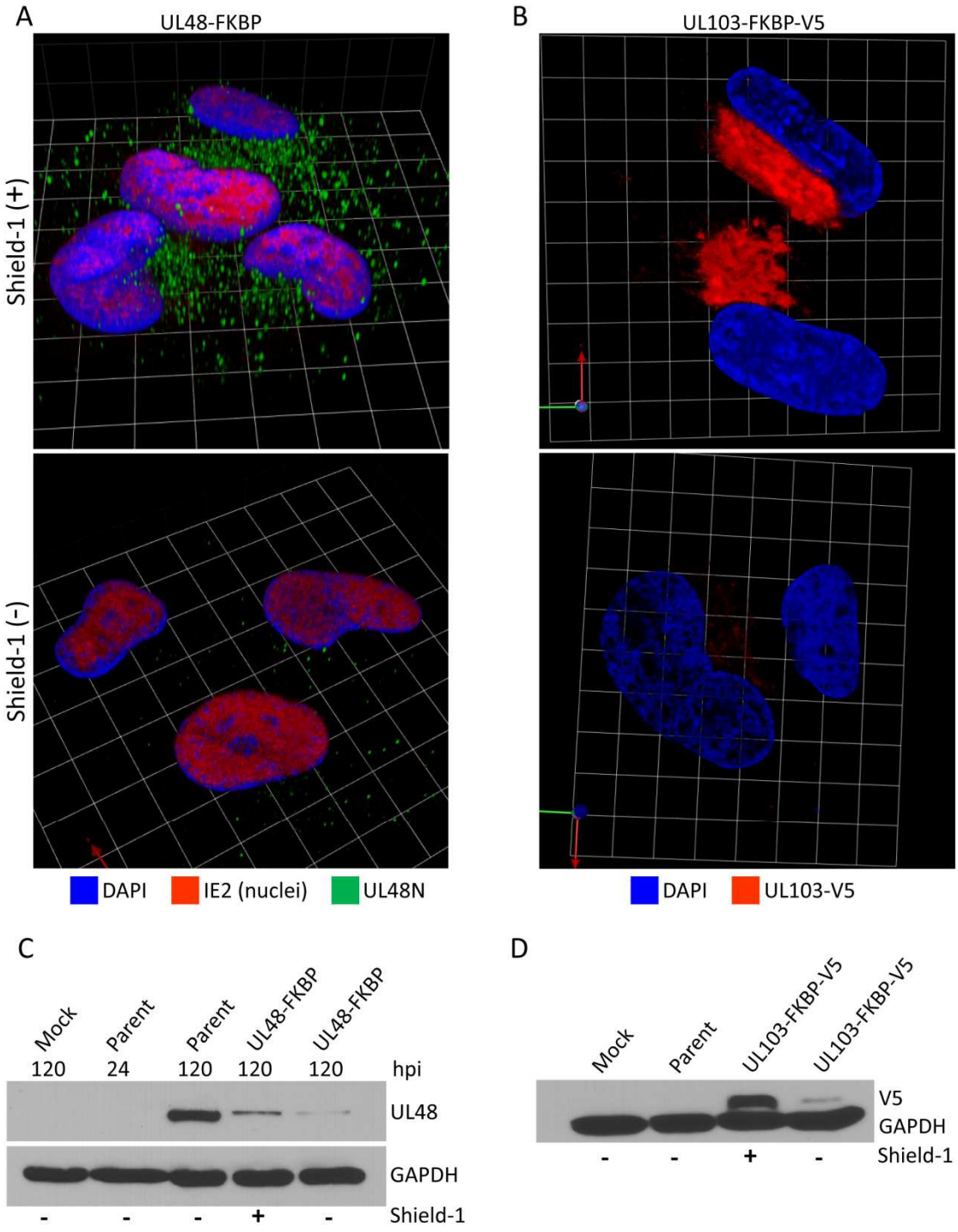

Figure 8. **Verification of regulated protein degradation.** The UL48-FKBP and UL103-FKBP-V5 tagged proteins were analyzed by (A and B) confocal immunofluorescence microscopy, and (C and D) immunoblots in the presence and absence of Shield-1. HFFs were infected for 120h at a MOI of 0.1. pUL48 was detected using an antibody against its N-terminus (C), and pUL103 was detected using an anti-V5 antibody (D).

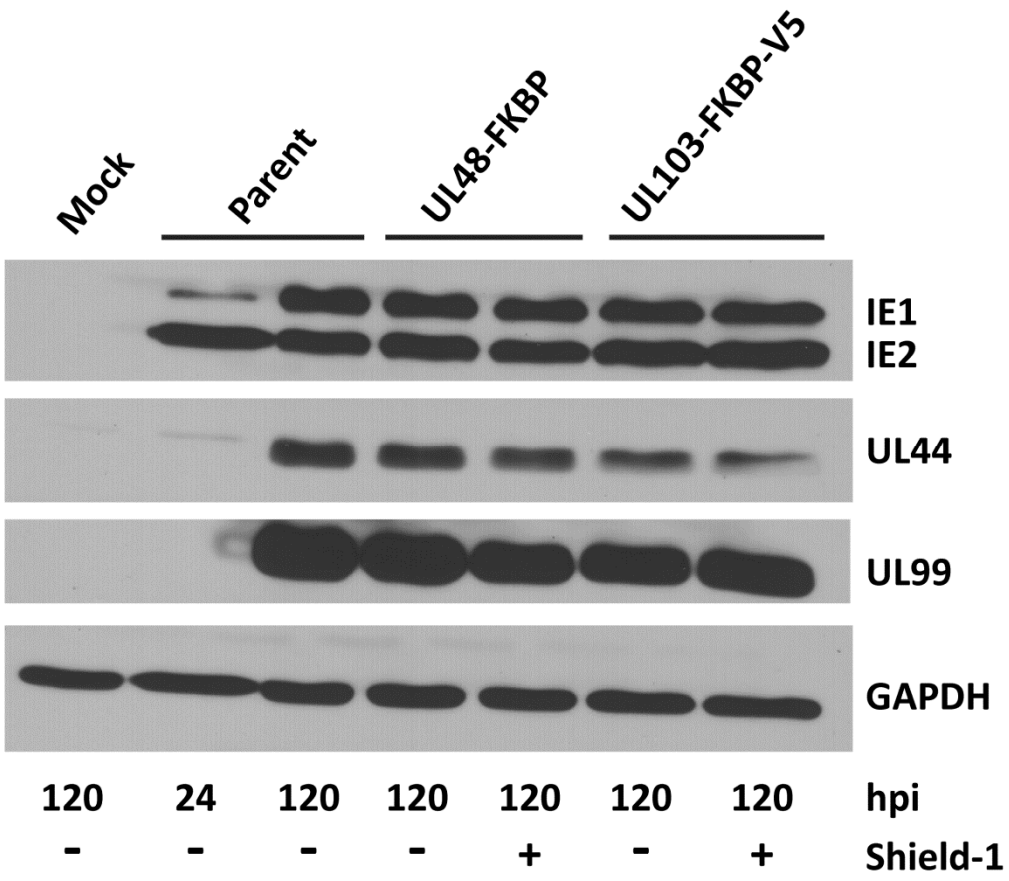

Figure 9. **Effect of protein destabilization on other HCMV proteins.** Cells were infected (MOI = 0.1) with UL48-FKBP and UL103-FKBP in the presence and absence of Shield-1 and then analyzed by immunoblots at 24 and 120 hpi, using antibodies against representative immediate early (IE1 and IE2), early (UL44), and late (pp28/UL99) viral proteins. GAPDH was used as a loading control.

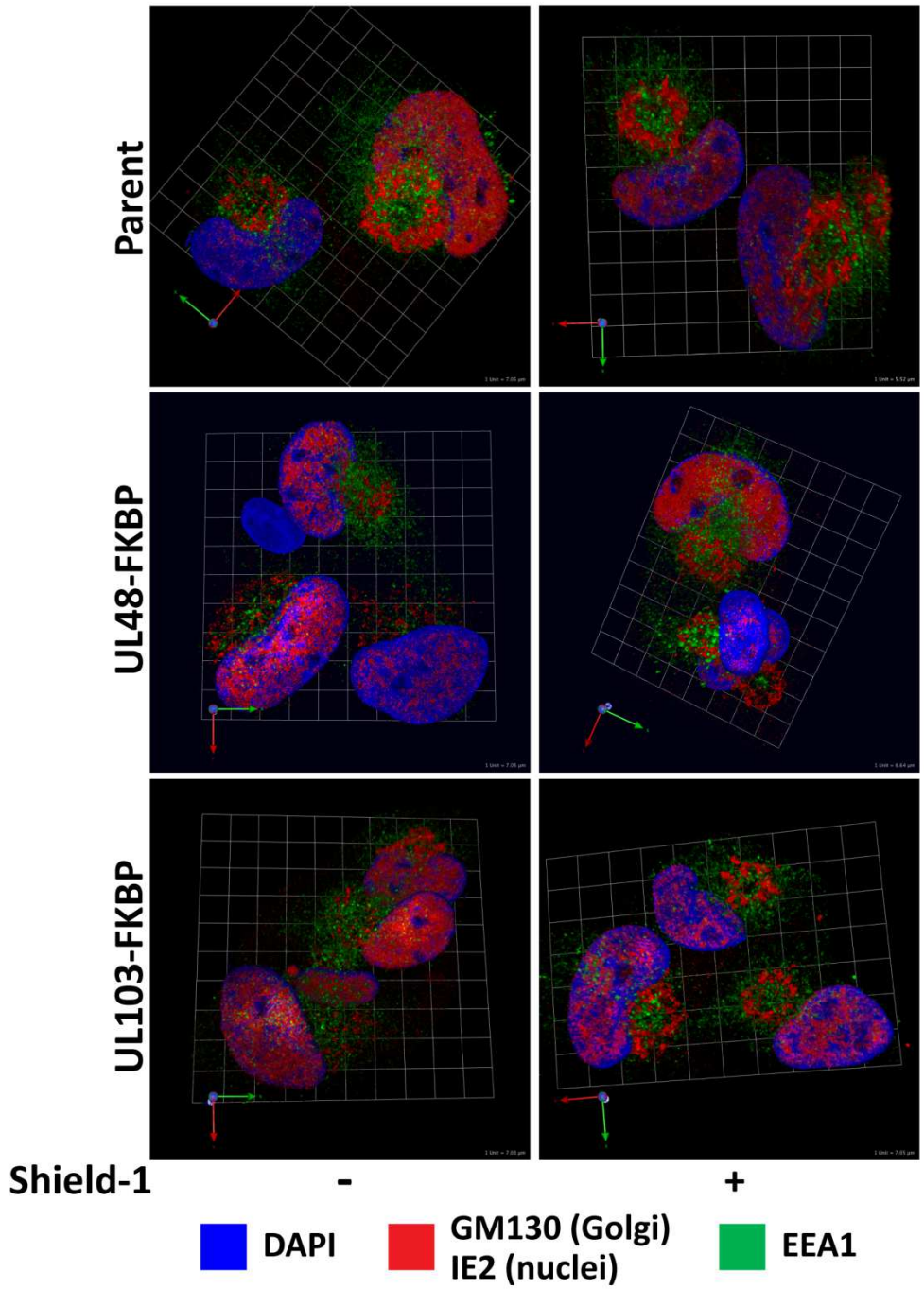

Figure 10. **Effects of regulated protein degradation on cVAC biogenesis.** Cells were infected with the indicated viruses in the presence or absence of Shield-1 for 120 hr and then stained for cellular markers of the cVAC (cytoplasmic staining) and infection (IE2, nuclear staining). Shield-1 had no effect on assembly complex development for the parental virus, whereas destabilization of pUL48 and pUL103 led to dispersal of early/recycling endosomes, and absence of the characteristic Golgi ring.

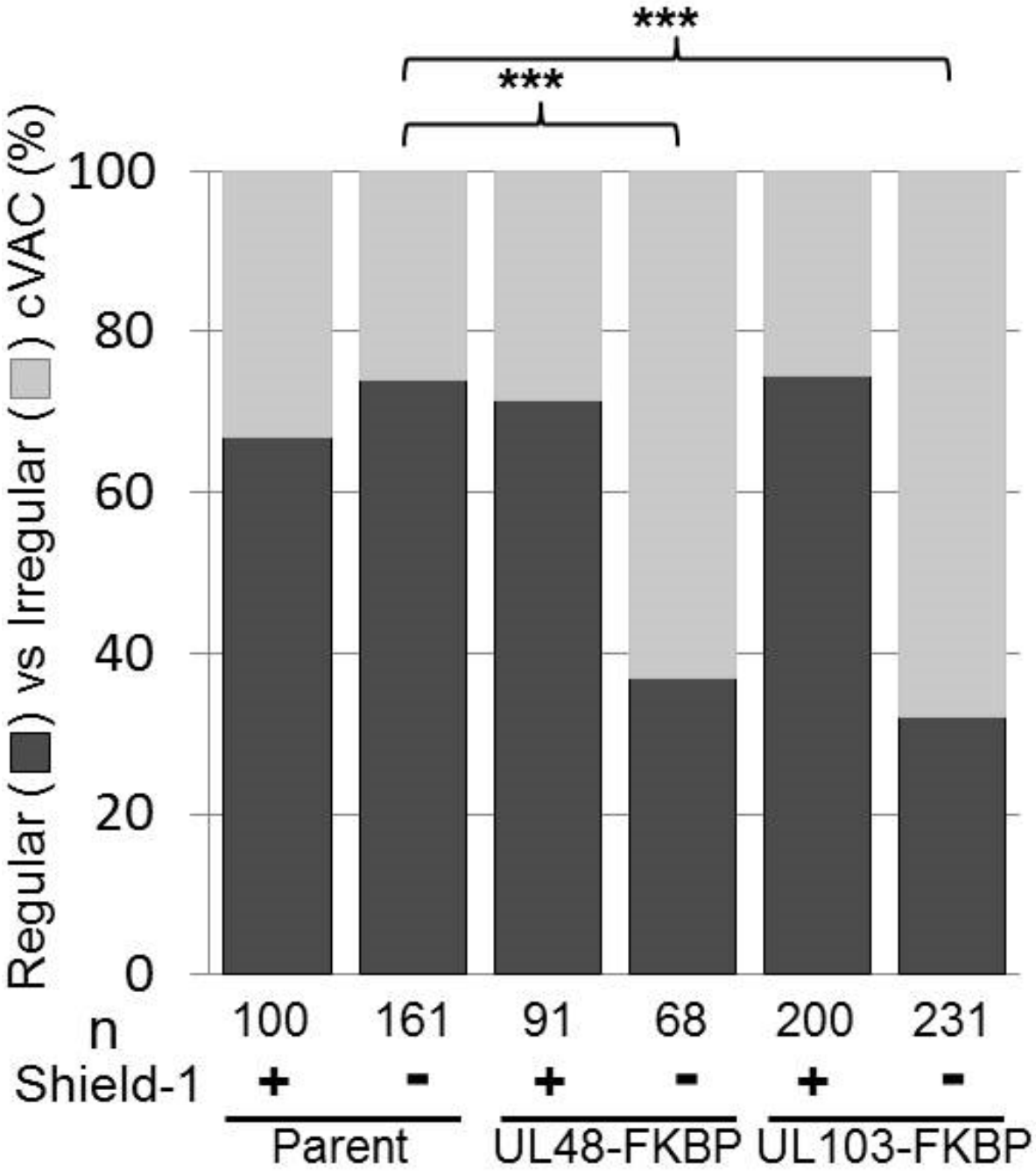

Figure 11. **Relative abundance of regular vs irregular cVAC structures in the presence and absence of Shield-1.** Regular structures displayed circular Golgi rings and a concentration of EEA1-positive vesicles inside the rings. Irregular structures had fragmented or abnormal Golgi shapes, and/or dispersal of EEA1-positive vesicles. Statistical significance was measured using the Chi Square test (***, $p<0.0001$). n, number of cells counted.

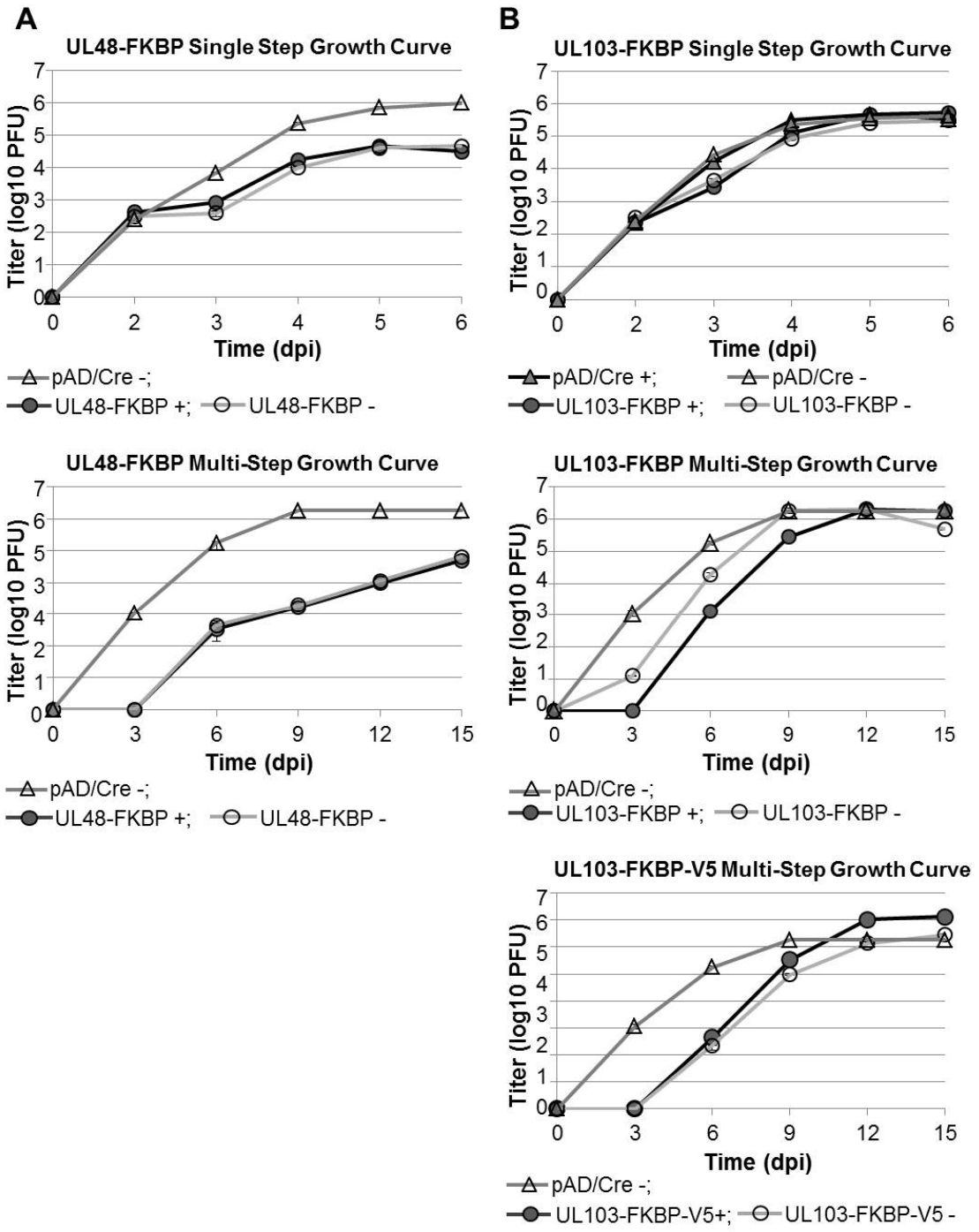

Figure 12. **Growth properties of recombinant extracellular viruses in the presence and absence of Shield-1.** (A) Replication of UL48-FKBP. (B) Replication of UL103-FKBP and UL103-FKBP-V5. Virus replication at high (MOI = 3) and low (MOI = 0.01) MOI (single step and multi-step growth curves, respectively) in presence or absence of Shield-1. +, cells infected in the presence of Shield-1; -, cells infected in the absence of Shield-1. Virus titers were determined in triplicate; the standard errors are too small to be seen in the graphs.

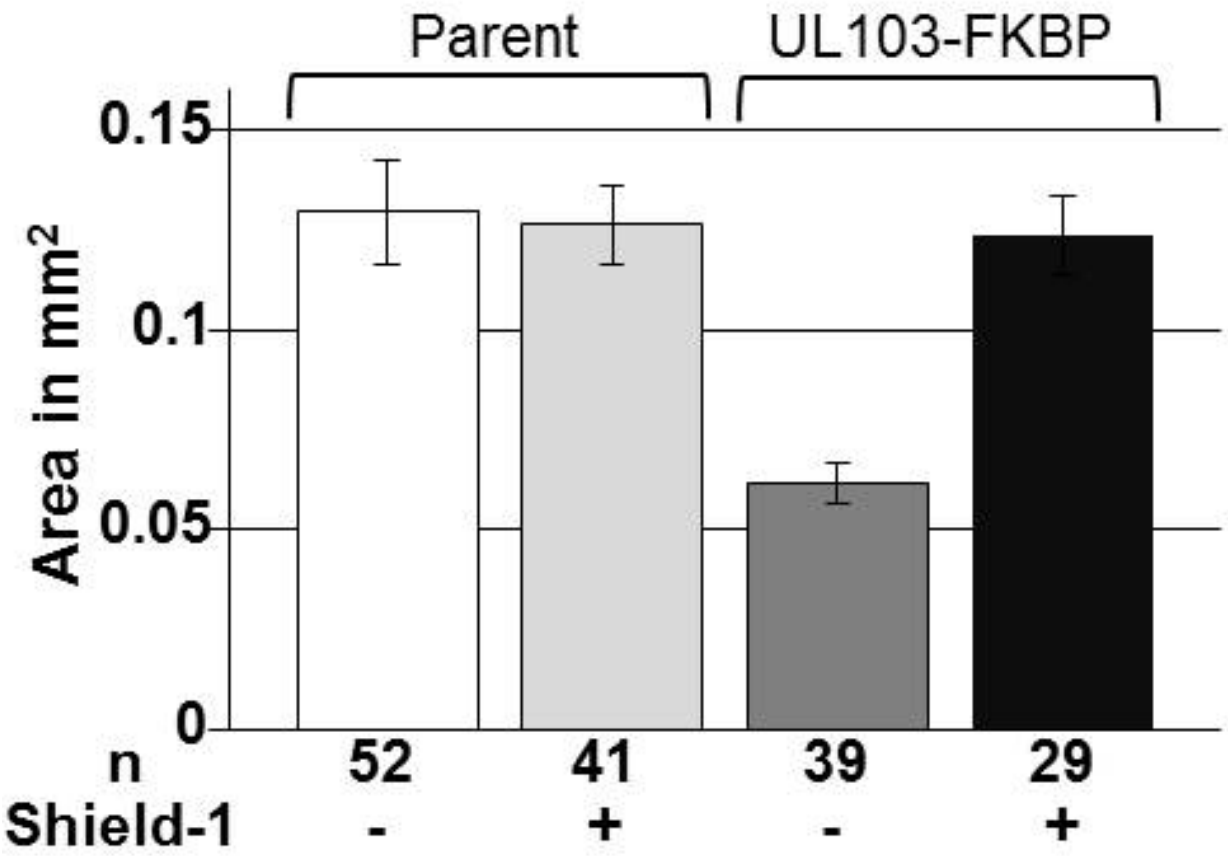

Figure 13. **Plaque sizes of UL103 recombinant viruses in the presence and absence of Shield-1 at 10 dpi.** Plaque size (area) = mm^2 +/- SEM, as measured from photographs by using ImageJ (NIH) (128). In the absence of Shield-1, UL103-FKBP plaque sizes were significantly smaller than for the other three conditions (*t* test, $p < 10^{-5}$).

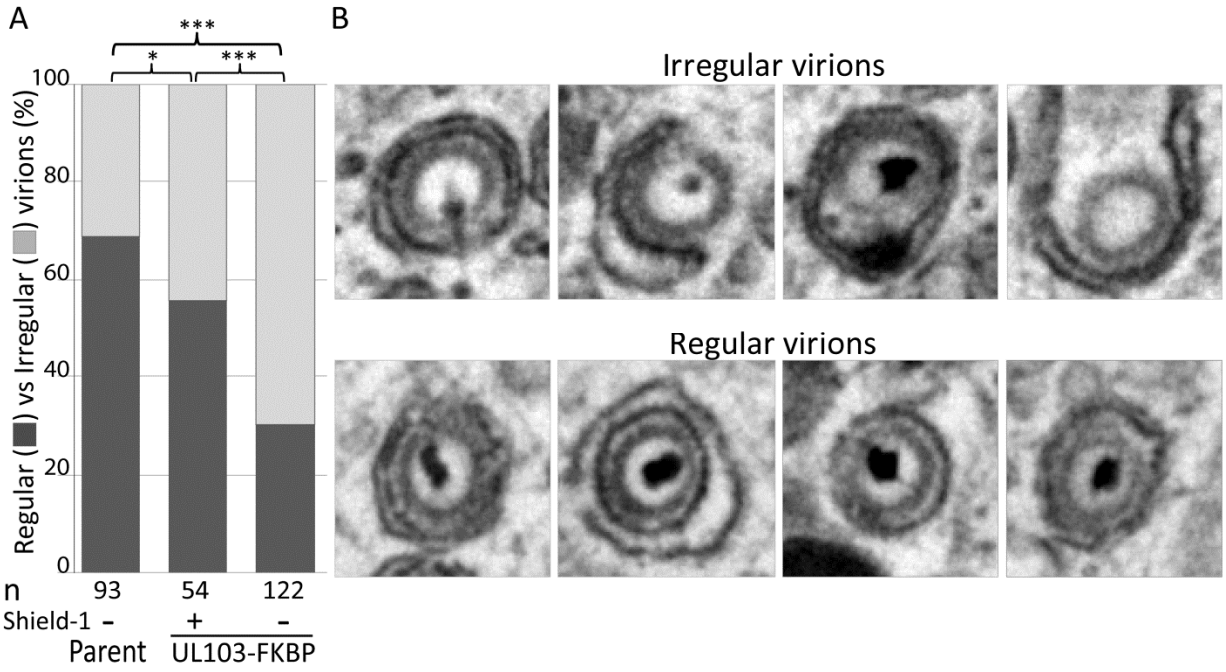

Figure 14. **Comparison of regular vs. irregular virions inside infected cells in the presence or absence of Shield-1.** Regular virions contain DNA and an envelope. Irregular virions are in the process of envelopment or display an abnormal structure. Statistical significance was measured using the Chi Square test (*, $p < 0.1$; ***, $p < 0.0015$). n, indicates the amount of viral particles counted.

CHAPTER THREE

VIRAL AND CELLULAR INTERACTION PARTNERS OF pUL103

Introduction

Human cytomegalovirus (HCMV) induces a wide range of profound modifications of host cell biology, including changes in cell morphology, cell cycle, metabolism, intrinsic and innate immunity, and the endosecretory machinery. Alterations in the endosecretory machinery include remodeling of the Golgi and early endosomal compartments to form the cytoplasmic virion assembly compartment (cVAC), where the mature tegument is acquired, secondary envelopment occurs, and vesicles containing mature virions are transported to the plasma membrane for release.

cVAC biogenesis is contingent on the expression of specific HCMV miRNAs and late genes (105). Previously, we identified pUL48, pUL94, and pUL103 as being important for cVAC biogenesis (129). When pUL103 is degraded during infection, the cVAC does not form properly. pUL103 is a tegument protein that is conserved across the Herpesviridae (HSV UL7 homolog)(Table 1). pUL103 and its homologs are important for efficient production of infectious virions at low and high MOI. Ahlqvist and Mocarski, as well as our lab, have identified roles of pUL103 in cell-to-cell spread, virion envelopment and egress (58, 129). The mechanisms employed by HCMV pUL103 and its relatives remain elusive.

Identification of protein-protein interactions can provide insights into the activities of pUL103 during infection. Four HCMV proteins (pUL22, pUL48, pUL71, and pUL103) were previously identified as pUL103 binding partners. In a yeast two-hybrid analysis interactions were detected between pUL103 and itself, pUL22A, and pUL48N (120). An interaction between pUL103 and pUL71 was identified by co-IP and bimolecular

fluorescence complementation in uninfected cells (70). However, none of these interactions were confirmed in the context of HCMV infection. During HSV-1 infection, proper localization and incorporation into the virion of pUL7 (the HSV pUL103 homolog) is dependent on its interaction with pUL51 (homolog of HCMV pUL71) (88). In addition, HSV-1 pUL7 binds to the mitochondrial protein adenine nucleotide translocator (ANT2), an interaction of uncertain significance (82). Viral and cellular binding partners of pUL103 have not been studied in HCMV infected cells, leaving a void in understanding the biological roles and mechanisms of pUL103.

To address this gap, we employed a set of complementary proteomics approaches that employed co-IP and proximity biotinylation (BioID) to identify viral and cellular proteins that interact with pUL103. Co-IP and the BioID system are well-suited for detection of interactions that are strong and direct. The BioID system also enables detection of weak, indirect, and transient interactions. The differences in these complementary methods provide internal controls that reduce the number of false positives, and interactions highly enriched in both approaches are more likely to be specific. Using these methods, we identified multiple novel interactions with viral and cellular proteins. pUL103 interacted with several cellular antiviral proteins, including IFI16, and interacts with DNA-associated proteins and is present in nuclei. We also found that pUL103 binds to ALIX (a component of the ESCRT machinery) via a novel ALIX-binding site, a role for pUL103 in the redistribution of ALIX to the cVAC, and that deletion of the ALIX binding site had a dominant negative effect on HCMV replication.

Materials and methods

Cell culture and virus stocks. Human foreskin fibroblasts (HFFs) below passage 20 were grown in Dulbecco modified Eagle medium (HyClone-Thermo Fisher Scientific, Waltham, MA) supplemented with 10% fetal bovine serum, 2 mM GlutaMAX (Life Technologies, Grand Island, NY), and 1% minimal nonessential amino acids (HyClone-Thermo Fisher Scientific, Rockford, IL). Virus stocks were propagated by infecting 80% confluent HFFs at an MOI of 0.01 and collecting supernatant every 4 days. Virions present in cell culture supernatants were purified by centrifugation at 2700 rpm for 15 min to remove cell debris, and then ultracentrifugation (70,000 x g for 1 h) through a 20% sorbitol cushion. Pelleted virions were resuspended and stored at -80ºC in DMEM containing 10% FBS. Titers of virus stocks were determined by plaque assay on confluent monolayers.

Plasmids. All cloning was performed in *Escherichia coli* DH5α. To construct the BioID-UL103 plasmid (p), full length UL103 was amplified from pAD/Cre (primers listed in Table 2) and inserted into the pcDNA3.1 mycBioID (Addgene, Cambridge, MA plasmid #35700) (130) using *Xho*I and *Afl*II. UL103-V5-His(v) described in the following section was used to generate UL103-V5-His(p) by inserting the V5-His-tagged UL103 gene into pcDNA3.1 between the *Kpn*I and *Xba*I sites. Alanine substitutions and deletion mutants were created by overlap extension PCR, followed by incorporation into UL103-V5-His(p). All constructs were verified by DNA sequencing.

Recombinant viruses (BioID and V5-His). Viruses were constructed by recombineering using the HCMV AD169 bacterial artificial chromosome pAD/Cre (kindly provided by Dong Yu) in SW105 cells (provided by the Court lab at the National Cancer

Institute). The UL103-V5-His and UL103-BioID mutants were created by inserting a gene cassette at the extreme c-terminus of UL103. The GalK/Kan cassette was PCR amplified from pYD-C630 (provided by Dong Yu) using 70-bp primers, 20-bp of which corresponded to flanking sequences in pYD-C630 and the remaining 50-bp were homologous to sites upstream and downstream of the UL103 stop codon (Table 2). Induction of the lambda RED recombinase in SW105 cells harboring pAD/Cre and the gene cassette lead to homologous recombination followed by selection of transformed colonies on LB-plates containing kanamycin. Single colonies were screened by BAC digestion and PCR.

To construct the scarless UL103-V5-His or UL103-BioID mutants, the GalK/kan cassette was replaced by homologous recombination with another cassette containing V5-His or BioID and the homologous ends described above (Table 2). SW105 cells carrying UL103 with the replacement cassette were negatively selected for on 2-deoxy-galactose (DOG) minimal plates. Galactose negative colonies were streaked on MacConkey agar plates supplemented with chloramphenicol and galactose. Non-fermenting colonies were picked and screened by BAC digestion, PCR, and open reading frame sequence analysis.

Co-Immunoprecipitation (co-IP). Cells (approximately $3.0x10^7$) were either transfected with 30 µg of plasmid or inoculated at an MOI of 0.1. Transfected cells were harvested after 48 hr, and infected cells were harvested 5 dpi using radioimmunoprecipitation assay (RIPA) buffer (10 mM HEPES [pH 7.4], 1% sodium deoxycholate, 1X protease inhibitors [Roche, Indianapolis, IN], 150 mM NaCl, 1% Nonidet P-40, 0.1% SDS). Protein was extracted by passing the lysate through a 27

gauge needle 10 times, centrifuging at 13,000 rpm for 10 min, and collecting the supernatant. Antibodies were conjugated to the beads by mixing 20 µl of protein A/G Plus Agarose (Santa Cruz Biotechnology, Dallas, Texas) and 1 µg of antibody in 0.5 ml of PBS at 4°C overnight. Antibody-bead complexes were washed twice in PBS and then incubated with cell lysates overnight at 4°C in a tube rotator. Non-specific interactions were stripped from the immunocomplex by washing three times with RIPA buffer. For mass spectrometry analysis, beads were spun at 2000xg and resuspended in 50 µl of 50 mM ammonium bicarbonate. For binding partner verification, immunocomplexes were washed with PBS, and the pellet was resuspended in 30 µl of 2X Laemmli sample buffer for immunoblot analysis.

BioID. Transfected and infected cells were incubated with 50 µM biotin 24 hours prior to harvesting. Cells lysed as described above were incubated at 4°C overnight with 500 µl of streptavidin conjugated to magnetic beads (New England Biolabs, Ipswich, MA). Beads were washed once in 1.5 ml of wash buffer 1 (2% SDS in dH_2O), once with wash buffer 2 (0.1% deoxycholate, 1% Triton X-100, 500 mM NaCl, 1 mM EDTA, and 50 mM Hepes, pH 7.5), once with wash buffer 3 (250 mM LiCl, 0.5% NP-40, 0.5% deoxycholate, 1 mM EDTA, and 10 mM Tris, pH 8.1), and then twice with wash buffer 4 (50 mM Tris, pH 7.4, and 50 mM NaCl). To evaluate sample integrity, 10% of the total was retained for immunoblots. The remaining beads were spun at 2000xg and resuspended in 50 µl of 50 mM ammonium bicarbonate for mass spectrometry.

Mass spectrometry. Samples were digested overnight using sequencing-grade trypsin (Promega) in 25 mM ammonium bicarbonate and 10% acetonitrile. The resulting peptides were separated by reverse phase chromatography (Acclaim PepMap100 C18

column, Thermo Scientific), followed by ionization with the Nanospray Flex Ion Source (Thermo Scientific), and introduced into an Orbitrap FusionTribrid mass spectrometer (Thermo Scientific). Primary data analysis was done using Proteome Discoverer 1.4 (Thermo), which incorporated the Mascot (Matrix Science) algorithm. Mascot searched the SwissProt_2014_06 and UniProt_Hum_Compl_All database for viral and cellular proteins respectively. Secondary analysis was performed with Scaffold 4.3.4 (Proteome Software) set to a minimum protein identification probability of ≥99% and 2 cellular or 3 viral unique peptides at ≥99% minimum peptide identification probability. Proteins identified by Scaffold were normalized by size using the normalized spectral abundance factor (NSAF) (131). Non-specific cellular interactions were filtered out using the contaminant repository for affinity purification (CRAPome) (132).

Cell Fractionation. HFFs were collected and pelleted in ice cold PBS. Following pellet resuspension in 900 µl of mild lysis buffer (0.1% NP40 in PBS), 300 µl were removed as whole cell lysate. Remaining cell lysate was centrifuged for 10 seconds. 300 µl of the supernatant was removed as the cytoplasmic fraction, while the pellet was washed in 1 ml of lysis buffer followed by another 10 seconds spin to pellet the nuclear fraction. The nuclear pellet was resuspended in 180 µl of 1X SDS-Laemmli buffer. Whole cell lysates and nuclear fractions were sonicated prior to immunoblots.

Immunoblots. Protein was quantified by bicinchoninic acid (BCA) assay (Pierce Biotechnology, Rockford, IL). For cell lysates, 50 µg of protein was solubilized in 2X SDS-Laemmli buffer followed by SDS-PAGE. Separated proteins were transferred to nitrocellulose membranes (Whatman, Florham Park, NJ), probed with primary antibodies, and then reacted with HRP-conjugated goat anti-mouse/rabbit IgG

secondary antibodies (Thermo Scientific, Rockford, IL). Reactions were detected with the Supersignal West Pico Chemiluminescent substrate (Bio-Rad, Hercules CA) on autoradiography film (GE Healthcare, Pittsburgh, PA). Antibodies are listed in Table 3.

Immunofluorescence assays (IFA). HFFs were seeded at 80% confluency one day prior to infection on 0.2% gelatin-coated 8-well glass chamber slides (Thermo Fisher Scientific, Waltham, MA). The following day, cells were infected at an MOI of 0.1 and then fixed in paraformaldehyde and stained at 120 hpi as previously described (129). Primary antibodies are listed in Table 3. Fluor-tagged secondary antibodies (Alexa Fluor 488-conjugated goat anti-rabbit IgG and Alexa Fluor 568-conjugated goat anti-mouse IgG) were from Life Technologies (Grand Island, NY). Mounting was done with Vectashield containing DAPI (4',6-diamidino-2-phenylindole) (Vector Laboratories Inc., CA). Imaging was done on a Nikon E800 fluorescence microscope and a Leica TCS SP5 laser scanning confocal microscope.

Results

Experimental design. Affinity purification followed by mass-spectrometry can be used to identify proteins pulled-down by a bait protein. The proteins identified can be true interacting partners, but false positives are common, arising due to reasons that can include non-specific interactions with the beads, antibody, protein tag, and sticky or highly abundant proteins. To increase the likelihood of identifying biologically meaningful interactions, we limited confounding by false positives through the use of two independent methods of affinity purification: co-immunoprecipitation (co-IP) and proximity labeled biotinylation (BioID). Co-IP detects proteins that strongly interact with the bait protein, while the BioID system uses BirA*, a promiscuous biotin ligase that biotinylates proteins within ~10 nm of the tagged protein (130). Each method uses different beads, antibodies, tags, and binding/elution conditions. The differences in these complementary methods provide internal controls that reduce the number of false positives, while proteins highly enriched in both approaches are more likely to be specific.

As shown in Table 4, experiments involved plasmids (p) and recombinant viruses (v) with tags fused to pUL103. Plasmids included one construct that expresses the BirA* protein alone, one with BirA* fused to the pUL103 N-terminus (BioID-pUL103(p)), and one in which the V5-His tag was added to the C-terminus of pUL103 (UL103-V5-His(p)). Two recombinant viruses were also used, in which the tags were attached to the C-terminus of pUL103 (UL103-BioID(v) and UL103-V5-His(v)). For infection experiments, we inoculated cells at an MOI of 0.1 with either UL103-V5-His(v) or UL103-BioID(v) and harvested the cells 5 days post infection. A low MOI infection allows simultaneous

analysis of cells at multiple stages of infection, giving us a broad overview of the viral and cellular proteins that interact with pUL103.

Collectively, these constructs and conditions enable identification of interactions of pUL103 with cellular proteins in the absence of other viral proteins, with HCMV proteins in infected cells, with cellular proteins in infected cells, and with cellular proteins enhanced during infection.

Effect of tags on virus replication, expression, and localization of pUL103. To determine if the affinity tags influenced the localization or activity of pUL103 we conducted immunofluorescence and virus replication plaque assays. In transfected cells, UL103-V5-His(p) and BioID-UL103(p) were abundant in perinuclear regions that correspond to ER and Golgi structures (Fig. 15A), while BioID(p) alone was dispersed diffusely throughout the cell cytoplasm (data not shown). During infection, UL103-V5-His(v) and UL103-BioID(v) localized to the assembly compartment, consistent with previous reports (Fig. 15A) (58, 129). In multi-step growth experiments, UL103-BioID(v) produced titers similar to the parent, while UL103-V5-His(v) replication was delayed, taking 6 days to reach parental levels (Fig. 15B). Our previous results using an FKBP tag also showed a lag in extracellular virus production, suggesting that some tags at the extreme C-terminus of pUL103 perturb virion production at earlier times after infection (129). Neither tag had a discernable effect on pUL103 localization or production of infectious progeny at late stages of viral replication.

Viral proteins identified by AP-MS. Mass spectrometry returned 5566 total viral spectral hits, which correspond to 49 HCMV proteins using co-IP and 47 proteins with BioID (outlined in Fig. 16A). Altogether, 53 viral proteins were identified, which

indicates high overlap using both methods. Larger proteins tend to generate higher spectral counts than smaller proteins, so we used the normalized spectral abundance factor (NSAF) to normalize the HCMV proteins based on size. To determine the most significant interactions, the HCMV proteins displaying an NSAF greater than 0.5 were plotted on a UL103-BioID vs UL103-V5-His graph (Fig. 16B). The highest NSAF values were seen for pp65 (21.6 UL103-BioID and 23.4 UL103-V5-His), but pp65 was also pulled down in untagged AD169 control lanes indicating a non-specific interaction (data not shown). The second highest NSAF value for UL103-V5-His was pUL103 (NSAF=13.25), demonstrating sufficient immunoprecipitation of the pUL103-V5-His protein with the V5 antibody. The tegument hub protein, pUL25 was also highly abundant in both approaches (6.7 UL103-BioID and 4.0 UL103-V5-His), but lack of a pUL25 specific antibody prohibited further verification. Other proteins enriched were pUL44, pUL112/113, pUL84, pUL71, pUL50, pUL45, pUL86, IE2, pUL34, pUL47, and pUL56. The identification of pUL71 by our pull-downs as well as Fischer and Mertens in transfected cells, provides validity to our dual method approach and evidence that pUL103 interacts with pUL71 during infection (70). In addition, Roller and Fetters showed that the homologues of pUL103 and pUL71 (HSV pUL7 and pUL51) form a complex in HSV1 infected cells (88).

Verification of interactions with viral proteins. We detected many previously unidentified pUL103 viral binding partners (Fig. 16B). The properties of the highest scoring viral proteins revealed many to be DNA associated (pUL34, IE2, pUL44, pUL84, etc.). This was surprising, since our lab and others have shown pUL103 immunofluorescence staining to be strictly cytoplasmic in infected cells (58, 129) (Fig.

15A). Nonetheless, the HSV1 and HSV2 homologs of pUL103 (HSV pUL7) can be present in nuclei (82, 89). To assess the nuclear presence of pUL103 we performed three-dimensional confocal microscopy on HCMV infected cells. Although much less intense than the cytoplasmic fluorescence, in central slices of the z-series (approximately equidistant from apical and basal surfaces), weak, but unambiguous nuclear staining for pUL103 was present in nuclei (Fig. 17A). We also performed cellular fractionation followed by western blots and found that pUL103 is present in the nuclear fractions of cells (Fig. 17B).

We employed immunoprecipitation and immunoblotting to verify interactions of pUL103 with three of the DNA associated viral proteins (IE2, UL34, and UL44). IE2 and pUL34 were verified by pull-downs with a V5 antibody followed by immunoblotting. Each blot showed a band in the UL103-V5-His IP lane, but not in the parent or control lanes (Figs. 17C and 17D). pUL44 is approximately 46 kDa and is obscured by the 50 kDa heavy chain antibody band. Because of this, pUL103-V5-His was immunoprecipitated with a pUL44 antibody and then probed with anti-His. There was a clear band in the UL103-V5-His (Fig. 17C, lane 3) that co-migrates with pUL103 in the total cell lysates (Fig. 17C, lane 6). These results provide evidence for the specificity obtained by merging results obtained with two independent affinity-based pull-down approaches, and revealed novel interactions of pUL103 with IE2, pUL34 and pUL44.

Interactions of pUL103 with cellular proteins. We used the dual affinity purification approach to identify the binding partners of pUL103 in transfected and HCMV infected cells. Mass spectrometry detected a total of 2953 cellular proteins pulled down by both methods. As mentioned previously, the NSAF formula was applied for

spectral count normalization. Our initial mass spectrometry dataset included proteins (tubulins, actins, ribosomal, and mitochondrial) that were abundant in the BioID-UL103(p) control or had high CRAPome scores, indicating non-specific interactions. To eliminate background, we only considered proteins that had a UL103-BioID(v) NSAF value higher than the NSAF of the BioID(p) control, and a CRAPome score lower than 100. We utilized two methods of analysis; NSAF to identify all the cellular protein interactions (Fig. 18A) and NSAF fold-change of infected cells versus uninfected cells to detect interactions enhanced during infection (Fig. 18C). Stringent cutoffs of 3 and 2 were used for NSAF and for NSAF fold-change, respectively, to identify pUL103 binding partners that are potentially of biological significance (Fig. 18B and 18D). A total of 13 cellular proteins met these criteria, with 6 being shared between both analyses (Table 5 and Figs. 18A and 18C).

Among the highly enriched proteins are several involved in innate immune responses (IFI16, STAT1, ISG15, MYD88, and IFIT1). All of these antiviral proteins had low NSAF scores or were undetected in transfected cells, thus the interactions might be attributed to elevated protein expression in infected cells. However, the mRNA levels of IFI16 decreased by 71% and 62% in fibroblasts infected for 96 hours with HCMV strains Towne and AD169 (133); a similar decrease is evident in immunoblots of infected cell lysates (Fig. 19A). Importantly, the IFI16 interaction was verified by forward and reverse co-IP, suggesting a novel role for pUL103 in the regulation of innate immune signaling during infection (Fig. 19A).

Another category of proteins identified in these analyses includes proteins involved in formation and trafficking of vesicle (MYO1C, PDCD6IP, and COPB1), which

may interact with pUL103 during virion envelopment and egress. Pulldowns in transfected and infected cells confirmed the binding of pUL103 to the ESCRT-associated protein, ALIX (Fig. 19B). Interestingly, amino acid motif analysis of pUL103 revealed two potential “late” or “L” domains that bind ALIX at the C-terminus (Fig. 20A). ALIX binding domains are well-characterized motifs present in retrovirus gag proteins that are sites of interaction with ALIX important for virion budding at the plasma membrane (reviewed in (134)). These results led us to further explore the pUL103-ALIX interaction.

Mutational analysis of ALIX binding motifs in uninfected cells. The amino acids YPNL at position 230 to 233 in pUL103 represent a type 1 late domain (134). The YPNL present in pUL103 corresponds to the YPX_nL ALIX binding motif (X is any residue and n can range from 1 to 3). In non-normalized transfection experiments with single and multiple amino acid substitution of the YPNL motif had little effect on pUL103-ALIX interaction (Fig. 20B).

Fifteen amino acids upstream of YPNL, is a sequence, GWPVGLGLL, that has properties that suggest it might serve as an ALIX site. The high similarity between tryptophan and tyrosine allow them to sometimes be interchanged, as seen in SIVwrcPbb Gag p6, in which the YPXL motif is replaced by WPXL (135). The GWPVGLGLL sequence thus conforms to both type 1(YPX_nL) and type 3 ($\Phi YX_n\Phi X_nL$) late domain motifs. In experiments in which levels of pUL103 were normalized relative to GAPDH, mutation of either of the putative pUL103 late domains led to at least 50% reduction in ALIX that was pulled down in uninfected cells (Fig. 19C). These results are

consistent with pUL103 containing two motifs together are important for its interaction with ALIX.

Influence of pUL103 on ALIX localization. Given the involvement of ALIX in vesiculation events similar to those associated with secondary envelopment, we examined ALIX localization during infection. By IFA, ALIX was diffusely distributed throughout the cytoplasm of uninfected cells, but strongly localized to the cVAC at late times post infection (Fig. 21A). To assess the location of ALIX in the absence of pUL103, we used a UL103-FKBP-V5 virus that contains a regulatable destabilization domain attached to UL103 (129). In the presence of Shield-1, pUL103 was stabilized and abundant in the cVAC along with ALIX (Fig. 22A). Removal of Shield-1 reduced the amount of pUL103 and ALIX in the assembly complex by 34% and 56% respectively (3D quantification of at least 14 cells per condition). The effect on ALIX was not due to differential ALIX expression, as immunoblots showed that levels of ALIX were similar in mock infected cells and in cells infected with either the parental or V5-His-tagged UL103 viruses, and regardless of whether the UL103-FKBP-V5 virus was treated with Shield-1 (Fig. 21B). These results demonstrate that HCMV infection results in pUL103-regulated localization of ALIX to the cVAC.

Discussion

HCMV pUL103 is a conserved herpesvirus tegument protein that is involved in several processes, including cell-to-cell spread, cVAC biogenesis, and virion envelopment and egress. We identified its interaction partners to provide novel insights into its molecular functions and biological roles. Several pUL103 binding partners were identified in transfection and yeast two-hybrid systems, but none have been characterized in the context of infection (70, 120). HCMV infection induces profound changes in host cells, altering the localization, production, and function of cellular proteins. In addition, in the absence of infection, interactions among viral proteins, as well as interactions of viral proteins with cellular proteins (e.g., antiviral proteins) do not occur. To address these gaps, we infected cells with recombinant viruses that express forms of pUL103 that were tagged to enable independent forms of pull-downs (co-IP and BioID). This was followed by mass spectrometry to identify interacting partners. By restricting our analysis to interactions that scored highly in both of the complimentary methods, we increased the likelihood of selecting specific, high-value biologically relevant interactions worthy of further study, while limiting the number of false positives and incidental interactions. The set of viral and cellular binding partners we identified for pUL103 suggest that it, and possibly its homologs in other herpesviruses, interact with nuclear proteins that bind DNA, and play roles in the regulation of antiviral responses and in formation, transport, and targeting of intracellular vesicles. The latter activities may be important during during cVAC biogenesis, and subsequently during secondary envelopment and egress.

Interactions of pUL103 with other HCMV proteins. The viral proteins that met our screening criteria belong to several distinct functional categories, including tegument proteins, DNA-binding proteins, and capsid and nuclear egress proteins. pUL103-pUL71 was previously shown to interact outside the context of infection in co-transfection and bimolecular fluorescence complementation experiments (70), and interactions between the HSV homologs (pUL7 and UL51) of these proteins were detected in infected cells (88). Our detection of this interaction provides validation for our dual pulldown approach.

Of the interactions that scored highly in both the V5 and BioID experiments, follow-up pull-down experiments were performed with antibodies against pUL34, pUL44, and IE2; in each instance, the interactions were detected only in cells infected with the UL103-V5-His virus, and not in mock infected cells or cells infected with untagged parental virus. These results provide further evidence that the interactions characterized by high NSAF scores in both the V5- and BioID-based proteomic analyses are sufficiently specific to justify follow-up studies.

The most prominent interaction with dual high NSAF scores was observed between pUL103 and the HCMV tegument protein pUL25. pUL25 is expressed at late times post infection, strongly localizes to the cVAC, and is incorporated into the three major types of virus particles: mature virions, noninfectious enveloped particles, and dense bodies (136, 137). The reported interactions of pUL25 with several other tegument proteins suggests it serves as an organizing hub for incorporating viral proteins into enveloped particles (120). Further analysis of the pUL103-pUL25 interaction is warranted.

We did not detect the previously described interactions between pUL103 and HCMV pUL22A and pUL48N, which were identified in a yeast two-hybrid system but not verified by co-IP in transfected cells (120). In yeast cells, pUL103 may lack posttranslational modification(s) or have alternative folding that exposes or creates artificial binding sites. While we acknowledge their limitations, tagged recombinant viruses can provide useful representations of protein-protein interactions during infection. The specificity of such methods can be enhanced by screening on the basis of dual high positivity using co-IP and Bio-ID methods.

Nuclear pUL103. Identification of five viral DNA associated proteins with dual NSAF values above 0.5 (Fig. 16B) and the co-IP verification of three of these (pUL34, pUL44, and IE2), suggests a nuclear role for pUL103. This was unexpected given that pUL103 appears to be strictly cytoplasmic by IFA in HCMV infected cells. Only after substantially increased exposure times were we able to detect a faint but discernable pUL103 signal in nuclei (Fig. 17A). Immunoblots of fractionated cells confirmed the presence of pUL103 in the nuclear fraction. Nuclear pUL103 has also been described for the HSV homolog (pUL7), in which IFA and transmission immunoelectron microscopy analysis detected pUL7 in infected cell nuclei (88, 89). The function of nuclear pUL103 is unknown, but may involve a conserved domain, present in the pUL103 homologs of all members of the herpesviridae. The conserved domain is homologous with a segment of DNA topoisomerase III of *Schizosaccharomyces pombe;* this protein releases supercoil tension that is introduced during DNA replication and transcription (89, 138). The presence of this conserved domain, in conjunction with its

observed nuclear localization and interaction with HCMV DNA associated proteins suggests a heretofore undefined role for pUL103 in nuclear events.

Interactions of pUL103 with cellular proteins. Our interest at this stage is to identify interactions unique to pUL103 that are more likely to be of true biological significance. Because of this, we applied the stringent screening criteria, described in the Results section and in Fig. 16A, understanding that we likely excluded some true interactions. For instance, HSV pUL7 can pull-down the mitochondrial protein, ANT2 (82). We found a dual high scoring interaction between ANT2 and pUL103 in transfected and in infected cells, but because ANT2 has a CRAPome score of 223, it did not pass our screening filter. Even though the interaction might be biologically meaningful, we did not pursue it here.

Most of the proteins that passed our screening criteria are involved in innate antiviral responses and vesicle formation/trafficking (Fig. 18A). A cellular protein from each category was verified in reciprocal pull-down experiments, providing evidence that these represent true interactions.

A novel role for pUL103 in innate immunity? A possible role for pUL103 in regulation of innate immunity is difficult to evaluate in uninfected cells. With the exception of STAT1, none of the antiviral interaction partners were detected in our transfection experiments. In infected cells, the presence of pathogen-associated molecular patterns (PAMPs) activates the antiviral response. Relocalization, increased expression, or phosphorylation can lead to interactions with viral binding partners. We identified four antiviral proteins that displayed dual high NSAF scores and verified the interaction with IFI16 by reciprocal co-IP. The abundance of antiviral proteins detected

demonstrates that pUL103 is capable of interacting with and modulating the innate immune response either directly or indirectly.

We did our proteomic experiments after low moi infections (moi - = 0.1). In addition to cells at the late stage of infection, at the time of harvest (5 dpi), the cultures would have included non-synchronously infected cells at the earliest stages of infection. We were thus able to sample material from various stages of infection. Virion tegument proteins are introduced into the host cell immediately upon fusion of the viral and host cell membranes. The release of tegument proteins pp65 and pp71 into host cells are known to be critical for subverting the innate immune response and helping to establish an environment conducive to productive infection (139, 140). pUL103 is a virion associated tegument protein and may have a similar function when engaging antiviral proteins (54). In addition, virion associated and newly synthesized pUL103 could interact with antiviral proteins to facilitate cVAC biogenesis. Recent work by Xie and colleagues showed that HCMV makes use of interferon-induced transmembrane proteins (IFITMs) for cVAC assembly and virion production (71). The biological role of the pUL103 interaction with antiviral proteins is being assessed.

Potential roles for pUL103 in biogenesis and trafficking of intracellular vesicles. Identification of three proteins (COPB1, MYO1C, and ALIX) involved in formation and trafficking of vesicles suggests a connection to the known role of pUL103 in virion envelopment and egress. The COPB1 mediates Golgi fragmentation during the M-phase of the cell cycle and retrograde transport from the Golgi to the ER (141, 142). MYO1C is involved in trafficking GLUT4 to the plasma membrane, and participates in lipid raft organization (143-145). These cellular proteins have functions that encompass

activities of the sort that would be involved in cVAC biogenesis and trafficking of virions to the cytoplasmic membrane, a subject for future study.

The specificity of the pUL103-ALIX interaction was demonstrated by a combination of dual high NSAF scores using both proteomic approaches, a low CRAPome score for ALIX, NSAF scores higher for pUL103 pull-downs than for free BioID, pull-downs in cells transfected with pUL103-V5-His, and positive pull-downs in cells infected with UL103-V5-His(v) but not with the untagged parental virus. Proteins that bind to ALIX typically interact via ALIX-specific late domains that are important for virion production in many RNA and DNA viruses (146-150). Late domains in retrovirus gag proteins can bind the V domain of ALIX to facilitate viral budding at the cell membrane (reviewed in (134, 149, 150)). For DNA viruses, vaccinia viruses use an ALIX binding domain for extracellular virion production, and Epstein-Barr virus, a gammaherpesvirus, exploits ALIX for vesicle formation and nuclear egress of capsids (146, 148). The use of ALIX and ESCRT machinery is thus a common theme for virion production for many viruses.

By sequence analysis, we identified two adjacent ALIX-binding motifs in pUL103, one that conforms to canonical Type1 and Type 3 motifs, and one that matches the Type 1 motif (Fig. 20A). We evaluated mutations in these motifs in pull-down experiments, and found that changes in the Type 1 motif had little effect by themselves, while deletion of the Type1 or 3 motif or substitution of five critical residues with alanines led to >60% reduction in the amount of ALIX pulled down by pUL103-V5-His.

Our identification of two adjacent ALIX binding domains in HCMV pUL103 and the strong infection and pUL103 influenced or induced localization of ALIX to the cVAC

during infection suggest involvement of ALIX in HCMV envelopment and egress, perhaps during secondary envelopment. However, siRNA knockdown and dominant negative versions of ALIX had no effect on HCMV virion production (48, 78). This raises the possibility that HCMV employs redundant ESCRT-related pathways during the late stages of virion biogenesis. Recombinant viruses with altered pUL103 ALIX binding domains are under construction to enable elucidation of the role of the pUL103-ALIX interaction during infection.

A major challenge for identification of interacting partners is the abundance of false-positives that are typically observed. To address this, we employed parallel analysis of interacting partners pulled down using two affinity based methods (V5-His and BioID). By coupling dual high NSAF cutoffs with other stringent selection criteria we effectively screened for high value interactions. Detection of the previously identified pUL71 interaction, and verification of pUL44, IFI16, and ALIX interactions by reverse co-IP, indicates our screening process selected for biologically plausible interactions. The collection of viral and cellular proteins identified provides novel insights into the biological functions of pUL103 and its respective homologs. This provides a robust foundation for future studies.

Table 7. Properties of HCMV pUL103 and its alphaherpesvirus UL7 homologs

Virus	Protein Kinetics	Size (aa)	Properties			
			Deletion	Localization	Interactions	Ref
herpes simplex virus 1 (HSV-1)	delayed early or early late	296	Essential or nonessential, decrease in viral titers (up to 3 logs), 50% reduction in plaque size	Nuclear and juxtanuclear. Present in mature virions	ANT2 pUL51 (HCMV pUL71)	(70, 73, 79)
herpes simplex virus 2 (HSV-2)	late	296	N/A	Nuclear and juxtanuclear. Present in mature virions	A,B, and C capsids (weak)	(80)
pseudorabies virus (PRV)	delayed early or early late	266	Nonessential, decrease in viral titers (up to 0.5 logs), 60% reduction in plaque size, inefficient secondary envelopment, and a delay in neuroinvasion	N/A	N/A	(71, 78)
bovine herpes virus 1 (BHV-1)	early	300	Nonessential, reduction in viral titers	Cytoplasmic, not present in mature virions	N/A	(77)
human cytomegalovirus (HCMV)	early late	250	Nonessential (up to 3.5 logs), decrease in viral titers, 60% reduction in plaque size, delayed secondary envelopment and release of dense bodies and virions	Juxtanuclear with Golgi markers. Present in mature virions	pUL103 pUL22A pUL48N pUL71	(56, 111, 121)

Table 8. Primers used for generating recombinant viruses

Plasmid	Primer sequence	Amplification target
BioID-UL103(p)	5'-GAAGCGCAGAGAAGCTCGAGATGGAGGCCCTGATGATCCG-3'	UL103 gene
	5'-ATCAGCGGTTTAAACTTAAGTCACTCTTCCTCTCCTCGTT-3'	
UL103-V5-His(p)	5'-GTACCGAGCTCGGATCCACTATGGAGGCCCTGATGATCCG-3'	UL103-V5-His gene
	5'-TAGACTCGAGCGGCCGCCACTCAATGGTGATGGTGATGAT-3'	

Virus	Primer sequence*	Amplification target
UL103-GalK/kan	5'-GTTGCGTGTTTTTTTTTTTTCTATGATATGCGTGTCTAGTTCGCTTCTCAgctggagctccaccgcgggaagttc-3'	GalK/kan
	5'-TGCCCTCACCCCCCAAGCTGCCGCCGCGCTGGGAACGAGGAGAGGAAGAGatgggagtgcaggtggaaaccatc-3'	
UL103-BioID	5'-CGTGTTGCGTGTTTTTTTTTTTTCTATGATATGCGTGTCTAGTTCGCTTCTCActtctctgcgcttctcagggag-3'	mycBioID tag
	5'-TGCCCTCACCCCCCAAGCTGCCGCCGCGCTGGGAACGAGGAGAGGAAGAGgaacaaaaactcatctcagaagagg-3'	
UL103-V5-His	5'-GTTGCGTGTTTTTTTTTTTTCTATGATATGCGTGTCTAGTTCGCTTCtcaatggtgatggtgatgatgaccggta-3'	V5-His tag
	5'-TGCCCTCACCCCCCAAGCTGCCGCCGCGCTGGGAACGAGGAGAGGAAGAGggtaagcctatccctaaccctctcc-3'	

*The uppercase sequences correspond to the 50-bp segments of viral DNA needed for recombination into the viral genome. The lowercase sequences are regions needed to enable amplification of exogenous sequences (e.g., the V5 epitope) intended to be inserted into the BAC

Table 9. Antibodies used in IFA and immuoblot assays

Antibody Target	Host/isotype, clone	Source, catalog no.
Epitope tag		
V5 (14 amino acids)	Mouse monoclonal/IgG2a	Life Technologies, R960-25
His (6 amino acids)	Rabbit polyclonal	Rockland 600-401-382
Cellular		
GAPDH (36 kDa)	Mouse monoclonal/IgG1, clone GA1R	Thermo Scientific, MA5-15738
GM130 (130 kDa)	Mouse monoclonal/IgG1(κ), clone 35/GM130	BD Biosciences, 610822
EEA1 (180 kDa)	Rabbit polyclonal	Abcam, ab2900
IFI16 (85-95 kDa)	Mouse monoclonal/IgG1, clone 1G7	Santa Cruz, sc-8023
Myo18A (230,190 kDa)	Mouse monoclonal/IgG1, clone H-10	Santa Cruz, sc-365328
ALIX (96 kDa)	Rabbit polyclonal	Abcam, ab76608
HCMV		
IE1 and IE2 (IE1, 72 kDa;IE2, 86 kDa)	Mouse monoclonal/IgG1(κ), clone CH160	Virusys, P1215
IE2 (86 kDa)	Mouse monoclonal, clone 8B1.2	Chemicon (millipore), MAB810
pUL44 (CMV ICP36), 46 kDa	Mouse monoclonal/IgG1(κ), clone 10D8	Virusys, CA006-100
UL34-R4	Rabbit polyclonal	Bonita Biegalke (Ohio University)

Table 10. Constructs and experiment conditions

Constructs	Condition	Affinity ligand	Beads
BioID(p)	Transfected	Streptavidin	Magnetic
BioID-UL103(p)	Transfected	Streptavidin	Magnetic
UL103-BioID(v)	Transfected	Streptavidin	Magnetic
UL103-V5-His(p)	Infected	V5	Agarose A/G
UL103-V5-His(v)	Infected	V5	Agarose A/G

Table 11. Properties of the cellular proteins meeting selection criteria

Gene	Property	Infected		Transfected	
		NSAF V5, BioID	NSAF FC V5, BioID	NSAF BioID(p)	CRAPome
TUBB3	Microtubule assembly	19.1, 13.5	1.1, 1.3	9.5	N/A
SERPINH1 (HSP70)	Collagen biosynthesis and folding	10.6, 4.8	3.1, 6.1	0.3	78
STAT1	Antiviral transcription activator	6.2, 4.6	3.9, 8.9	0.9	23
ISG15	Ubiquitin-like protein with antiviral activity	6.0, 3.1	6.0, 3.1	0.0	5
IFI16	Viral DNA sensor that triggers innate immune response	4.9, 21.5	4.9, 21.5	0.4	9
MYO1C	Intracellular vesicle transport. Nuclear isoform functions in transcription initiation	4.7, 9.3	3.2, 12.6	0.9	66
IFIT1	RNA-binding protein that inhibits viral replication and translation initiation	4.2, 3.1	4.2, 3.1	0.0	4
SEC61A1	Associated with ER ribosomes for assembly of membrane and secretory proteins	3.9, 3.5	0.8, 2.5	1.4	28
PDCD6IP (ALIX)	Associated with ESCRT machinery sorting of protein cargo into MVBs	3.6, 5.9	0.7, 3.3	1.9	55
COPB1	Mediates retrograde Golgi-to-ER transport	3.0, 3.6	0.6, 1.9	1.2	92

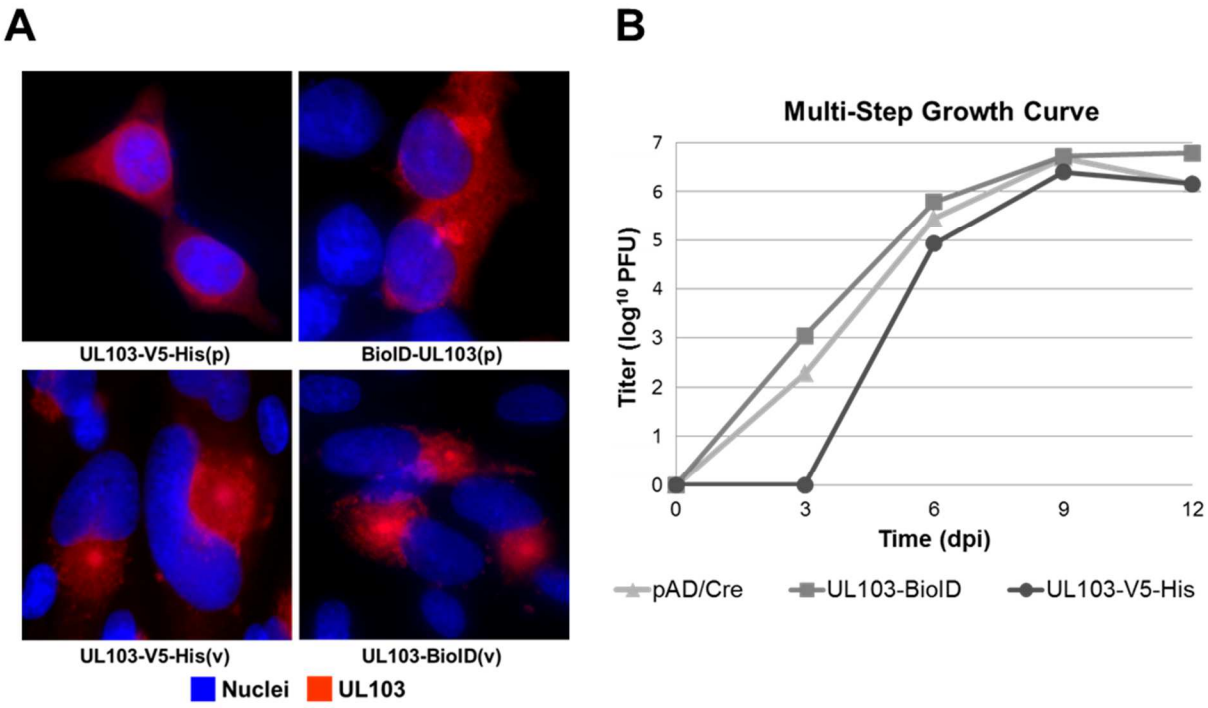

Figure 15. **The effect of tagged pUL103 on localization and viral growth.** (A) HFFs were either transfected (p) for 48 hours or infected (v) at an MOI of 0.2 for 120 hours, then analyzed by fluorescence microscopy. pUL103 was visualized using a V5 antibody against the V5-His epitope or a myc antibody targeting the BioID tag. (B) Replication of UL103-V5-His and UL103-BioID recombinant viruses were evaluated by multi-step growth curves (MOI=0.1). Virus titers were performed in triplicate.

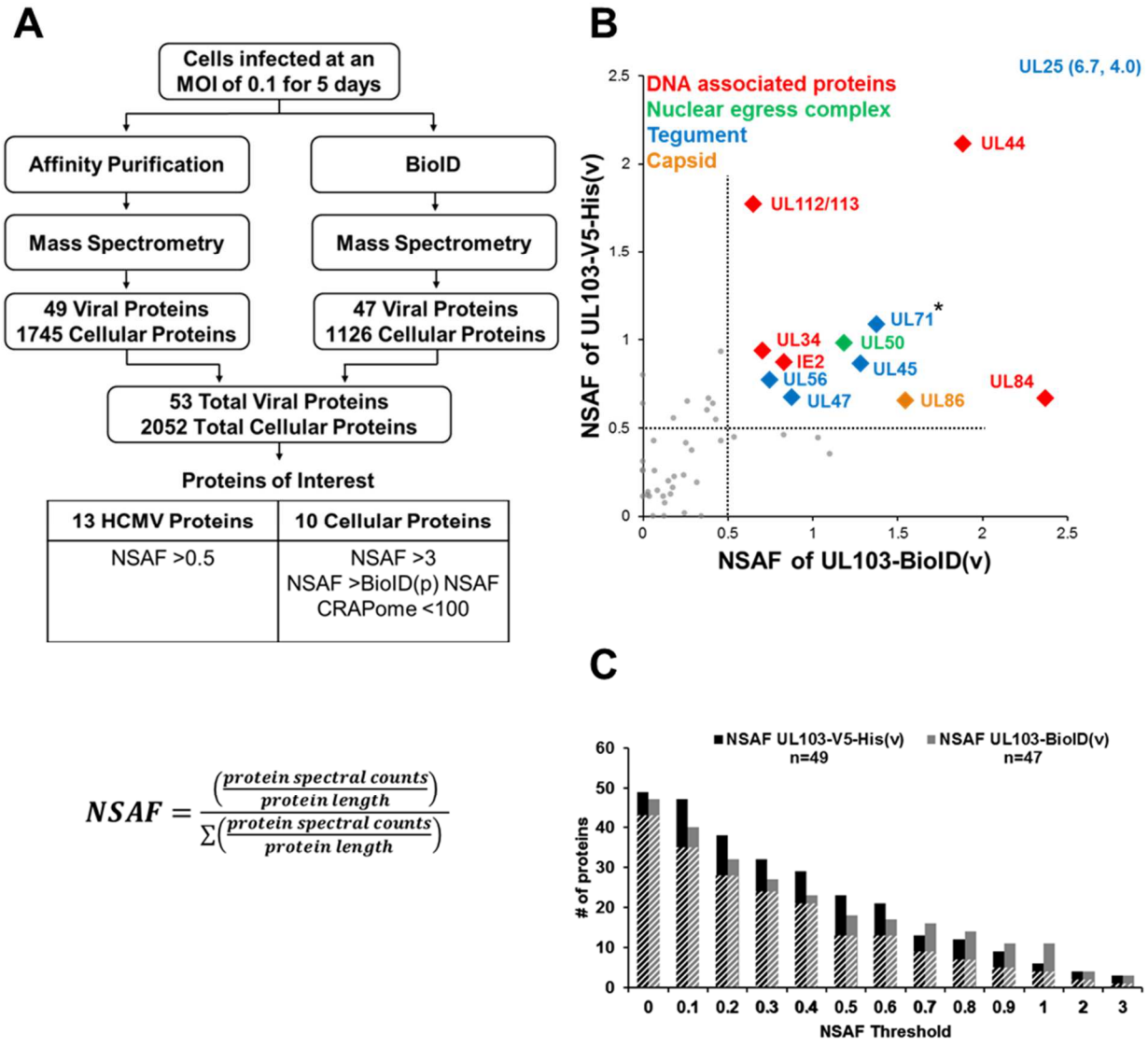

Figure 16. **Experimental scheme and graphical representation of enriched HCMV proteins.** (A) HFFs were infected for 120 h at an MOI of 0.1 with UL103-V5-His(v) or UL103-BioID(v) and immunocomplexes were pulled-down with antibodies to V5 or biotin respectively. Mass spectrometry spectral counts were normalized based on size using the normalized spectral abundance factor (NSAF) formula. (B) Scatter plot of viral protein NSAFs from co-immunoprecipitation and proximity labeled biotinylation experiments. The dotted line separates the viral proteins with an NSAF > 0.5 (colored) from those less enriched (gray). Asterisk (*) indicates a known interaction. (C) Bar graph of all the viral proteins identified at increasing NSAF thresholds. The stripes indicate proteins shared by both methods.

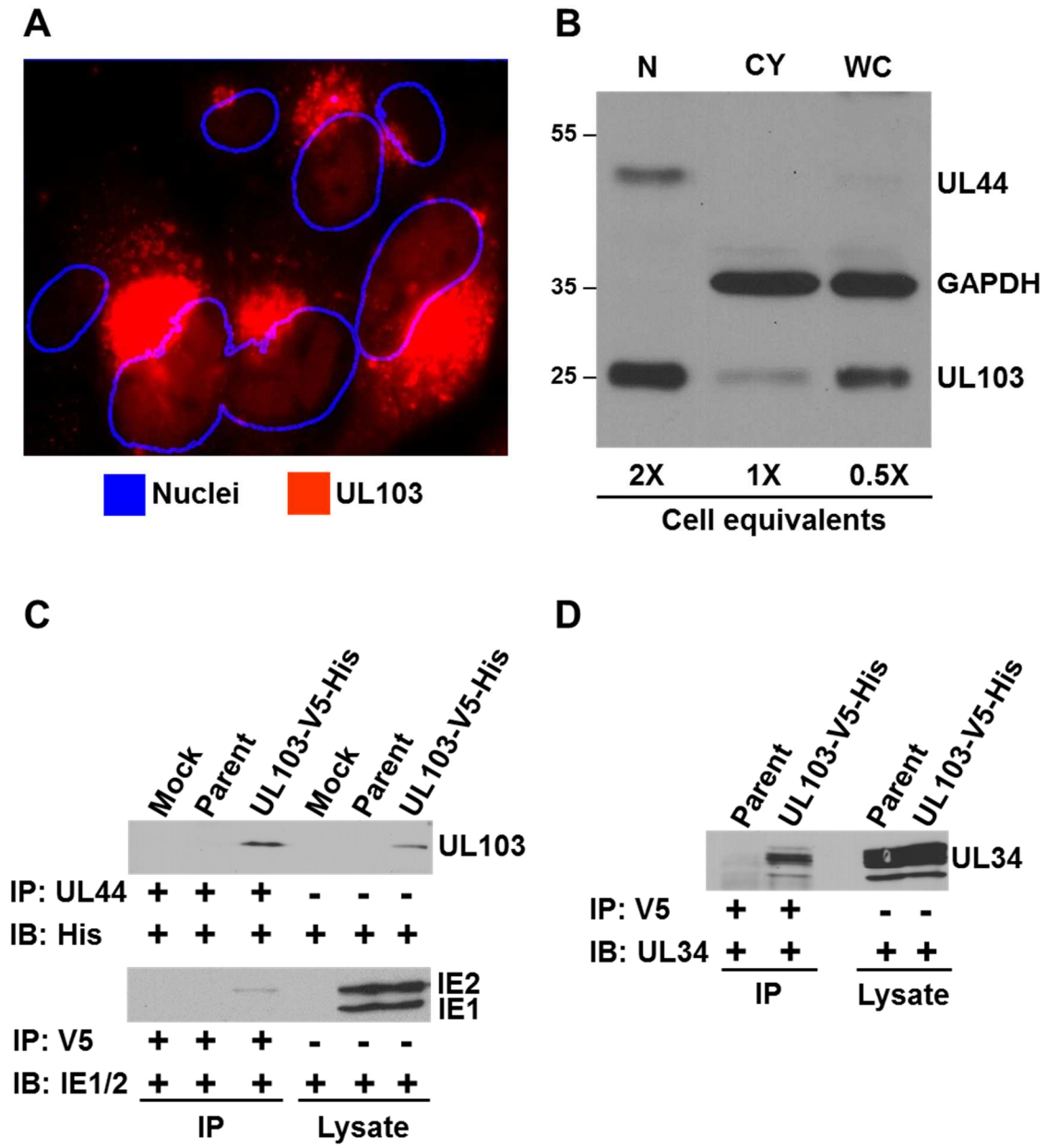

Figure 17. **Localization of pUL103 in infected cells and co-immunoprecipitation verification of viral proteins.** (A and B) HFFs were infected with UL103-V5-His(v) for 96 h at an MOI of 0.1 and probed with anti-V5 antibody. (A) The pUL103-V5-His tagged protein was analyzed by confocal microscopy. The center slice of a z-stack is shown with the nuclei outlined using ImageJ. (B) Cellular fractionation of infected cells using antibodies against UL44 and GAPDH to determine nuclear (N) and cytoplasmic (CY) fractions respectively. (C and D) Pull-downs were performed with anti-UL44 or anti-V5 on HFFs infected for 120 h at an MOI of 0.1. The immunoprecipitating antibody (IP) and the probing antibody (IB) are listed to the left of each blot. Immunoblots were probed with antibodies against His tagged UL103, IE1/2, and UL34

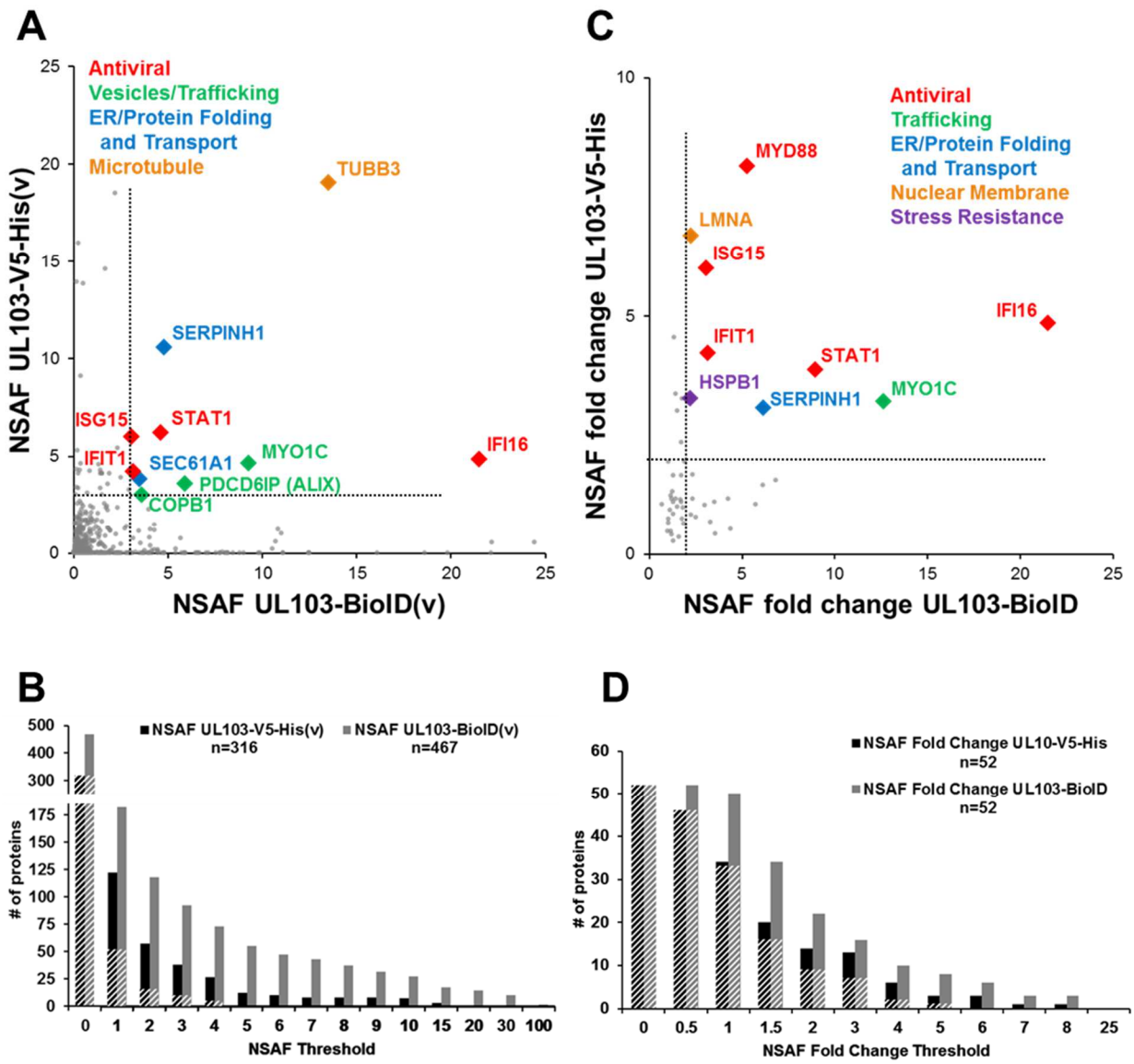

Figure 18. **Charts of the NSAF and NSAF fold change of cellular protein interactions.** (A) After filtering out non-specific interactions, the cellular NSAF of the of UL103-V5-His(v) and UL103-BioID(v) was plotted against each other. The function of the most enriched interactions (NSAF >3) are shown. (C) NSAF fold change selects for cellular interactions enhanced during infection. Fold changes greater than 2 highlights multiple antiviral proteins. (B and D) Charts showing all the cellular proteins at increasing cutoff values. The stripes indicate proteins shared by both methods.

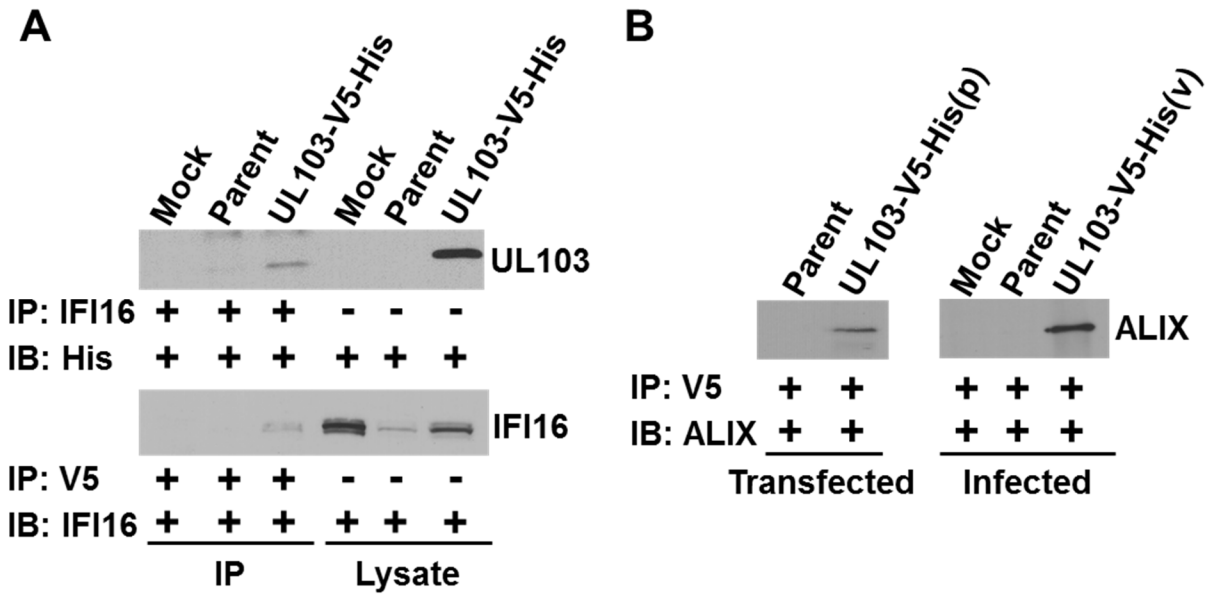

Figure 19. **Co-immunoprecipitation verification of IFI16 and ALIX interactions.** (A) HFFs were infected for 120 h at an MOI of 0.1 and affinity purification was conducted on the left three lanes while the right three lanes contain protein from cell lysates. The immunoprecipitating antibody (IP) and the probing antibody (IB) are listed to the left of each blot. pUL103 was purified with IFI16 in reciprocal pull down assays. (B) Affinity purification of pUL103 using a V5 antibody verified the interaction with ALIX in transfected and infected cells.

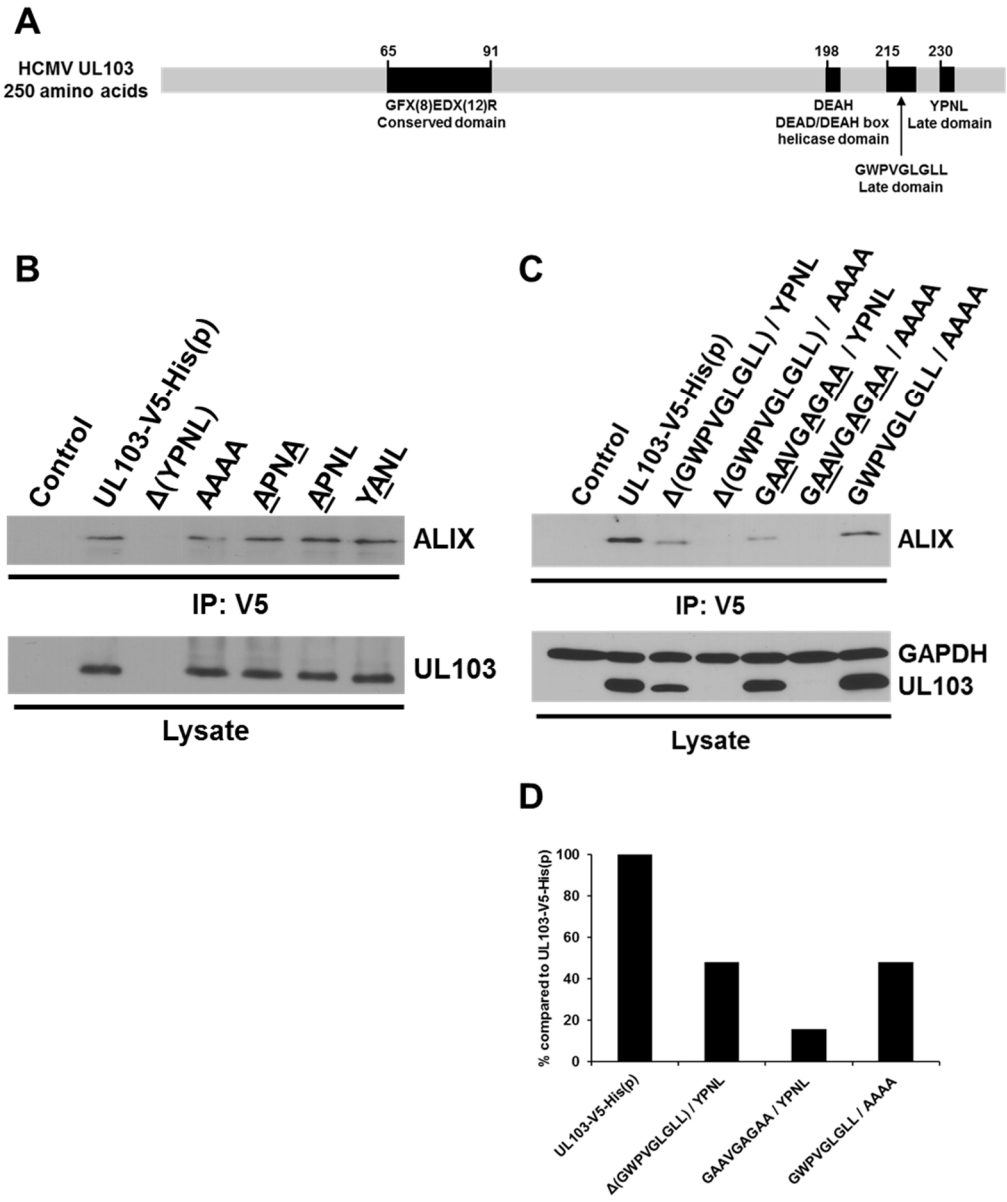

Figure 20. **pUL103 amino acid sequence schematic and mutational analysis of late domains.** (A) Map of HCMV pUL103 gene depicting a herpesvirus conserved region ($GFX_8EDX_{12}R$), along with HCMV specific helicase and late domains. (B and C) Co-immunoprecipitations of pUL103 using a V5 antibody in transfected cells. (B) Alanine substitutions within the ALIX motif had little to no effect on the pUL103-ALIX interaction. (C) Alteration of the first or second ALIX binding motif reduced the quantity of ALIX pulled down with pUL103. (D) The quantity of ALIX immunoprecipitated per condition was measured by densitometry and divided by normalized pUL103. The amount of pUL103 produced was normalized by taking the ratio of GAPDH to pUL103.

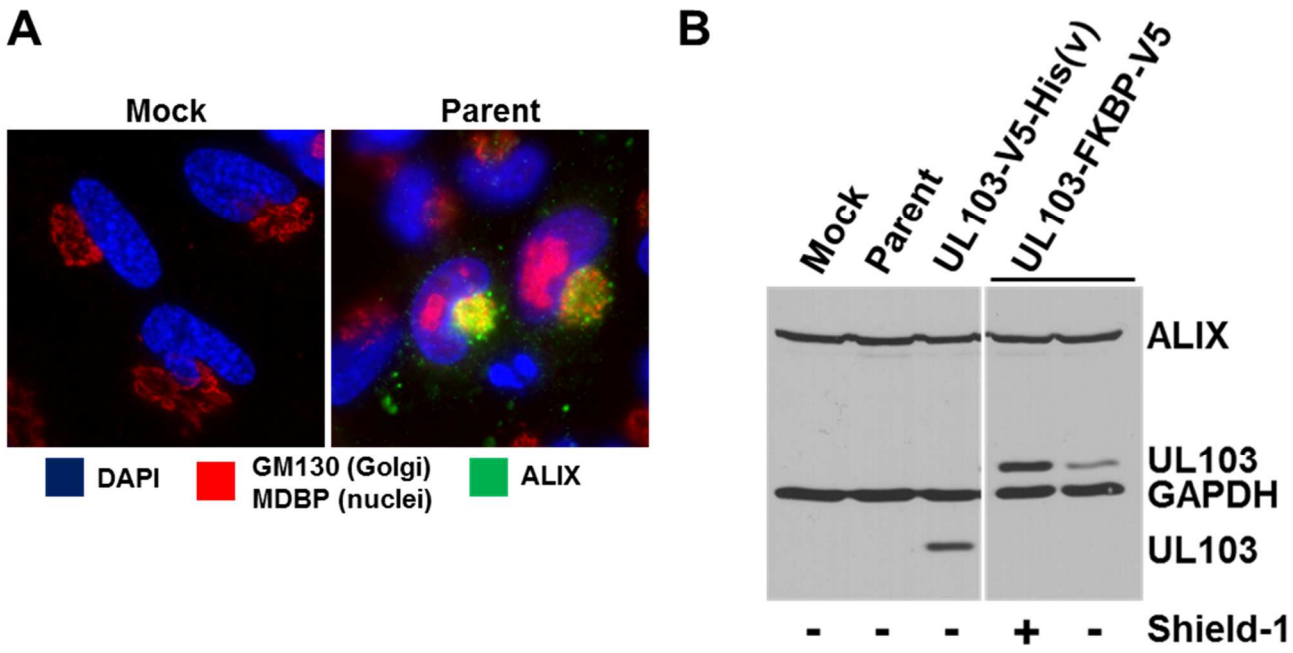

Figure 21. **ALIX redistribution during infection.** (A and B) ALIX localization and proteins levels were detected in uninfected and infected HFFs (MOI of 0.1, 120 hpi) by IFA and immunoblot. (A) Infection enhances ALIX staining which overlaps cVAC markers. (B) The protein levels ALIX were unchanged with each condition.

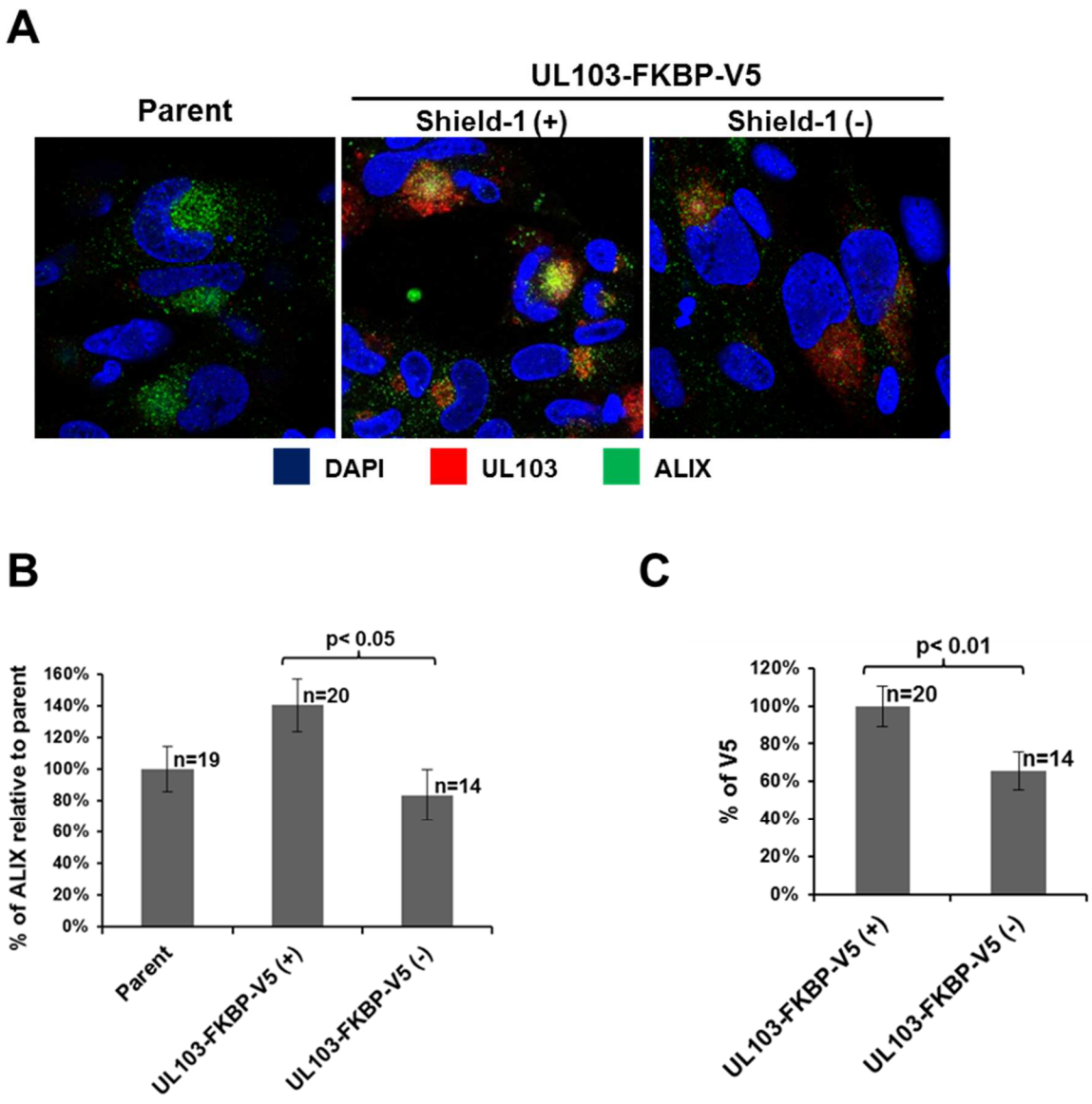

Figure 22. **ALIX redistribution involves pUL103.** (A) The localization of ALIX during pUL103 regulation by the Shield-1 ligand. (B) 3D quantitation of ALIX mean fluorescence intensity in the cVAC relative to the parent (measured using ImageJ). A significant change was seen only in the presence and absence of pUL103. (C) The same cVAC area was used for 3D quantitation of pUL103 by mean fluorescence intensity.

Chapter Four

Conclusions and Discussion

Human cytomegalovirus (HCMV) infection has multiple effects on host cells, including remodeling the cytoplasm to form the cytoplasmic virion assembly complex (cVAC), the site of final virion assembly. The HCMV genes specifically responsible for initiating and regulating cVAC biogenesis have not been defined. Our work set out to determine which HCMV genes are involved in this process. Previous work in our lab described the three dimensional structure of the cVAC using cellular markers against Golgi, trans-Golgi and early endosomes components. These cellular markers were used as indications of proper cVAC development. An siRNA screen targeting 26 early-late and late genes identified three HCMV genes (UL48, UL94, and UL103) whose silencing had major effects on cVAC development. To ensure the protein product of these genes is specifically involved; we created two recombinant viruses with a protein destabilization tag attached to UL48 or UL103. Degradation of either protein resulted in the disrupted cVAC assembly, validating the siRNA results. The set of viral genes identified is by no means all-encompassing as other immediate early or early genes were not included in our analysis.

It is important to note, that all three proteins involved in cVAC biogenesis are tegument proteins incorporated into mature virions (54). Tegument proteins introduced into host cells upon entry may facilitate cVAC development, yet whether these proteins play a role during early or late stages of infection has yet to be addressed. The incomplete degradation of these proteins using the FKBP destabilization domain has

prevented these types of analyses. However, the partial degradation of pUL48 and pUL103 is sufficient to disrupt cVAC formation, suggesting that wild-type expression levels are necessary for efficient virion production.

In addition to cVAC biogenesis, pUL103 is a highly conserved, multifunctional herpesvirus tegument protein involved in several processes, including cell-to-cell spread and virion envelopment and egress. To further understand the mechanisms of action and predict additional functions of pUL103, we sought to identify its interaction partners. To do so, we employed two complementary methods, co-immunoprecipitation (co-IP) and BioID, to detect viral and cellular proteins that interact with pUL103 in uninfected and HCMV infected cells. Our approach identified a multitude of pUL103 binding partners. To identify interactions of potentially high value, we selected for interactions highly abundant in both approaches and applied stringent selection criteria. The viral and cellular proteins that passed our selection criteria are associated with DNA, the antiviral response, and the biogenesis and transport of cytoplasmic vesicles.

Analysis of some of these interactions expanded our current understanding of the pUL103 multifunctional repertoire; we detected HCMV pUL103 in nuclei of infected cells, identified two functional ALIX binding domains, and established a role for pUL103 in ALIX localization during infection. This provides novel insights to the biological functions of pUL103 that may also be exercised by its homologous herpesvirus counterparts.

REFERENCES

1. **Vidal JB.** 1873. Ann Dermatol Syphiligr. **1**.
2. **Burnet JM, Williams SW.** 1939. Herpes Simplex: A new point of view. Med J Aust **1:**637.
3. **Knipe DM, Howley PM, Griffin DE, Lamb RA, Martin MA, Roizman B (ed).** 2013. Fields virology. Lippincott Williams & Wilkins, Philadelphia.
4. **Ryckman BJ, Jarvis MA, Drummond DD, Nelson JA, Johnson DC.** 2006. Human cytomegalovirus entry into epithelial and endothelial cells depends on genes UL128 to UL150 and occurs by endocytosis and low-pH fusion. J Virol **80:**710-722.
5. **Compton T, Nepomuceno RR, Nowlin DM.** 1992. Human cytomegalovirus penetrates host cells by pH-independent fusion at the cell surface. Virology **191:**387-395.
6. **Bate SL, Dollard SC, Cannon MJ.** 2010. Cytomegalovirus seroprevalence in the United States: the national health and nutrition examination surveys, 1988-2004. Clin Infect Dis **50:**1439-1447.
7. **Manicklal S, Emery VC, Lazzarotto T, Boppana SB, Gupta RK.** 2013. The "silent" global burden of congenital cytomegalovirus. Clin Microbiol Rev **26:**86-102.
8. **Tyms AS, Taylor DL, Parkin JM.** 1989. Cytomegalovirus and the acquired immunodeficiency syndrome. J Antimicrob Chemother **23 Suppl A:**89-105.
9. **Holbrook JT, Jabs DA, Weinberg DV, Lewis RA, Davis MD, Friedberg D.** 2003. Visual loss in patients with cytomegalovirus retinitis and acquired

immunodeficiency syndrome before widespread availability of highly active antiretroviral therapy. Arch Ophthalmol **121:**99-107.

10. **Heiden D, Tun N, Maningding E, Heiden M, Rose-Nussbaumer J, Chan KN, Khizniak T, Yakubenko A, Lewallen S, Keenan JD, Saranchuk P.** 2014. Training clinicians treating HIV to diagnose cytomegalovirus retinitis. Bull World Health Organ **92:**903-908.
11. **Heiden D, Saranchuk P, Tun N, Audoin B, Cohn J, Durier N, Holland G, Drew WL, t Hoen E.** 2014. We urge WHO to act on cytomegalovirus retinitis. Lancet Glob Health **2:**e76-77.
12. **Einsele H, Hebart H, Kauffmann-Schneider C, Sinzger C, Jahn G, Bader P, Klingebiel T, Dietz K, Loffler J, Bokemeyer C, Muller CA, Kanz L.** 2000. Risk factors for treatment failures in patients receiving PCR-based preemptive therapy for CMV infection. Bone Marrow Transplant **25:**757-763.
13. **Li CR, Greenberg PD, Gilbert MJ, Goodrich JM, Riddell SR.** 1994. Recovery of HLA-restricted cytomegalovirus (CMV)-specific T-cell responses after allogeneic bone marrow transplant: correlation with CMV disease and effect of ganciclovir prophylaxis. Blood **83:**1971-1979.
14. **Prentice HG, Gluckman E, Powles RL, Ljungman P, Milpied NJ, Camara R, Mandelli F, Kho P, Kennedy L, Bell AR.** 1997. Long-term survival in allogeneic bone marrow transplant recipients following acyclovir prophylaxis for CMV infection. The European Acyclovir for CMV Prophylaxis Study Group. Bone Marrow Transplant **19:**129-133.

15. **Ljungman P, de La Camara R, Milpied N, Volin L, Russell CA, Crisp A, Webster A.** 2002. Randomized study of valacyclovir as prophylaxis against cytomegalovirus reactivation in recipients of allogeneic bone marrow transplants. Blood **99:**3050-3056.

16. **Peggs KS, Preiser W, Kottaridis PD, McKeag N, Brink NS, Tedder RS, Goldstone AH, Linch DC, Mackinnon S.** 2000. Extended routine polymerase chain reaction surveillance and pre-emptive antiviral therapy for cytomegalovirus after allogeneic transplantation. Br J Haematol **111:**782-790.

17. **Versalovic J, Carroll KC, Funke G, Jorgensen JH, Landry ML, Warnock DW (ed).** 2011. Manual of clinical microbiology. ASM Press, Washington DC.

18. **Ogawa H, Suzutani T, Baba Y, Koyano S, Nozawa N, Ishibashi K, Fujieda K, Inoue N, Omori K.** 2007. Etiology of severe sensorineural hearing loss in children: independent impact of congenital cytomegalovirus infection and GJB2 mutations. J Infect Dis **195:**782-788.

19. **Swanson EC, Schleiss MR.** 2013. Congenital cytomegalovirus infection: new prospects for prevention and therapy. Pediatr Clin North Am **60:**335-349.

20. **Murphy E, Yu D, Grimwood J, Schmutz J, Dickson M, Jarvis MA, Hahn G, Nelson JA, Myers RM, Shenk TE.** 2003. Coding potential of laboratory and clinical strains of human cytomegalovirus. Proc Natl Acad Sci U S A **100:**14976-14981.

21. **Murphy E, Rigoutsos I, Shibuya T, Shenk TE.** 2003. Reevaluation of human cytomegalovirus coding potential. Proc Natl Acad Sci U S A **100:**13585-13590.

22. **Stern-Ginossar N, Weisburd B, Michalski A, Le VT, Hein MY, Huang SX, Ma M, Shen B, Qian SB, Hengel H, Mann M, Ingolia NT, Weissman JS.** 2012. Decoding human cytomegalovirus. Science **338:**1088-1093.

23. **Kari B, Gehrz R.** 1993. Structure, composition and heparin binding properties of a human cytomegalovirus glycoprotein complex designated gC-II. J Gen Virol **74 (Pt 2):**255-264.

24. **Fairley JA, Baillie J, Bain M, Sinclair JH.** 2002. Human cytomegalovirus infection inhibits epidermal growth factor (EGF) signalling by targeting EGF receptors. J Gen Virol **83:**2803-2810.

25. **Vanarsdall AL, Wisner TW, Lei H, Kazlauskas A, Johnson DC.** 2012. PDGF receptor-alpha does not promote HCMV entry into epithelial and endothelial cells but increased quantities stimulate entry by an abnormal pathway. PLoS Pathog **8:**e1002905.

26. **Feire AL, Koss H, Compton T.** 2004. Cellular integrins function as entry receptors for human cytomegalovirus via a highly conserved disintegrin-like domain. Proc Natl Acad Sci U S A **101:**15470-15475.

27. **Spear PG, Longnecker R.** 2003. Herpesvirus entry: an update. J Virol **77:**10179-10185.

28. **Child SJ, Hakki M, De Niro KL, Geballe AP.** 2004. Evasion of cellular antiviral responses by human cytomegalovirus TRS1 and IRS1. J Virol **78:**197-205.

29. **Gilbert MJ, Riddell SR, Plachter B, Greenberg PD.** 1996. Cytomegalovirus selectively blocks antigen processing and presentation of its immediate-early gene product. Nature **383:**720-722.

30. **Odeberg J, Plachter B, Branden L, Soderberg-Naucler C.** 2003. Human cytomegalovirus protein pp65 mediates accumulation of HLA-DR in lysosomes and destruction of the HLA-DR alpha-chain. Blood **101:**4870-4877.

31. **Baldick CJ, Jr., Marchini A, Patterson CE, Shenk T.** 1997. Human cytomegalovirus tegument protein pp71 (ppUL82) enhances the infectivity of viral DNA and accelerates the infectious cycle. J Virol **71:**4400-4408.

32. **Schierling K, Stamminger T, Mertens T, Winkler M.** 2004. Human cytomegalovirus tegument proteins ppUL82 (pp71) and ppUL35 interact and cooperatively activate the major immediate-early enhancer. J Virol **78:**9512-9523.

33. **Paulus C, Nevels M.** 2009. The human cytomegalovirus major immediate-early proteins as antagonists of intrinsic and innate antiviral host responses. Viruses **1:**760-779.

34. **Castillo JP, Yurochko AD, Kowalik TF.** 2000. Role of human cytomegalovirus immediate-early proteins in cell growth control. J Virol **74:**8028-8037.

35. **Lukac DM, Harel NY, Tanese N, Alwine JC.** 1997. TAF-like functions of human cytomegalovirus immediate-early proteins. J Virol **71:**7227-7239.

36. **Greaves RF, Mocarski ES.** 1998. Defective growth correlates with reduced accumulation of a viral DNA replication protein after low-multiplicity infection by a human cytomegalovirus ie1 mutant. J Virol **72:**366-379.

37. **Nevels M, Paulus C, Shenk T.** 2004. Human cytomegalovirus immediate-early 1 protein facilitates viral replication by antagonizing histone deacetylation. Proc Natl Acad Sci U S A **101:**17234-17239.

38. **Park JJ, Kim YE, Pham HT, Kim ET, Chung YH, Ahn JH.** 2007. Functional interaction of the human cytomegalovirus IE2 protein with histone deacetylase 2 in infected human fibroblasts. J Gen Virol **88:**3214-3223.

39. **Pari GS, Anders DG.** 1993. Eleven loci encoding trans-acting factors are required for transient complementation of human cytomegalovirus oriLyt-dependent DNA replication. J Virol **67:**6979-6988.

40. **Pari GS, Kacica MA, Anders DG.** 1993. Open reading frames UL44, IRS1/TRS1, and UL36-38 are required for transient complementation of human cytomegalovirus oriLyt-dependent DNA synthesis. Journal of Virology **67:**2575-2582.

41. **Xu Y, Cei SA, Rodriguez Huete A, Colletti KS, Pari GS.** 2004. Human cytomegalovirus DNA replication requires transcriptional activation via an IE2- and UL84-responsive bidirectional promoter element within oriLyt. J Virol **78:**11664-11677.

42. **Mettenleiter TC.** 2002. Herpesvirus assembly and egress. J Virol **76:**1537-1547.

43. **Sharma M, Bender BJ, Kamil JP, Lye MF, Pesola JM, Reim NI, Hogle JM, Coen DM.** 2015. Human cytomegalovirus UL97 phosphorylates the viral nuclear egress complex. J Virol **89:**523-534.

44. **Tooze J, Hollinshead M, Reis B, Radsak K, Kern H.** 1993. Progeny vaccinia and human cytomegalovirus particles utilize early endosomal cisternae for their envelopes. Eur J Cell Biol **60:**163-178.

45. **Cepeda V, Esteban M, Fraile-Ramos A.** 2010. Human cytomegalovirus final envelopment on membranes containing both trans-Golgi network and endosomal markers. Cell Microbiol **12:**386-404.

46. **Homman-Loudiyi M, Hultenby K, Britt W, Soderberg-Naucler C.** 2003. Envelopment of human cytomegalovirus occurs by budding into Golgi-derived vacuole compartments positive for gB, Rab 3, trans-golgi network 46, and mannosidase II. J Virol **77:**3191-3203.

47. **Das S, Vasanji A, Pellett PE.** 2007. Three-dimensional structure of the human cytomegalovirus cytoplasmic virion assembly complex includes a reoriented secretory apparatus. J Virol **81:**11861-11869.

48. **Tandon R, AuCoin DP, Mocarski ES.** 2009. Human cytomegalovirus exploits ESCRT machinery in the process of virion maturation. J Virol doi:JVI.01093-09 [pii];10.1128/JVI.01093-09 [doi].

49. **Fraile-Ramos A, Cepeda V, Elstak E, van der SP.** 2010. Rab27a is required for human cytomegalovirus assembly. PLoS One **5:**e15318.

50. **Indran SV, Britt WJ.** 2011. A role for the small GTPase Rab6 in assembly of human cytomegalovirus. J Virol **85:**5213-5219.

51. **Sanchez V, Greis KD, Sztul E, Britt WJ.** 2000. Accumulation of virion tegument and envelope proteins in a stable cytoplasmic compartment during human cytomegalovirus replication: characterization of a potential site of virus assembly. J Virol **74:**975-986.

52. **Theiler RN, Compton T.** 2002. Distinct glycoprotein O complexes arise in a post-Golgi compartment of cytomegalovirus-infected cells. J Virol **76:**2890-2898.

53. **Gibson W.** 2008. Structure and formation of the cytomegalovirus virion. Curr Top Microbiol Immunol **325:**187-204.

54. **Varnum SM, Streblow DN, Monroe ME, Smith P, Auberry KJ, Pasa-Tolic L, Wang D, Camp DG, Rodland K, Wiley S, Britt W, Shenk T, Smith RD, Nelson JA.** 2004. Identification of proteins in human cytomegalovirus (HCMV) particles: the HCMV proteome. J Virol **78:**10960-10966.

55. **Phillips SL, Bresnahan WA.** 2012. The human cytomegalovirus (HCMV) tegument protein UL94 is essential for secondary envelopment of HCMV virions. J Virol **86:**2523-2532.

56. **Silva MC, Yu QC, Enquist L, Shenk T.** 2003. Human cytomegalovirus UL99-encoded pp28 is required for the cytoplasmic envelopment of tegument-associated capsids. J Virol **77:**10594-10605.

57. **AuCoin DP, Smith GB, Meiering CD, Mocarski ES.** 2006. Betaherpesvirus-conserved cytomegalovirus tegument protein ppUL32 (pp150) controls cytoplasmic events during virion maturation. J Virol **80:**8199-8210.

58. **Ahlqvist J, Mocarski E.** 2011. Cytomegalovirus UL103 controls virion and dense body egress. J Virol **85:**5125-5135.

59. **Yu X, Shah S, Lee M, Dai W, Lo P, Britt W, Zhu H, Liu F, Zhou ZH.** 2011. Biochemical and structural characterization of the capsid-bound tegument proteins of human cytomegalovirus. J Struct Biol **174:**451-460.

60. **Hensel G, Meyer H, Gartner S, Brand G, Kern HF.** 1995. Nuclear localization of the human cytomegalovirus tegument protein pp150 (ppUL32). J Gen Virol **76 (Pt 7):**1591-1601.

61. **Irmiere A, Gibson W.** 1985. Isolation of human cytomegalovirus intranuclear capsids, characterization of their protein constituents, and demonstration that the B-capsid assembly protein is also abundant in noninfectious enveloped particles. J Virol **56:**277-283.

62. **Meyer HH, Ripalti A, Landini MP, Radsak K, Kern HF, Hensel GM.** 1997. Human cytomegalovirus late-phase maturation is blocked by stably expressed UL32 antisense mRNA in astrocytoma cells. J Gen Virol **78 (Pt 10):**2621-2631.

63. **Tandon R, Mocarski ES.** 2008. Control of cytoplasmic maturation events by cytomegalovirus tegument protein pp150. J Virol **82:**9433-9444.

64. **Jones TR, Lee SW.** 2004. An acidic cluster of human cytomegalovirus UL99 tegument protein is required for trafficking and function. J Virol **78:**1488-1502.

65. **Sanchez V, Sztul E, Britt WJ.** 2000. Human cytomegalovirus pp28 (UL99) localizes to a cytoplasmic compartment which overlaps the endoplasmic reticulum-golgi-intermediate compartment. J Virol **74:**3842-3851.

66. **Seo JY, Britt WJ.** 2008. Multimerization of tegument protein pp28 within the assembly compartment is required for cytoplasmic envelopment of human cytomegalovirus. J Virol **82:**6272-6287.

67. **Phillips SL, Cygnar D, Thomas A, Bresnahan WA.** 2012. Interaction between the human cytomegalovirus tegument proteins UL94 and UL99 is essential for virus replication. J Virol **86:**9995-10005.

68. **Womack A, Shenk T.** 2010. Human cytomegalovirus tegument protein pUL71 is required for efficient virion egress. MBio **1**.

69. **Schauflinger M, Fischer D, Schreiber A, Chevillotte M, Walther P, Mertens T, J. vE.** 2011. The tegument protein UL71 of human cytomegalovirus is involved in late envelopment and affects multivesicular bodies. J Virol doi:JVI.01540-10 [pii];10.1128/JVI.01540-10 [doi].

70. **Fischer D.** 2012. Dissecting functional motifs of the human cytomegalovirus tegument protein pUL71. Doctoral. University of Ulm.

71. **Xie M, Xuan B, Shan J, Pan D, Sun Y, Shan Z, Zhang J, Yu D, Li B, Qian Z.** 2015. Human cytomegalovirus exploits interferon-induced transmembrane proteins to facilitate morphogenesis of the virion assembly compartment. J Virol **89:**3049-3061.

72. **Garrus JE, von Schwedler UK, Pornillos OW, Morham SG, Zavitz KH, Wang HE, Wettstein DA, Stray KM, Cote M, Rich RL, Myszka DG, Sundquist WI.** 2001. Tsg101 and the vacuolar protein sorting pathway are essential for HIV-1 budding. Cell **107:**55-65.

73. **Demirov DG, Ono A, Orenstein JM, Freed EO.** 2002. Overexpression of the N-terminal domain of TSG101 inhibits HIV-1 budding by blocking late domain function. Proc Natl Acad Sci U S A **99:**955-960.

74. **Garnier L, Wills JW, Verderame MF, Sudol M.** 1996. WW domains and retrovirus budding. Nature **381:**744-745.

75. **Puffer BA, Parent LJ, Wills JW, Montelaro RC.** 1997. Equine infectious anemia virus utilizes a YXXL motif within the late assembly domain of the Gag p9 protein. J Virol **71:**6541-6546.

76. **Fisher RD, Chung HY, Zhai Q, Robinson H, Sundquist WI, Hill CP.** 2007. Structural and biochemical studies of ALIX/AIP1 and its role in retrovirus budding. Cell **128:**841-852.

77. **Strack B, Calistri A, Craig S, Popova E, Gottlinger HG.** 2003. AIP1/ALIX is a binding partner for HIV-1 p6 and EIAV p9 functioning in virus budding. Cell **114:**689-699.

78. **Fraile-Ramos A, Pelchen-Matthews A, Risco C, Rejas MT, Emery VC, Hassan-Walker AF, Esteban M, Marsh M.** 2007. The ESCRT machinery is not required for human cytomegalovirus envelopment. Cell Microbiol **9:**2955-2967.

79. **Patel AH, MacLean JB.** 1995. The product of the UL6 gene of herpes simplex virus type 1 is associated with virus capsids. Virology **206:**465-478.

80. **Dijkstra JM, Fuchs W, Mettenleiter TC, Klupp BG.** 1997. Identification and transcriptional analysis of pseudorabies virus UL6 to UL12 genes. Arch Virol **142:**17-35.

81. **Newcomb WW, Juhas RM, Thomsen DR, Homa FL, Burch AD, Weller SK, Brown JC.** 2001. The UL6 gene product forms the portal for entry of DNA into the herpes simplex virus capsid. J Virol **75:**10923-10932.

82. **Tanaka M, Sata T, Kawaguchi Y.** 2008. The product of the Herpes simplex virus 1 UL7 gene interacts with a mitochondrial protein, adenine nucleotide translocator 2. Virol J **5:**125.

83. **Chambers J, Angulo A, Amaratunga D, Guo H, Jiang Y, Wan JS, Bittner A, Frueh K, Jackson MR, Peterson PA, Erlander MG, Ghazal P.** 1999. DNA

microarrays of the complex human cytomegalovirus genome: profiling kinetic class with drug sensitivity of viral gene expression. J Virol **73:**5757-5766.

84. **Yu D, Silva MC, Shenk T.** 2003. Functional map of human cytomegalovirus AD169 defined by global mutational analysis. Proc Natl Acad Sci U S A **100:**12396-12401.

85. **Dunn W, Chou C, Li H, Hai R, Patterson D, Stolc V, Zhu H, Liu F.** 2003. Functional profiling of a human cytomegalovirus genome. Proc Natl Acad Sci U S A **100:**14223-14228.

86. **Schmitt J, Keil GM.** 1996. Identification and characterization of the bovine herpesvirus 1 UL7 gene and gene product which are not essential for virus replication in cell culture. J Virol **70:**1091-1099.

87. **Fuchs W, Granzow H, Klopfleisch R, Klupp BG, Rosenkranz D, Mettenleiter TC.** 2005. The UL7 gene of pseudorabies virus encodes a nonessential structural protein which is involved in virion formation and egress. J Virol **79:**11291-11299.

88. **Roller RJ, Fetters R.** 2015. The herpes simplex virus 1 UL51 protein interacts with the UL7 protein and plays a role in its recruitment into the virion. J Virol **89:**3112-3122.

89. **Nozawa N, Daikoku T, Yamauchi Y, Takakuwa H, Goshima F, Yoshikawa T, Nishiyama Y.** 2002. Identification and characterization of the UL7 gene product of herpes simplex virus type 2. Virus Genes **24:**257-266.

90. **Mettenleiter TC, Klupp BG, Granzow H.** 2009. Herpesvirus assembly: an update. Virus Res **143:**222-234.

91. **Johnson DC, Baines JD.** 2011. Herpesviruses remodel host membranes for virus egress. Nat Rev Microbiol **9:**382-394.

92. **Resnik KS, DiLeonardo M, Maillet M.** 2000. Histopathologic findings in cutaneous cytomegalovirus infection. Am J Dermatopathol **22:**397-407.

93. **Buchkovich NJ, Maguire TG, Alwine JC.** 2010. Role of the endoplasmic reticulum chaperone BiP, SUN domain proteins, and dynein in altering nuclear morphology during human cytomegalovirus infection. J Virol **84:**7005-7017.

94. **Severi B, Landini MP, Govoni E.** 1988. Human cytomegalovirus morphogenesis: an ultrastructural study of the late cytoplasmic phases. Arch Virol **98:**51-64.

95. **Schauflinger M, Villinger C, Mertens T, Walther P, von EJ.** 2013. Analysis of human cytomegalovirus secondary envelopment by advanced electron microscopy. Cell Microbiol **15:**305-314.

96. **Das S, Pellett PE.** 2007. Members of the HCMV US12 family of predicted heptaspanning membrane proteins have unique intracellular distributions, including association with the cytoplasmic virion assembly complex. Virology **361:**263-273.

97. **Prichard MN, Britt WJ, Daily SL, Hartline CB, Kern ER.** 2005. Human cytomegalovirus UL97 kinase is required for the normal intranuclear distribution of pp65 and virion morphogenesis. J Virol **79:**15494-15502.

98. **Das S, Pellett PE.** 2011. Spatial relationships between markers for secretory and endosomal machinery in human cytomegalovirus-infected cells versus those in uninfected cells. J Virol **85:**5864-5879.

99. **Hollinshead M, Johns HL, Sayers CL, Gonzalez-Lopez C, Smith GL, Elliott G.** 2012. Endocytic tubules regulated by Rab GTPases 5 and 11 are used for envelopment of herpes simplex virus. EMBO J **31:**4204-4220.

100. **Indran SV, Ballestas ME, Britt WJ.** 2010. Bicaudal D1-dependent trafficking of human cytomegalovirus tegument protein pp150 in virus-infected cells. J Virol **84:**3162-3177.

101. **Azzeh M, Honigman A, Taraboulos A, Rouvinski A, Wolf DG.** 2006. Structural changes in human cytomegalovirus cytoplasmic assembly sites in the absence of UL97 kinase activity. Virology **354:**69-79.

102. **Prichard MN, Gao N, Jairath S, Mulamba G, Krosky P, Coen DM, Parker BO, Pari GS.** 1999. A recombinant human cytomegalovirus with a large deletion in UL97 has a severe replication deficiency. J Virol **73:**5663-5670.

103. **Tandon R, Mocarski ES.** 2011. Cytomegalovirus pUL96 is critical for the stability of pp150-associated nucleocapsids. J Virol **85:**7129-7141.

104. **Bughio F, Elliott DA, Goodrum F.** 2013. An endothelial cell-specific requirement for the UL133-UL138 locus of human cytomegalovirus for efficient virus maturation. J Virol **87:**3062-3075.

105. **Hook LM, Grey F, Grabski R, Tirabassi R, Doyle T, Hancock M, Landais I, Jeng S, McWeeney S, Britt W, Nelson JA.** 2014. Cytomegalovirus miRNAs target secretory pathway genes to facilitate formation of the virion assembly compartment and reduce cytokine secretion. Cell Host Microbe **15:**363-373.

106. **Yu D, Smith GA, Enquist LW, Shenk T.** 2002. Construction of a self-excisable bacterial artificial chromosome containing the human cytomegalovirus genome and mutagenesis of the diploid TRL/IRL13 gene. J Virol **76:**2316-2328.

107. **Warming S, Costantino N, DL C, Jenkins NA, Copeland NG.** 2005. Simple and highly efficient BAC recombineering using galK selection. Nucleic Acids Res **33:**e36.

108. **Banaszynski LA, Chen LC, Maynard-Smith LA, Ooi AG, Wandless TJ.** 2006. A rapid, reversible, and tunable method to regulate protein function in living cells using synthetic small molecules. Cell **126:**995-1004.

109. **Perng YC, Qian Z, Fehr AR, Xuan B, Yu D.** 2011. The human cytomegalovirus gene UL79 is required for the accumulation of late viral transcripts. J Virol **85:**4841-4852.

110. **Das S, Skomorovska-Prokvolit Y, Wang FZ, Pellett PE.** 2006. Infection-dependent nuclear localization of US17, a member of the US12 family of human cytomegalovirus-encoded seven-transmembrane proteins. J Virol **80:**1191-1203.

111. **Kim ET, Oh SE, Lee YO, Gibson W, Ahn JH.** 2009. Cleavage specificity of the UL48 deubiquitinating protease activity of human cytomegalovirus and the growth of an active-site mutant virus in cultured cells. J Virol **83:**12046-12056.

112. **Misaki R, Nakagawa T, Fukuda M, Taniguchi N, Taguchi T.** 2007. Spatial segregation of degradation- and recycling-trafficking pathways in COS-1 cells. Biochem Biophys Res Commun **360:**580-585.

113. **Misaki R, Morimatsu M, Uemura T, Waguri S, Miyoshi E, Taniguchi N, Matsuda M, Taguchi T.** 2010. Palmitoylated Ras proteins traffic through

recycling endosomes to the plasma membrane during exocytosis. J Cell Biol **191:**23-29.

114. **Husebye H, Aune MH, Stenvik J, Samstad E, Skjeldal F, Halaas O, Nilsen NJ, Stenmark H, Latz E, Lien E, Mollnes TE, Bakke O, Espevik T.** 2010. The Rab11a GTPase controls Toll-like receptor 4-induced activation of interferon regulatory factor-3 on phagosomes. Immunity **33:**583-596.

115. **Alwine JC.** 2008. Modulation of host cell stress responses by human cytomegalovirus. Curr Top Microbiol Immunol **325:**263-279.

116. **Mocarski ES, Upton JW, Kaiser WJ.** 2011. Viral infection and the evolution of caspase 8-regulated apoptotic and necrotic death pathways. Nat Rev Immunol **12:**79-88.

117. **Pawliczek T, Crump CM.** 2009. Herpes simplex virus type 1 production requires a functional ESCRT-III complex but is independent of TSG101 and ALIX expression. J Virol **83:**11254-11264.

118. **Wang J, Loveland AN, Kattenhorn LM, Ploegh HL, Gibson W.** 2006. High-molecular-weight protein (pUL48) of human cytomegalovirus is a competent deubiquitinating protease: mutant viruses altered in its active-site cysteine or histidine are viable. J Virol **80:**6003-6012.

119. **Mocarski ES, Jr., Shenk T, Griffiths PD, Pass RF.** 2013. Cytomegaloviruses, p 1960-2014. *In* Knipe DM, Howley PM, Griffin DE, Cohen JI, Lamb RA, Martin MA, Racaniello VR, Roizman B (ed), Fields Virology, 6 ed. Lippincott Williams & Wilkins, Philadelphia.

120. **To A, Bai Y, Shen A, Gong H, Umamoto S, Lu S, Liu F.** 2011. Yeast two hybrid analyses reveal novel binary interactions between human cytomegalovirus-encoded virion proteins. PLoS One **6:**e17796.

121. **Phillips SL, Bresnahan WA.** 2011. Identification of binary interactions between human cytomegalovirus virion proteins. J Virol **85:**440-447.

122. **Mocarski ES, Jr.** 2007. Betaherpes viral genes and their functions, p 204-230. *In* Arvin A, Campadelli-Fiume G, Mocarski E, Moore PS, Roizman B, Whitley R, Yamanishi K (ed), Human herpesviruses: biology, therapy, and immunoprophylaxis doi:NBK47435 [bookaccession]. Cambridge University Press, Cambridge.

123. **Roizman B, Campadelli-Fiume G.** 2007. Alphaherpes viral genes and their functions, p 70-92. *In* Arvin A, Campadelli-Fiume G, Mocarski E, Moore PS, Roizman B, Whitley R, Yamanishi K (ed), Human Herpesviruses: Biology, Therapy, and Immunoprophylaxis doi:NBK47364 [bookaccession]. Cambridge University Press, Cambridge.

124. **Hyun JJ, Park HS, Kim KH, Kim HJ.** 1999. Analysis of transcripts expressed from the UL47 gene of human cytomegalovirus. Arch Pharm Res **22:**542-548.

125. **Wing BA, Johnson RA, Huang ES.** 1998. Identification of positive and negative regulatory regions involved in regulating expression of the human cytomegalovirus UL94 late promoter: role of IE2-86 and cellular p53 in mediating negative regulatory function. J Virol **72:**1814-1825.

126. **Wing BA, Lee GC, Huang ES.** 1996. The human cytomegalovirus UL94 open reading frame encodes a conserved herpesvirus capsid/tegument-associated virion protein that is expressed with true late kinetics. J Virol **70:**3339-3345.

127. **Wing BA, Huang ES.** 1995. Analysis and mapping of a family of 3'-coterminal transcripts containing coding sequences for human cytomegalovirus open reading frames UL93 through UL99. J Virol **69:**1521-1531.

128. **Schneider CA, Rasband WS, Eliceiri KW.** 2012. NIH Image to ImageJ: 25 years of image analysis. Nat Methods **9:**671-675.

129. **Das S, Ortiz DA, Gurczynski SJ, Khan F, Pellett PE.** 2014. Identification of human cytomegalovirus genes important for biogenesis of the cytoplasmic virion assembly complex. J Virol **88:**9086-9099.

130. **Roux KJ, Kim DI, Raida M, Burke B.** 2012. A promiscuous biotin ligase fusion protein identifies proximal and interacting proteins in mammalian cells. J Cell Biol **196:**801-810.

131. **Zybailov B, Mosley AL, Sardiu ME, Coleman MK, Florens L, Washburn MP.** 2006. Statistical analysis of membrane proteome expression changes in Saccharomyces cerevisiae. J Proteome Res **5:**2339-2347.

132. **Mellacheruvu D, Wright Z, Couzens AL, Lambert JP, St-Denis NA, Li T, Miteva YV, Hauri S, Sardiu ME, Low TY, Halim VA, Bagshaw RD, Hubner NC, Al-Hakim A, Bouchard A, Faubert D, Fermin D, Dunham WH, Goudreault M, Lin ZY, Badillo BG, Pawson T, Durocher D, Coulombe B, Aebersold R, Superti-Furga G, Colinge J, Heck AJ, Choi H, Gstaiger M, Mohammed S, Cristea IM, Bennett KL, Washburn MP, Raught B, Ewing RM,**

Gingras AC, Nesvizhskii AI. 2013. The CRAPome: a contaminant repository for affinity purification-mass spectrometry data. Nat Methods **10:**730-736.

133. **Gurczynski SJ, Das S, Pellett PE.** 2014. Deletion of the human cytomegalovirus US17 gene increases the ratio of genomes per infectious unit and alters regulation of immune and endoplasmic reticulum stress response genes at early and late times after infection. J Virol **88:**2168-2182.

134. **Votteler J, Sundquist WI.** 2013. Virus budding and the ESCRT pathway. Cell Host Microbe **14:**232-241.

135. **Liegeois F, Lafay B, Formenty P, Locatelli S, Courgnaud V, Delaporte E, Peeters M.** 2009. Full-length genome characterization of a novel simian immunodeficiency virus lineage (SIVolc) from olive Colobus (Procolobus verus) and new SIVwrcPbb strains from Western Red Colobus (Piliocolobus badius badius) from the Tai Forest in Ivory Coast. J Virol **83:**428-439.

136. **Battista MC, Bergamini G, Boccuni MC, Campanini F, Ripalti A, Landini MP.** 1999. Expression and characterization of a novel structural protein of human cytomegalovirus, pUL25. J Virol **73:**3800-3809.

137. **Baldick CJ, Jr., Shenk T.** 1996. Proteins associated with purified human cytomegalovirus particles. J Virol **70:**6097-6105.

138. **Win TZ, Goodwin A, Hickson ID, Norbury CJ, Wang SW.** 2004. Requirement for Schizosaccharomyces pombe Top3 in the maintenance of chromosome integrity. J Cell Sci **117:**4769-4778.

139. **Saffert RT, Kalejta RF.** 2006. Inactivating a cellular intrinsic immune defense mediated by Daxx is the mechanism through which the human cytomegalovirus

pp71 protein stimulates viral immediate-early gene expression. J Virol **80:**3863-3871.

140. **Browne EP, Shenk T.** 2003. Human cytomegalovirus UL83-coded pp65 virion protein inhibits antiviral gene expression in infected cells. Proc Natl Acad Sci U S A **100:**11439-11444.

141. **Nickel W, Brugger B, Wieland FT.** 2002. Vesicular transport: the core machinery of COPI recruitment and budding. J Cell Sci **115:**3235-3240.

142. **Misteli T.** 1996. Molecular mechanisms in the disassembly and reassembly of the mammalian Golgi apparatus during M-phase. FEBS Lett **389:**66-69.

143. **Brandstaetter H, Kendrick-Jones J, Buss F.** 2012. Molecular roles of Myo1c function in lipid raft exocytosis. Commun Integr Biol **5:**508-510.

144. **Brandstaetter H, Kishi-Itakura C, Tumbarello DA, Manstein DJ, Buss F.** 2014. Loss of functional MYO1C/myosin 1c, a motor protein involved in lipid raft trafficking, disrupts autophagosome-lysosome fusion. Autophagy **10:**2310-2323.

145. **Chen XW, Leto D, Chiang SH, Wang Q, Saltiel AR.** 2007. Activation of RalA is required for insulin-stimulated Glut4 trafficking to the plasma membrane via the exocyst and the motor protein Myo1c. Dev Cell **13:**391-404.

146. **Honeychurch KM, Yang G, Jordan R, Hruby DE.** 2007. The Vaccinia Virus F13L YPPL Motif Is Required for Efficient Release of Extracellular Enveloped Virus. Journal of Virology **81:**7310-7315.

147. **Bardens A, Doring T, Stieler J, Prange R.** 2011. Alix regulates egress of hepatitis B virus naked capsid particles in an ESCRT-independent manner. Cell Microbiol **13:**602-619.

148. **Lee CP, Liu PT, Kung HN, Su MT, Chua HH, Chang YH, Chang CW, Tsai CH, Liu FT, Chen MR.** 2012. The ESCRT machinery is recruited by the viral BFRF1 protein to the nucleus-associated membrane for the maturation of Epstein-Barr Virus. PLoS Pathog **8:**e1002904.

149. **Zhai Q, Landesman MB, Robinson H, Sundquist WI, Hill CP.** 2011. Identification and structural characterization of the ALIX-binding late domains of simian immunodeficiency virus SIVmac239 and SIVagmTan-1. J Virol **85:**632-637.

150. **Freed EO.** 2002. Viral late domains. J Virol **76:**4679-4687.

ABSTRACT

THE ROLES OF HUMAN CYTOMEGALOVIRUS TEGUMENT PROTEINS pUL48 AND pUL103 DURING INFECTION

by

DANIEL A. ORTIZ

December 2015

Advisor: Dr. Philip E. Pellett

Major: Immunology and Microbiology

Degree: Doctor of Philosophy

Human cytomegalovirus (HCMV) is a large double-stranded DNA virus that causes severe disease in newborns and immunocompromised patients. During infection, HCMV is able to reconfigure the host cell machinery to establish a virus producing factory, termed the cytoplasmic virion assembly complex (cVAC). Generating drugs that affect cVAC development or function provides an alternative mode of action for HCMV antivirals that can essentially eliminate virion production. The objective of this work is aimed at identifying regulators of cVAC biogenesis that may serve as potential drug targets.

We identified three HCMV genes (UL48, UL94, and UL103) whose silencing or protein degradation had major effects on cVAC development, including failure to form the Golgi ring and dispersal of markers of early and recycling endosomes. In addition, we found that mutant viruses expressing an unstable form of the UL103 protein causes a reduction in plaque size and the aberrant formation of intracellular virions.

To help define the mechanisms of action and predict additional functions of pUL103, we investigated its viral and cellular protein-protein interactions. We applied a dual method approach, co-immunoprecipitation and proximity biotinylation affinity purification followed by mass spectrometry to enrich for pUL103 interaction partners in uninfected and HCMV infected cells. This led to identification of pUL103 in nuclei, delineation of a novel ALIX binding domain, and a role for pUL103 in ALIX localization in infected cells.

AUTOBIOGRAPHICAL STATEMENT

I was born in 1986 at the Advocate Christ Medical Center in Oak Lawn, Illinois. At the early age of three we moved to the suburbs of Hanover Park where my family has lived ever since. My interest in research truly began at the University of Illinois Champaign-Urbana where I volunteered for Dr. Scott E. Martin working on *Listeria monocytogenes* virulence factors and the efficacy of antimicrobial solutions. My growing interest in pathogenic organisms led me to the PhD program at Wayne State University. I joined the laboratory of Dr. Philip E. Pellett in June of 2011. There, I continued the work of Dr. Subhendu Das in identifying viral genes necessary for building a virus factory in host cells. In addition to research, I was fortunate to have met Dr. Hossein Salimnia, Chief of the Microbiology Division at Detroit Medical Center, who introduced me to clinical microbiology. This particular area of microbiology fascinates me, as it enables me to work in a setting with pathogenic organisms, laboratory diagnosis, and translational research. I am excited for what lies ahead in pursuing a career path as a clinical laboratory director.